Helsinki University of Technology Publications in Materials Science and Metallurgy
Teknillisen korkeakoulun materiaalitekniikan ja metallurgian julkaisuja
Espoo 2003 TKK-MK-151

ON HEARTH PHENOMENA AND HOT METAL CARBON CONTENT IN BLAST FURNACE

Doctoral Thesis

Kalevi Raipala

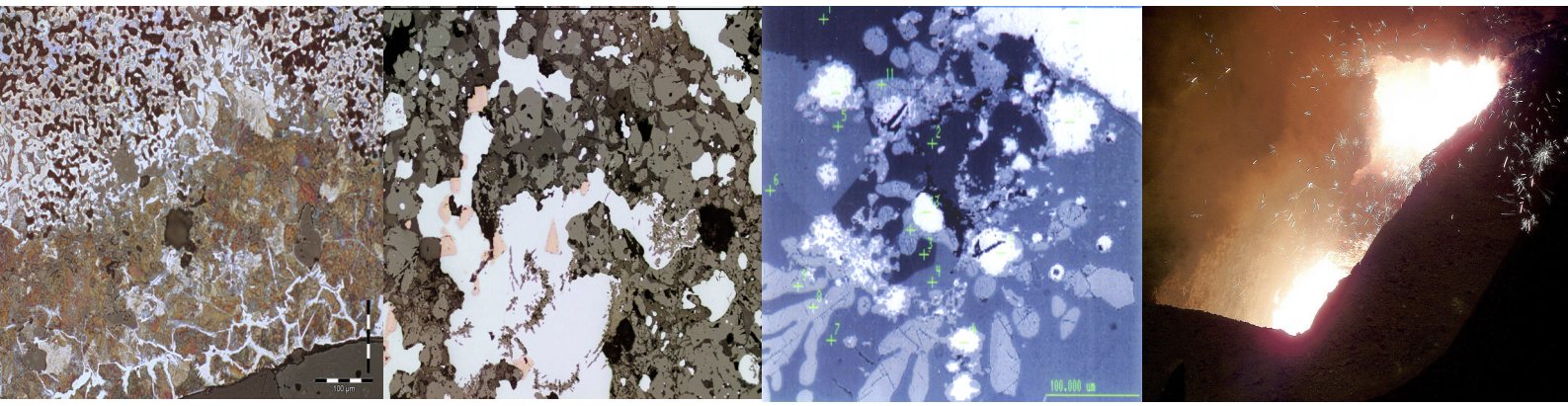

TEKNILLINEN KORKEAKOULU
TEKNISKA HÖGSKOLAN
HELSINKI UNIVERSITY OF TECHNOLOGY
TECHNISCHE UNIVERSITÄT HELSINKI
UNIVERSITE DE TECHNOLOGIE D'HELSINKI

Helsinki University of Technology Publications in Materials Science and Metallurgy
Teknillisen korkeakoulun materiaalitekniikan ja metallurgian julkaisuja
Espoo 2003 TKK-MK-151

ON HEARTH PHENOMENA AND HOT METAL CARBON CONTENT IN BLAST FURNACE

Kalevi Raipala

Dissertation for the degree of Doctor of Science in Technology to be presented with due permission of the Department of Materials Science and Rock Engineering for public examination and debate in Auditorium V1 at Helsinki University of Technology (Espoo, Finland) on the 14th of November, 2003, at 12 noon.

Helsinki University of Technology
Department of Materials Science and Rock Engineering
Laboratory of Metallurgy

Teknillinen korkeakoulu
Materiaali- ja kalliotekniikan osasto
Metallurgian laboratorio

Keywords: Blast furnace, Hearth, Deadman, Salamander, Hot metal, Sulphur, Carbon
UDC: 669.162.2; 66.041.53

Distribution:
Helsinki University of Technology
Laboratory of Metallurgy
P.O. Box 6200
FIN-02015 HUT, Finland
Tel. +358 9 451 2756
Fax. +358 9 451 2798
e-mail: lea.selin@hut.fi

Cover: Fig. 1: Micrograph of a partly reduced and carbonised pellet, Fig. 2: Micrograph of bottom scab structure, Fig. 3: SEM photo of bottom scab structure, Fig. 4: View of hot metal

ISBN 951-22-6748-9
ISSN 1455-2329

Picaset Oy

PREFACE

This work has been done during the years 1994-2003 in the Laboratory of Metallurgy, Department of Materials Science and Rock Engineering in Helsinki University of Technology under supervision of Professor Lauri Holappa to whom I wish to express my gratitude for his encouragement and guidance during this work. I would also express my gratitude to professor emeritus Kaj Lilius who stimulated me to begin this work and professor Jouko Härkki for his encouragement.

The experimental part and observation of blast furnaces in operation have been made mainly at Koverhar Steelworks of Fundia Wire Oy Ab and at Rautaruukki Steel Oy, both members of the Rautaruukki Group. I wish to thank Dr. Peter Sandvik and Dr. Veikko Heikkinen for their support during the work. Especially I would like to thank director Pertti Kostamo for his encouragement during these years. I would like to thank the personnel of Koverhar for their excellent work and support.

I wish to thank Mrs Kaisa Sirviö for supplying the large amount of chemical analyses needed and Mrs Anja Maaninka for her excellent help in microscopy.

Important samplings were made at the Experimental Blast Furnace of LKAB in Luleå, Sweden. I would like to express my gratitude to the management of Luossavaara-Kiirunavaara AB and especially to Dr. Lawrence Hooey and Mrs Anna Dahlstedt for their help during the test campaign.

I recall with gratitude the blast furnace co-operation committee and the former Corporate Research and Development organisation for the numerous fruitful discussion meetings.

Finally, I would like to thank my dear wife Kaarina for checking the language, for her patience, encouragement and support during the many years of this work.

Ekenäs, July 2003

Kalevi Raipala

CONTENTS

LIST OF SYMBOLS

A	Area
C_p	Molar heat capacity
C_S	Sulphide capacity
E	Modulus of elasticity
ΔG	Standard free energy
K	Equilibrium constant (in chapter 7.4 Overall rate constant)
L_S	Sulphur partitioning
N	Atomic fraction
O_{SL}	Solution loss oxygen
$\dot{Q}$	Heat flux/cross area
R	Gas constant
T	Absolute temperature
V	Volume
$\dot{V}$	Flow
a	Activity
d	Diameter
e	First order interaction parameter (Sub- and superscripts for components: i,j,k) wt-% reference state
f	Activity coefficient
g	Function
h_{th}	Distance between tap hole and bottom
k	Coefficient
l_b	Brick length
n*	Ash factor
$\dot{n}$	Molar flow (subscripts o = ore, c = coke, g = gas)
p	Pressure
r	Second order interaction parameter (Sub- and superscripts for components: i,j,k) wt-% reference state
t	Time
u	Heat content ratio
v	Velocity
α	Coefficient of linear expansion
η	Utilisation
λ	Thermal conductivity
θ	Temperature
ρ	Slag ratio

Other subscripts

HM	Hot metal
f	Flame
sat	Saturation
0	Initial

( ) Refers to slag component
[] Refers to metal
(s) Solid phase
(l) Liquid phase
(g) Gas phase

Abbreviations

BOF	Basic Oxygen Furnace
CCC	Centre Coke Charging
CRI	Coke Reactivity Index
CSR	Coke Strength After Reactivity Test
DCI	Deadman Cleanliness Index
DMT	Deadman Temperature
ERP	Extra heavy bottom oil
FEM	Finite Element Method
FR	Fuel Rate
LKAB	Luossavaara-Kiirunavaara Aktiebolag
MICUM	Coke strength index
SEM	Scanning Electron Microscope
SR	Slag Rate
TS	Sulphur Load
XRF	X-Ray Fluorescence
XRD	X-Ray Diffraction

1 INTRODUCTION

Blast furnace is the oldest (at least 700 years old /1/) but still the main method to produce molten raw iron, hot metal, for steel making and foundry purposes. New alternative processes are under development, but none of them has yet reached the same economy as the blast furnace, with same productivity and lower CO_2 emission. The blast furnace is a shaft furnace where coke and iron bearing burden are charged on the top and preheated gas is blown in from the lower part of the furnace. Descending iron oxides are reduced by the ascending gas and melted to form hot metal. The gangue minerals and coke ash melt to form slag. The molten products are tapped at certain intervals.

The blast furnace plant is a central part of an integrated steel works. It may consist of a coke plant, a sintering plant, one or more blast furnaces, a steel plant, a rolling mill, a power plant and an oxygen plant. Iron ore, pellets and coke can be bought for ore based steel making, but the blast furnace is essential for reduction of iron. In Fig. 1.1 the flow sheet of Koverhar plant is presented. Coke, oil and pellets are bought and continuous cast billets are the final products.

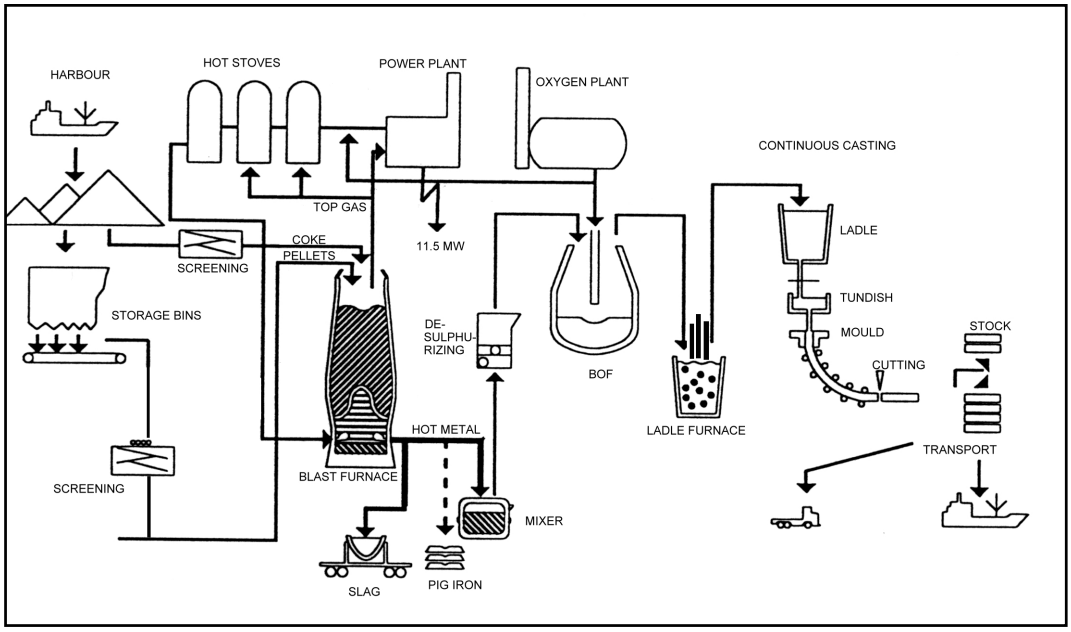

Fig. 1.1 *Flow sheet of Koverhar steel plant*

The customer of a blast furnace is usually a steel plant, sometimes a foundry. The steel plant needs a steady and sufficient supply of hot metal. The temperature must be high and the composition of hot metal stable. Required contents of certain elements can vary from plant to plant: some steelmakers want to have high carbon content, some higher silicon and some want to have desiliconized, desulphurized and dephosphorized pure iron.

The total quality of hot metal includes three main requirements: right composition, steady supply and total economy. In this presentation the focus is on the right composition without neglecting supply and economy. Physical and chemical conditions inside the blast furnace have a great influence on the three requirements. Economy does not include only raw materials but also production capacity, maintenance and capital. Most of the phenomena inside the blast furnace must be deduced from the measurements made from charged coke and ore as well as produced melts and gas because there are no sensors that could withstand the violent environment inside the furnace,

only thermocouples in the lining are available. The various (e.g. minutes, hours or weeks) time lags and time factors must be kept in mind when studying blast furnace phenomena. Deadman clogging and accretion formations are typical examples of slowly (during days and weeks) developing problems having a strong influence on total quality.

Adjusting the burden and thermal conditions of the process makes short-term control of hot metal composition. Certain elements are easily reduced. As it can be seen in Table 1.1, Cu, Ni, Sn, P etc. are reduced almost completely to the hot metal and choosing suitable raw materials is the only way to control them. In the table the missing fraction from 100 % means yield to slag. The heat level of the process controls silicon content. Sulphur content in hot metal is controlled by selecting raw materials and by controlling the slag basicity.

Table 1.1 *Typical yields of elements in production of basic iron (for BOF) in Koverhar*

Element	Yield to hot metal, %	Yield to gas phase, %
Fe	100	0
Mn	90	0
Cr	95	0
V	70	0
Ni	100	$<10^{*)}$
Co, Cu, Sn, As	100	0
Zn	0	1.0
P	98	0
S	10	5 - 10
F	0	1 - 2 /2/
Si	15	0
Ti	50	0
Ca, Ba, Mg	0	0
Al	0	0
K, Na	0	30 - 40

**) Escapes at low top gas temperatures as $Ni(CO)_4$ /2/*

Carbon content of hot metal has usually been taken as a more or less uncontrollable result of the melting process depending only on hot metal temperature and silicon content.

However, carbon content depends on several other factors and it can be controlled in desired direction as will be shown later. By applying certain simple rules and metallurgical thermodynamics, the total quality of hot metal can be maintained on high level.

Alkalies are considered to be troublemakers in the blast furnace process. They don't have a direct effect on hot metal quality, but indirectly they influence it by weakening coke strength, increasing fuel rate, building accretions on shaft walls, causing damage to hearth walls etc.

The campaigns of blast furnaces have grown longer during the last decades. The campaign length is usually calculated from a hearth lining to the next one. During the sixties and seventies a normal campaign lasted eight years. In the nineties the target was 15 years. Nowadays blast furnaces are designed to last 20 years or longer. There may be one or more intermediate overhauls in between including maintenance, some relining of the shaft and replacement of cooling elements. A proper hearth operation is essential in reaching long campaigns, e.g. 20 years. If the hearth operation is poor it may end in severe erosion of the hearth lining and shortening of the campaign. Poor hearth

operation also contributes to failing hot metal quality. Sulphur and carbon contents have strong interaction which may cause severe problems by clogging the hearth. Clogging can be triggered by many primary events. This vicious circle, resulting in low carbon and high sulphur content, not to mention total quality, will be explained later.

The main purpose of this work has been to find

- ✧ the factors influencing hot metal carbon content
- ✧ methods to control hot metal sulphur content and
- ✧ working methods to operate the blast furnace hearth.

Chapters 2-4 cover the blast furnace in general; its construction and operation briefly in order to understand the complexity of the process and its influence on hot metal quality. Chapters 5-8 deal with the author's experience and investigations of hearth operation, control of hot metal sulphur content and development of hot metal carbon content. Otherwise the source is given as reference.

2 BLAST FURNACE CONSTRUCTION IN GENERAL

2.1 Shaft

A blast furnace is a shaft furnace with an inner volume of 600 - 6000 m^3. The evolution of the furnace size during centuries from about 1 m^3 to 6000 m^3 has been restricted at first by blowing apparatus (bellows - piston blowers - turbines) and nowadays by coke crushing strength. The inner height of a charcoal blast furnace was typically 12 m and for a very large modern coke blast furnace the corresponding value is 33 m.

The furnace profile is a result of evolution, too. All heights, diameters and angles must be in certain relations to get an effective and long lasting blast furnace construction. When the height is restricted, the only way to increase the volume is to increase the diameters. As the penetration depth of the hot blast into the coke (raceway) is about 1.8 m and cannot be exceeded the passive volume in the middle of the furnace remains larger with an increased hearth diameter and the cohesive zone comes too close to the stock level. The burden in the centre of the furnace has not enough time to be reduced properly. The design of a blast furnace is based on experience, empirical formulas and scientific methods.

The gas offtakes are located at the furnace top. Usually there are four offtakes which are united 20 - 30 m above the top to a downcomer leading the top gas to the gas cleaning system.

The charging equipment is on the top of the furnace. The most common designs are the two-bell top (e.g. McKee) and the bell less top (Paul Wurth). A modern bell top includes movable armour. The burden, coke and ore are charged into the furnace through the charging equipment, which also acts as a gas seal. By using this equipment the materials are dumped in the furnace and distributed in a desired manner on the burden surface.

The steel shell is cooled with water circulating in stave coolers made of cast iron or copper. Hot blast is blown through water-cooled copper tuyeres located between the hearth and the bosh. The number of tuyeres depends on the hearth diameter. The distance between adjacent tuyeres is 1.5 - 2.0 meters. The blast is heated in hot stoves to 1000 - 1400 °C and distributed to the tuyeres. The number of stoves is usually three or four.

The hearth is lined with carbon bricks and sometimes completed with a so-called ceramic cup. (Fig. 2.1) Small furnaces have spray cooling on the hearth shell but larger ones have stave cooling inside the shell. As hearth phenomena are so crucial to the hot metal quality the hearth construction will be discussed more detailed in the following chapters.

2.2 Hearth geometry

The hearth height from the taphole to the tuyeres must be large enough to collect melted materials during the time between tappings. The hearth height is usually 4 - 8 m depending on the furnace size. The porosity of coke bed is taken to 0.3. The time between tappings for a single tap hole furnace varies from 30 to 90 minutes depending on tap hole clay properties.

The tap hole is an essential part of the blast furnace. It is 2 - 3 m long and it inclines 8 -12 ° inwards. In large furnaces the taphole number is two to four depending on size. In such furnaces

tappings are practically continuous - one taphole is always open and tappings from two tapholes are overlapping. The tap hole drill is used for opening the tap hole to cast the hot metal and slag. The hole diameter is chosen to get proper casting speed i.e. to get maximum slag time and good drainage of the hearth. The molten materials are led to the main trough where hot metal and slag are separated. The tap hole is closed with a clay gun.

The well depth from the inner end of the tap hole to the bottom is 20 % of the hearth diameter. The walls of the well part are inclined in order to minimize the coke free volume in the corner between the wall and the bottom.

A floating or slightly sitting yet not an inactive deadman (filling also the corners) gives the best conditions to an even flow through the deadman /4/. This may be achieved with

$$h_{TH} / d_H \geq 0.2 \qquad (2.1)$$

Where h_{TH} = distance between tap hole and bottom and
d_H = hearth diameter.

The hearth walls below the tap hole should have an inclination of 45 – 60 degrees.

2.3 Hearth cooling

In medium size and large blast furnaces the hearth walls are cooled with staves. The staves are inside the shell. The bottom is cooled with water pipes. Stave cooling keeps the shell clean and dry.

For small furnaces spray cooling is sufficient. The drawback of spray cooling is splashing of water and corrosion of the shell. Small and even medium size blast furnaces can have air cooling in the bottom.

Double jacket cooling is sometimes used to get rid of water splashing and to get closed water circulation. It may be dangerous if a hearth breakout occurs.

In large furnaces even heating of the middle part of the hearth bottom may be necessary.

2.4 Hearth lining materials

A state of the art is given by Kowalski et al. /4/. In the following only the most essential items are focused.

The usual carbon based grades are ‘common’ carbon, micropore carbon, super micropore, semi-graphite and graphite.

Carbon blocks are made of calcinated anthracite baked with tar at 1300 °C for one month.

Micropore grades are made of carbon blocks impregnated with tar in vacuum after baking and baked once again to reduce the size and number of pores. Some Al_2O_3 can be added to the base carbon mix. Impregnation reduces the number of pores greater than 10 µm thus preventing iron infiltration. Addition of Al_2O_3 prevents slag and iron attack.

In super micropore grades some metallic silicon and Al_2O_3 are mixed to the base carbon mix. Si_{met} has a strong effect on reducing the pore size.

Graphite blocks are made of carbon blocks by graphitizing them at 2400 - 3000 °C. Graphite blocks are used beneath the carbon layer to smooth out temperature gradients and to conduct heat to the side walls.

Semi-graphite products are made like carbon blocks by baking them at 1300 °C, but the carbon base is graphite. Hot pressed bricks are made of carbon or semi-graphite. These products have very low porosity and high thermal conductivity.

Ceramic materials used in composite designs are mullite (chamotte) and corundum with different type of bonding.

2.5 Hearth design

At present four main design types are dominating. The hearth lining can be very expensive, but because it must hold for 15-20 years, the price is of minor importance. The main materials are carbon-based blocks or bricks combined with high quality ceramics.

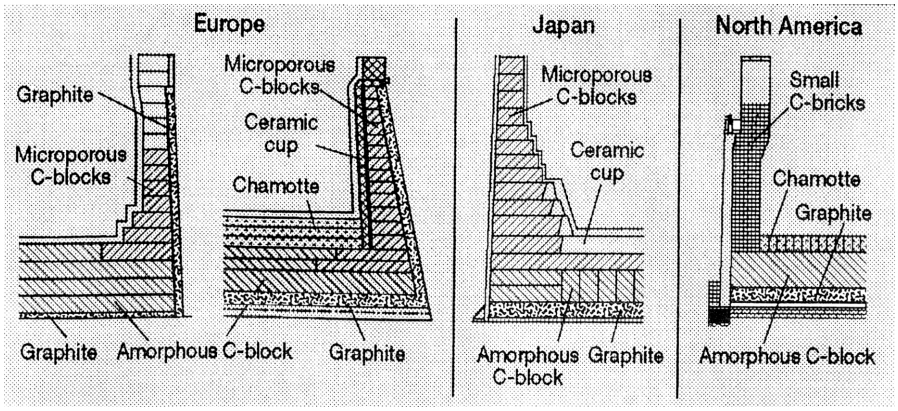

Fig. 2.1 *Typical hearth constructions /4/*

The most widely applied (European - Japanese) design could be called classic (Fig. 2.1). The lining is made of large, e.g. 500 × 500 × 2500 mm carbon blocks. The blocks are thoroughly machined and the lining glued with 0.5 mm joints. The gap between the lining and the shell is filled with carbon ramming mix to ensure good thermal conductivity. The hearth walls are lined with micropore or super micropore grade blocks. The lining at the tap hole area is made of super micropore blocks. The uppermost 500 - 1000 mm of the hearth bottom is made of ceramic material (ceramic plug).

In the North-American design the hearth walls are laid with small hot pressed carbon bricks and the bottom with large carbon beams. The bricks at the wall-side are glued to the steel shell in order to get good thermal conductivity between the shell and brick. The idea is to keep the inner surface cold to prevent carbon solution in the hot metal below the tap hole level or to promote slag solidification on the inner surface above the tap hole where solidified slag protects the carbon surface.

The ceramic cup is much like the classic, but it has somewhat thinner layers of carbon materials at the hearth walls and bottom. The inside of the carbon lining is covered with high alumina bricks. High alumina, cooled by carbon contact, withstands slag attack and solution to hot metal. The 850 °C isotherm (the brittle layer region) is moved in the ceramic part.
The ceramic cup extends the lifetime of the lining.

The thermal approach design is somewhat sophisticated /5/. Emphasis is placed on avoiding of thermal stresses in the carbon blocks:

$$\sigma = \frac{1}{2} \cdot E \cdot \alpha \cdot \dot{Q} \cdot \frac{l_b}{\lambda} \qquad (2.2)$$

Where σ = thermal stress
E = modulus of elasticity
α = coefficient of linear expansion
l_b = brick length
λ = thermal conductivity
$\dot{Q}$ = constant = (heat flux / cross area)

The thermal stress in the brick layer can be tolerable when l_b is short and λ high enough.

Semi-graphite is used in the sidewalls, graphite in the bottom and carbon beneath the graphite. The well has a ceramic plug. The wall bricks are carefully assembled with exactly calculated expansion joints in order to minimize thermal stresses and to prevent cracking during heating and operation.

To avoid solidification of iron at the hearth bottom a trade off must be made between cooling and refractory wear. Too effective bottom cooling extends the service life of the hearth bottom but increases the risks of solidification of the lower part of the deadman. A ceramic plug is a solution to this problem as well as heating of the bottom lining with steam instead of cooling it.

2.6 Hearth instrumentation

The hearth lining must be equipped with a sufficient number of thermocouples. It must be kept in mind that some thermocouples may fail during the years of operation. The thermocouples are laid in their places during the installation of the lining. The number and location of the thermocouples must be designed so that the calculation of the remaining lining thickness is possible. The number of the thermocouples can probably never be too large. When the furnace gets older many thermocouples may have failed, but the need to monitor the lining thickness and the deadman condition becomes more and more important. The thermocouples installed in a protection tube must be checked regularly to ensure the contact with the tube end wall. (Appendix 3)

In the bottom the thermocouples are easy to place between the block layers. In the sidewalls they are installed two by two to make it possible to calculate the remaining thickness of the lining. Heat flow sensors are also useful in hearth monitoring.

2.7 Hearth deterioration

The length of a blast furnace campaign depends on the durability of the hearth. Other parts of the furnace can be relined or replaced during a relatively short period of time but relining of the hearth takes so long that usually it will escalate to a complete revamp.

There are two main types of damage of the hearth lining:

1) A brittle layer in the middle of the side walls near the range of 850 °C isotherm. Five possible causes are presented:

   - ✧ Thermal stresses
   - ✧ Precipitation of carbon
     $2CO \rightarrow CO_2 + C$ (2.3)
   - ✧ Oxidation of zinc
     $Zn + CO_2 \rightarrow ZnO + CO$ (2.4)
   - ✧ Oxidation of carbon in the lining by water
     $H_2O + C \rightarrow H_2 + CO$ (2.5)
   - ✧ Precipitation of potassium compounds.

Zinc and potassium are always found in the brittle layer. Zn and K from raw materials are reduced in the lower part of the blast furnace and they are present as gas in hearth atmosphere, where p_{O2} is of magnitude 10^{-14} - 10^{-16} bar and temperature 1400 - 1500 °C.

Carbon monoxide is always present in the hearth atmosphere and water leakages from tuyeres or cooling elements into the furnace are common.

When the hearth linings have been excavated after blowing down the brittle layer has been observed. There is sometimes almost an empty 5 - 15 cm wide cylinder around the hearth with some porous relicts of carbon lining and sometimes it is filled with iron. Probably all these factors play their role in the lining deterioration.

2) Erosion of the sidewall and bottom below the taphole level. This is also called ”an elephant foot” or ”a mushroom” because of its curved shape. Erosion is caused by iron penetration into the pores of carbon block and dissolution of carbon to hot metal. Erosion proceeds at temperatures above 1150 °C, which is the liquidus of hot metal. Erosion is accelerated by temperature, low degree of carbon saturation and flow velocity of hot metal.

Hearth protection is of fundamental importance. Water leaks are the most common causes for lining damage and they must be repaired immediately. Erosion is more difficult to observe and prevent. Methods to monitor hearth operation and to prevent hearth damage are presented in the following chapters.

3 PHYSICAL ZONES IN BLAST FURNACE

3.1 General

It does not make sense to study hearth phenomena without considering the fundamentals of the whole blast furnace process in the furnace. Phenomena in the hearth depend greatly on events in upper zones and vice versa. Therefore all processes above the hearth must be considered. In short, the hearth is controlled by burdening and by blast parameters. Of course the thermal state and slag properties are of great importance.

When heat and mass transfer phenomena are studied it is convenient to divide the blast furnace in chemical and thermal zones (Fig. 3.1). Constructional parts of the blast furnace are presented in Fig. 3.2 and the zones of the burden in Fig. 3.3.

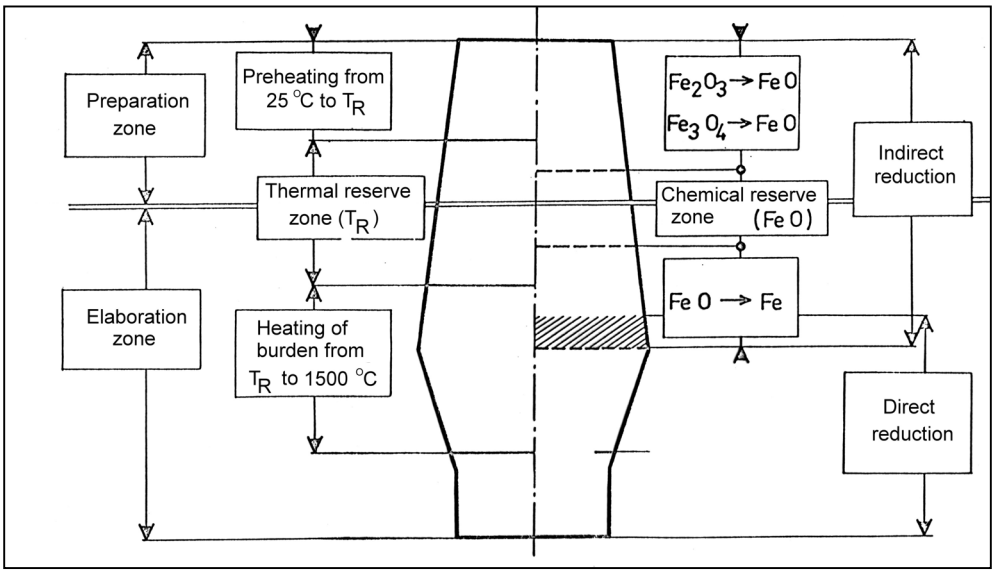

Fig. 3.1 *Chemical and thermal zones /56/*

All chemical reactions are strongly dependent on heat transfer between gas, solid and liquid. The heat content ratio u of counterflowing solid and gas must not exceed a certain value /6/.

$$u = \frac{\dot{n}_o \cdot C_{p,o} + \dot{n}_c \cdot C_{p,c}}{\dot{n}_g \cdot C_{p,g}} \qquad (3.1)$$

where u = heat content ratio

$\dot{n}_o, \dot{n}_c, \dot{n}_g$ = molar flows of ore, coke and gas

C_p = molar heat capacities of ore, coke and gas.

If a certain limit of heat content ratio (e.g. 0.9) is exceeded the preheating of the burden will be delayed and consequently also all chemical reactions lower in the shaft resulting in serious disturbances, e.g. a chilled hearth. The distribution of gas and solids along the shaft radius is not uniform. The gas flow is stronger compared to burden in the centre and close to the walls. There u is very low (e.g. 0.4). At the mid radius of the shaft u is close to ideal because the burden materials

are charged more to the wall side and their main movement is towards the raceways. That is why the u value calculated to the whole cross section of the shaft cannot be ideal (u=1).

3.2 Preparation zone (lumpy zone)

The burden must be placed on the solids surface, stock level, in a desired pattern e.g. by using movable armour or rotating chute. The distribution of ore/coke determinates the gas distribution. The first thing happening to the burden after it has been dumped into the furnace is evaporation of its moisture. If the material temperature is below the freezing point the heat of fusion must be taken into consideration. When the material is dried its temperature will rise rapidly and the reduction of iron oxides starts at about 400 °C.

At about 950 - 1000 °C there is a so called thermal reserve zone where the temperatures of gas and solid are close to each other and heat transfer from gas to solid is minor. From the chemical point of view there exists also a chemical reserve zone where the indirect reduction of wüstite is close to equilibrium and thus the reduction rate is slow.

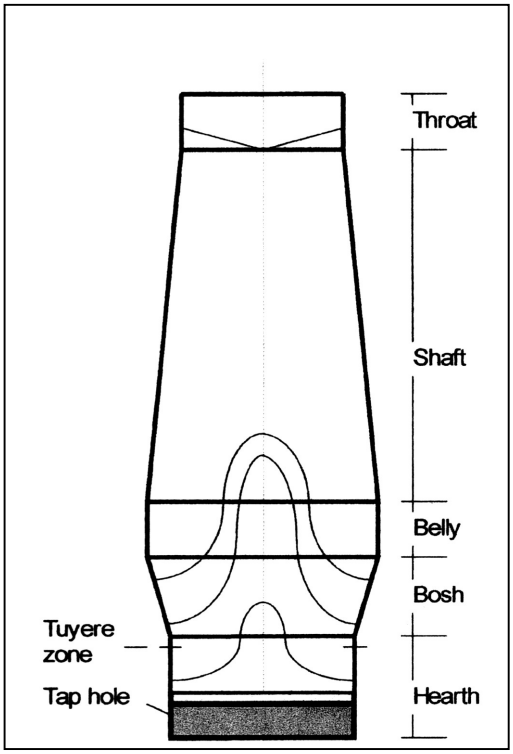

Fig. 3.2 *Parts of a blast furnace*

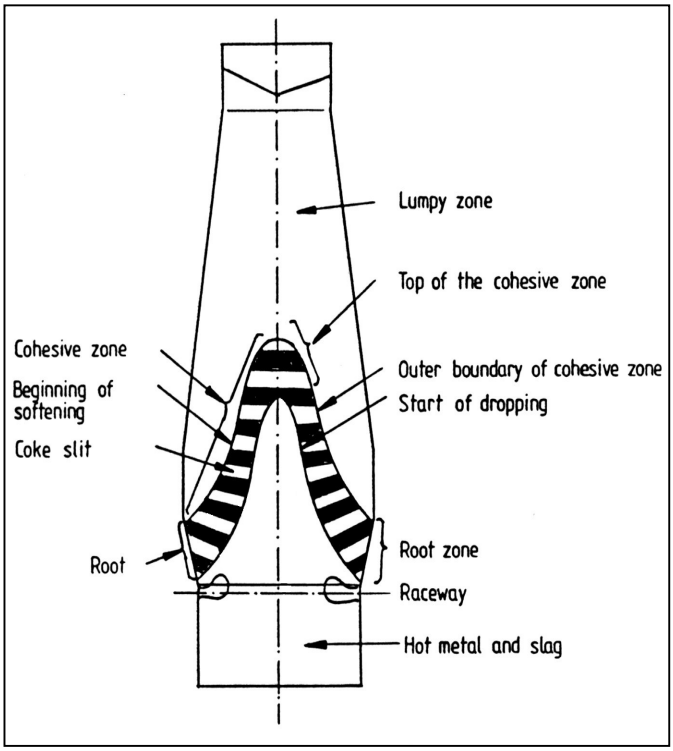

Fig. 3.3 *Zones of a blast furnace*

From 1000 to 1500 °C the temperature rise is rapid. Reactions between certain slag components start already in solid state. The cohesive zone begins where the reduced ore particles start to stick together. The sticking proceeds and the metal and slag phases separate. The metal phase dissolves carbon, silicon and sulphur from the gas phase and melts at about 1350 °C.

3.3 Cohesive zone

Dissections of blast furnaces have shown, that the shape of the cohesive zone (Fig. 3.3) is usually like V upside down /9/. W and L (Λ) are common, too. The cohesive zone penetrates coke and ore layers so that the softened and compressed ore layers form doughnut shaped rings leaving coke slits (”windows”) between them. The diameter of the rings is largest in the bosh diminishing upwards. The layers touching the furnace walls make the root. The root must always lie towards the bosh walls. In other words, the cohesive zone is a continuously regenerating vault that bears the weight of the burden leaving the active coke layer without pressure from overlying material.

The coke windows, slits, act as gas distributors. Therefore the coke and ore must not be mixed. In the outer edge of an ore ring the material is softening. The iron particles are stuck together and the slag phase is squeezed out. The composition of this primary slag is far from the final slag and very inhomogenous except when only self-fluxing sinter is used. The primary slag is usually rich in FeO depending on the local reduction degree. The fresh reduced iron adsorbs carbon, sulphur and silicon from the gas phase and melts from the inner side of the ring.

Controlling the cohesive zone shape is one of the most important tasks in the blast furnace operation. The shape has a crucial influence on the fuel rate, gas distribution, burden movement, and chemical reactions and hearth operation. The shape is controlled by burden distribution (ore/coke distribution and burden material size distribution). The raceway shape has a certain influence on the root part of the cohesive zone, but control actions should be only local and temporary. A more permanent effect of the raceway shape is caused by the deadman if it is large and impermeable. Then it bends the raceway upwards and steers the hot gas flow towards the bosh wall. This will cause a hanging cohesive zone (Fig. 3.4 (b)), which in turn transfers unreduced FeO to the slag resulting in poor desulphurization. Large amounts of injected fuel have a similar effect causing hanging cohesive zone.

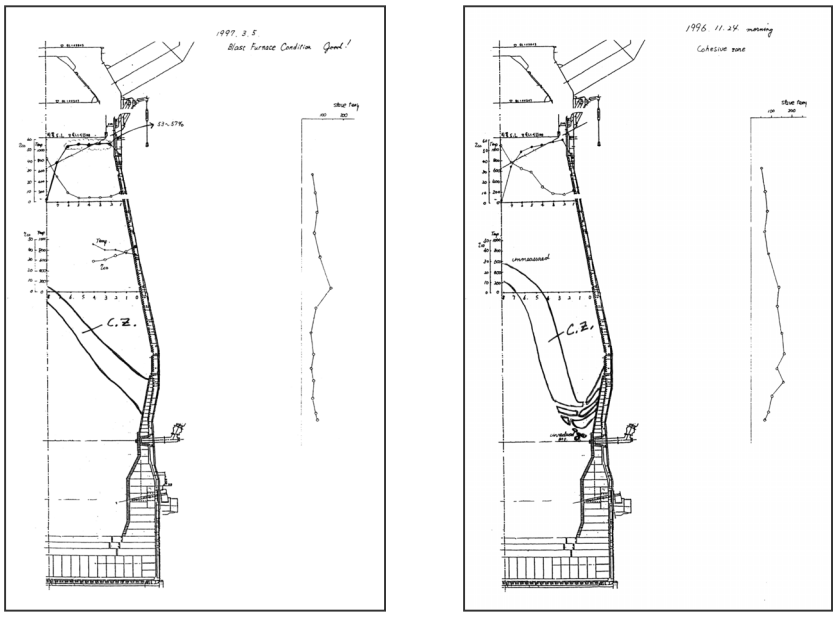

(a) (b)

Fig. 3.4 *The shape of the cohesive zone: (a) normal shape and good operation. Stave temperatures on the right side of the figure. (b) Hanging cohesive zone and poor operation. /8/*

3.4 Active coke layer

Between the deadman and the cohesive zone coke is flowing down and towards the raceways. Coke lumps are partly fluidized and flow freely down. If the clearance between the deadman and the cohesive zone is too narrow coke can not flow and the burden slips (Fig.3.5) /9/.

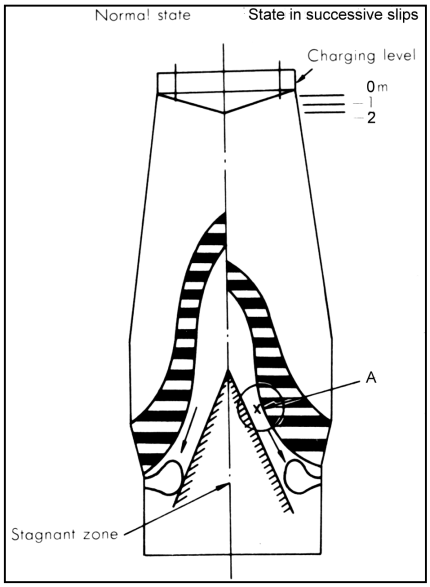

Fig.3.5 *Narrow section in active coke layer /9/*

When the burden slips the charging pattern is out of control because the charging level is lower than during a normal filling when new material is charged. This kind of disturbance is self-repeating if not corrected. Common actions are charging of extra coke, reducing the blast volume slightly and adjusting the filling pattern. Narrow section occurs frequently with the hanging cohesive zone.

3.5 Tuyere zone

In the tuyere zone hot blast penetrates through the tuyeres into the coke creating physical combustion zones - raceways. The raceway is normally a 1.5 – 2.5 m long cavity with a shape reminding of an upward bent pear. In the raceway the carbon in coke and injected materials react with oxygen in several steps resulting in bosh gas consisting of CO, H_2, N_2 and minor amounts of SiO, H_2S, COS, Ar etc. The physical heat of hot blast and the oxidation of carbon are the main sources of heat in the blast furnace process.

In the raceway cavity coke lumps circulate with high speed and are consumed by oxidation. When the coke has been reduced to a smaller size it is pressed towards the cavity wall by the dynamic pressure of the gas and new large coke is fed in the raceway via the active coke layer. CO_2 and H_2O consume the coke fines in the raceway atmosphere. The bottom of the raceway contains a lot of coke fines because of gravity and weaker gas penetration.

The raceway ends to the deadman. The deadman controls the length and shape of the raceway. If the deadman is loose and permeable, the raceway can reach its normal length, but if the deadman is solid, the raceway shortens and bends strongly upwards. (As mentioned in paragraph 3.3)

Other common rules are linked to oxygen enrichment and injection via tuyeres:

An increase in the oxygen content of the blast makes the raceway longer if no compensating control actions are made: There are more oxygen moles in the blast per time unit reacting to two moles of CO thus increasing the number of gas moles per time unit. The flame temperature gets also higher with increased oxygen. As a result the real volume of tuyere gas increase as well as its velocity and penetration depth. An increased injection rate of oil or coal powder moves the hottest point of the raceway towards the tuyere nose. The latter rule coincides probably with the soot formation, the inactive deadman and the hanging cohesive zone. This item will be discussed later in chapter 5.3.2.

The flow of molten slag and metal avoid the gas stream from the tuyeres and trickle down mainly through the space between the tuyeres.

3.6 Hearth

The hearth is mainly filled with coke. Molten iron and slag are collected in the empty spaces between the coke lumps and tapped out through the tap hole at certain intervals. Slag floats on the iron and iron droplets trickling down from the melting zone sink through the slag layer to the bottom. A major part of the reactions between the slag and the iron take place at this stage when the contact area between the slag and the metal is large compared to the stagnant slag area between the slag and metal layers. The coke in the middle of the hearth is more or less compact forming the so-called deadman. The coke between the deadman and the hearth walls is more loosely packed.

In a well working hearth iron and slag can flow straight through the coke bed towards the tap hole. If the deadman is clogged the hot metal quality fails and the campaign life of the hearth lining will be reduced. These phenomena will be discussed more detailed in the following chapters of this work.

4 DEADMAN

The hot metal quality and the blast furnace operation are strongly dependent on the hearth conditions. These conditions depend on burden distribution, cohesive zone shape, blast parameters, slag formation, cooling intensity and many other factors. In short, the deadman has an influence on all the zones above it.

The hearth of the iron blast furnace is a challenging object of research because of the extreme conditions. There are no sensors, which can operate continuously in an environment like in the hearth. Therefore all measurements must be made outside the hearth itself and the conclusions are based on these results.

4.1 Physical conditions

In the middle of the hearth, the tuyere zone and the lower bosh there is a space where coke descends with a strongly reduced velocity. Coke is relatively densely packed with a porosity of about 0.35 in this volume. This formation is called a deadman. Under normal operation of a blast furnace the deadman floats in hot metal and touches the bottom lining slightly in the middle or it fills the hearth completely but is loose packed. Anyway, the hot metal can flow straight towards the tap hole also from the opposite side of the hearth. The deadman reaches up to the upper bosh. The inclination from the top towards the tuyeres is about the same as the natural angle of repose for coke. The raceways are not interconnected and the space between them is filled with coke of different grain size. The coke properties in the hearth have been studied especially in dissected blast furnaces, Fig. 4.1 /10/.

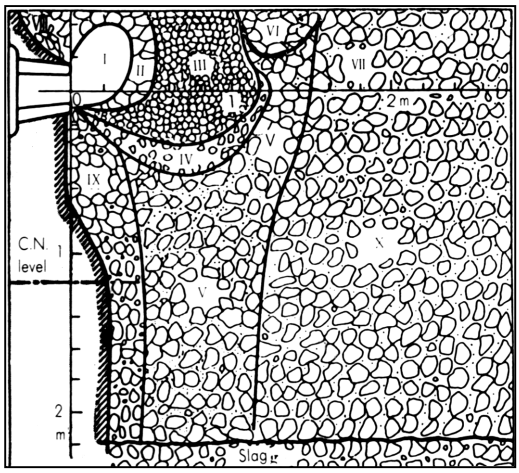

Fig.4.1 *Raceway and Hearth Conceptual View /9/*

I: Raceway cavity
II: Large coke lumps from active coke layer, circulating and burning
III: Small size coke packed in the back end of the raceway, oxidised by CO_2 and H_2O from the raceway
IV: Black fine-compacted layer (consisting of graphite, metal, slag and small lump coke), -"bird's nest"
V-VIII: A portion consisting of fine grains (under 5mm) and large lump coke. This coke moves relatively fast down by being dissolved in hot metal
IX: Medium-size, slowly moving round coke
X: Coke located in the hearth centre, the deadman

The bottoms of the raceway cavities (called “the bird’s nest“) have been found beneath the tuyere zone at a relatively constant distance from each other telling about regular sudden increase in descending velocity - apparently caused by tappings (Fig.4.2).

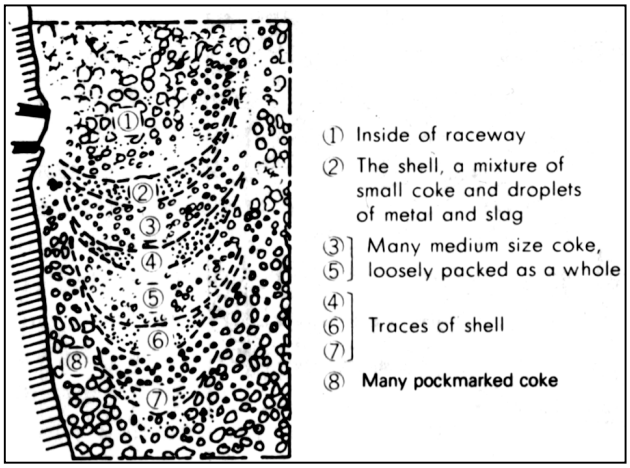

Fig.4.2 *”Bird's nest” observed from Kawasaki 2BF and 3BF /10/*

4.2 Function of deadman

4.2.1 Normal deadman

The renewal of deadman coke proceeds mainly by dissolving in hot metal and also by reaction (4.2) with FeO in the slag. According to an old rule of thumb, the renewal is estimated to take about four weeks.
Data from a tracer (radioactive Sc_2O_3) test gives more detailed information as can be seen from Table 4.1:

Table 4.1 *Replacement Period of Dead Coke Zone Measured with Radioactive Coke /9 /*

Test	Changing position of radioactive coke			Period before detection
1	Periphery	1.5 m from wall	Tuyere level	almost 10 h
2	Periphery	1.7 m from wall	Cinder notch level (1.2 m below tuyere level)	2.5 days
3	Midway	3.6 m from wall		18.5 days
4	Centre	7.9 m from wall		15.5 days

From this data the following conclusions have been made:
1) Coke in the peripheral zone is consumed in 2 - 3 days due to larger hot metal flow dissolving coke carbon.
2) Coke in the middle zone is consumed very slowly - during 15 - 19 days / 9 /

Even longer lag times have been reported. When the hearth coke is renewed and the porosity between coke lumps increases, the slag starts to run out earlier than with clogged coke (the slag ratio (4.1) increases). In Sollac the time delay of change in coke stability (I40 index) on slag ratio has been 6 weeks /59/ indicating elimination of clogging. For the same reason hot metal flows more at the wall side of the hearth when the centre is clogged and the heat loads are higher

compared to operation with open centre. A decrease in cooling losses have been observed after 9 weeks of adapting more stable coke /11/.

$$\text{slag ratio} = \rho = \frac{\text{slag tapping duration}}{\text{total tapping duration}} \tag{4.1}$$

The time for renewal depends also on the shape of the cohesive zone. For a V-shaped cohesive zone the coke in the centre is consumed faster and floating up towards the raceway also renews the coke in the periphery. This kind of cohesive zone is formed when the production rate of the furnace is strongly reduced. An old rule of thumb states the descending speed of hearth coke to 1 m/day.

Another carbon consuming reaction occurs with FeO in molten slag

$$FeO + C \rightarrow Fe + CO \tag{4.2}$$

This reaction takes place in the slag layer and above it. Sunahara et al./12/ made a study on deadman coke degradation by unreduced FeO in molten slag. Their conclusion was that the effect of disintegration caused by reaction with FeO in the slag couldn't be ignored for the disintegration behaviour of the deadman coke. Reaction (4.2) does not depend on CRI.

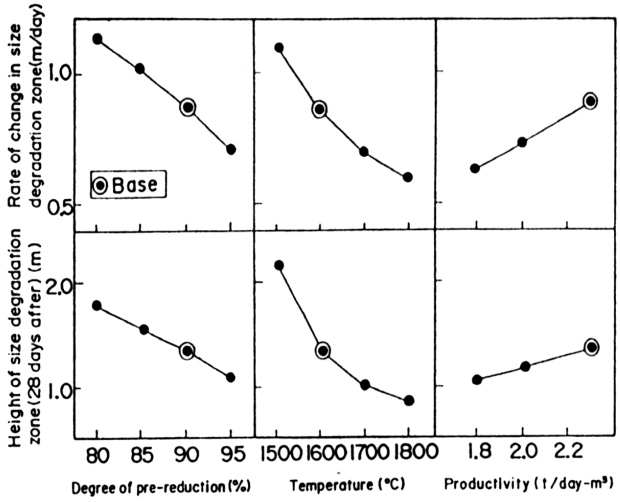

Fig. 4.3 *Influence of operation conditions on coke degradation /12/*

Model calculations based on experimental results show clear dependence on operation parameters: low degree of pre-reduction, low temperature and high productivity promote coke degradation as shown in Fig. 4.3.
The importance of coke properties becomes more stressed with high injection rates and large furnace volumes (as will be described in chapter 5.3.1) /13/

4.2.2 Floating deadman

A floating deadman is a common phenomenon. Saxén's group has investigated deadman porosity and floating phenomena /14,15,16,17/. Floating occurs when the buoyancy of the submerged coke encumbers the descent of burden material.

The floating of the deadman can be anticipated when the charging frequency and gas utilisation decrease before tapping. Slag delay (=total tapping time - slag tapping time) can be modelled rather well (Fig. 4.4) and further on it may be deduced if the deadman is sitting or floating (Fig. 4.5) /16/.

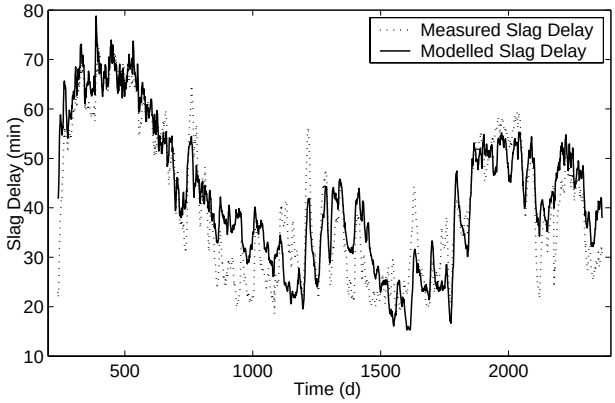

Fig. 4.4 *Modeled and measured slag delay at BF2 in Raahe /16/*

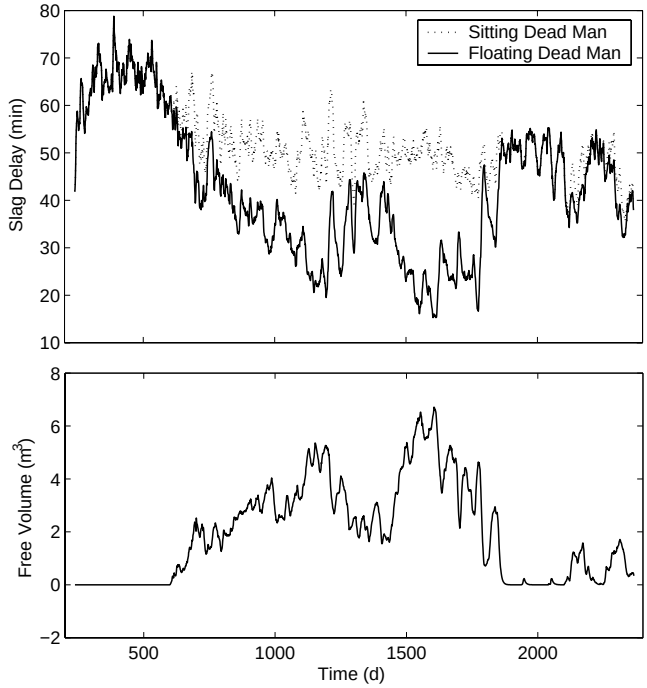

Fig. 4.5 *Upper figure: modelling of sitting and floating deadman as in Fig. 4.4. Lower figure: free volume if the deadman floats /16/*

Floating has desirable features but also some disadvantages. If the deadman floats it is not stuck to the cold bottom and it will sooner or later open and become active if it has been clogged. The negative effect is unsteady burden descent, which disturbs burden distribution and gas utilisation.

4.2.3 Inactive deadman

If the deadman becomes clogged it will cause poor hot metal quality, irregular burden descent, abnormal hearth erosion (so-called elephant foot) etc. These phenomena will be discussed later. An inactive deadman is caused by different factors, e.g. low coke strength, low production rate, too long maintenance stop, water leakage into the furnace, improper burden distribution, hearth construction, hearth erosion, peeling scaffolds etc. All these factors are significant.

An inactive deadman is "sitting" on the hearth bottom and usually not floating in the hot metal. It is perhaps more common in large blast furnaces but occurs also in smaller ones - depending on construction and operation. The coke in the deadman is closely packed and the space between coke particles is filled with coke breeze, solid metal, solid slag and unreduced ore. Calcined lime can also be found if it is used in the burden /8/.

Heat to the deadman is carried by dripping hot metal and slag. Heat is flowing out through the hearth wall and bottom cooling. Heat is also consumed by reaction (4.2). When the deadman has become inactive it is very difficult to get heat into it and melt the solidified slag and metal because the deadman is like a solid rock in the middle of the hearth. Hot metal and slag cannot trickle through it so they flow along the crust down to the active cylinder shaped part of the hearth. The operating part of the hearth is thus strongly reduced.

In some blast furnaces there are special tuyeres for a probe for sampling and/or temperature measurement. These measurements show the thermal state of the deadman. The deadman is inactive if the temperature is below 1400 °C, down to 1200 °C and even lower /11/. In a normal deadman the temperature is above 1400 °C, up to 1700 °C at the tuyere level.

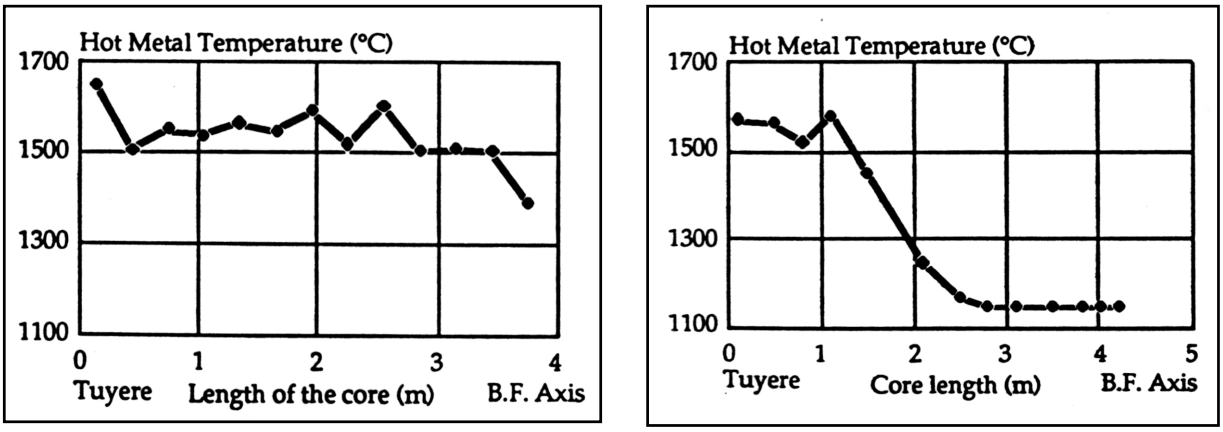

(a) (b)

Fig. 4.6 *Measured temperatures from tuyere nose to furnace axis. (a) Normal deadman and (b) inactive deadman /11/*

5 OBSERVATIONS AND INVESTIGATIONS ON HEARTH PHENOMENA AND HOT METAL COMPOSITION

The theme of this chapter is to explain methods to monitor the deadman and to control the hearth operation in order to get high quality hot metal with high carbon content. Hearth control needs patience because it may take weeks or even months to get response to control actions.

New kinds of problems have appeared with higher rates of oil injection:

- ✧ Disposition to clogged hearth
- ✧ High sulphur content in hot metal
- ✧ Low carbon content in hot metal.

The complexity of challenges can be disentangled piece by piece. The essential factors are discussed later in chapter 8 and this vicious circle will be illustrated in Fig. 8.1. A clogged hearth is a synonym for an inactive deadman. Also large slips and peeling scaffolds are potential problem makers.

5.1 Measurements in blast furnace hearth

The simplest measurement is the rod test. A 25 mm diameter steel rod is led trough tuyere peephole to measure the length of the raceway - from the tuyere nose to the back wall of the raceway. At the same time a trained operator can determine whether the back wall is soft or hard. This kind of measurements have been carried out in Koverhar since 1995. The method itself is older /12/.

Shortening of the raceways can be observed by the rod test when the deadman becomes inactive. This is a simple test and very reliable. The surface of a fully developed inactive deadman is rock hard and cannot be penetrated with the test rod using human force.

Numerical calculation of 1150 °C isotherm is calculated with FEM method and used in Koverhar /46/. Totally 47 thermocouples in the bottom and the hearth walls (Appendix 3) are used in the calculation. The 1150 °C isotherm is calculated once a day. It gives valuable information about the scull thickness in the hearth. A certain scull thickness is desired, because the scull protects the carbon lining from erosion. The scull thickness itself does not reveal a clogged hearth, but if the thickness in the middle of the hearth grows remarkably it is a warning signal.

> Calculation of hearth condition is made every morning on base of 47 thermocouple readings. FEM method is used. On the display (Fig. 5.1 and 5.2), for the upper figure, the section across the hearth can be selected (10 sections). The red area represents the remaining original lining (the minimum 1150 °C isotherm is always saved and used as "remaining"). The actual 1150 °C isotherm is then calculated using 24 h averages. The green area between actual 1150 °C isotherm and the red area represents the scull (salamander).
> The second figure on the display is an axonometric presentation of the 1150 °C surface. This figure can be rotated and tilted by using the slide bars on the right side of the display. The yellow-blue colouring presents scull thickness.

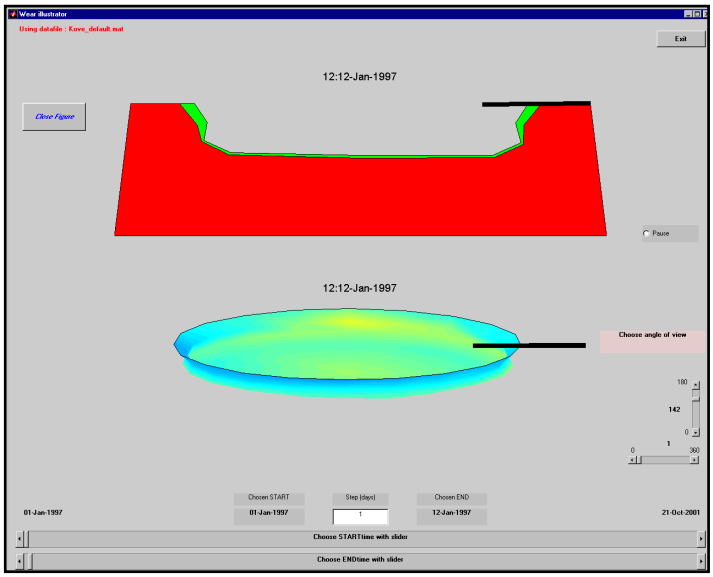

Fig.5.1 *Hearth monitoring 12-Jan-1997. Two years after relining. (Red = original lining, green = scull, black = tap hole location, blue-green = axonometric illustration of inner surface)*

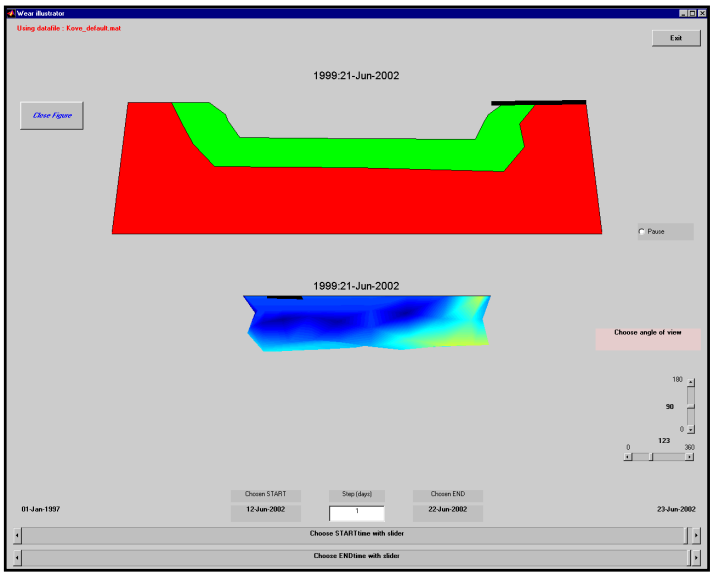

Fig. 5.2 *Hearth monitoring 21-Jun-2002. Seven years after relining. Some erosion and thick scull formation - but no inactivation of the deadman.*

5.2 Identification of inactive deadman

The inactivation of the deadman can be identified from at least the following symptoms:

- ✧ Temperatures in the hearth bottom decline
- ✧ Hearth wall temperatures increase
- ✧ Oxygen potential (FeO and MnO in slag) increases resulting in decreased desulphurization of hot metal
- ✧ Hot metal carbon decreases
- ✧ Slag tapping ratio (4.1) decreases
- ✧ Hot metal temperature is higher than usual with the same energy consumption and hot metal composition
- ✧ Shortening of the raceway can be observed
- ✧ Back walls of the raceways are hard (rod test)
- ✧ Shortening of the tap hole.

5.2.1 Bottom temperatures

Temperatures in the blast furnace bottom are clear indicators of the hearth circumstances. The only source of heat to the bottom is hot metal. The heat sinks are bottom cooling (air cooling or water pipes) and wall cooling (staves or spray cooling).

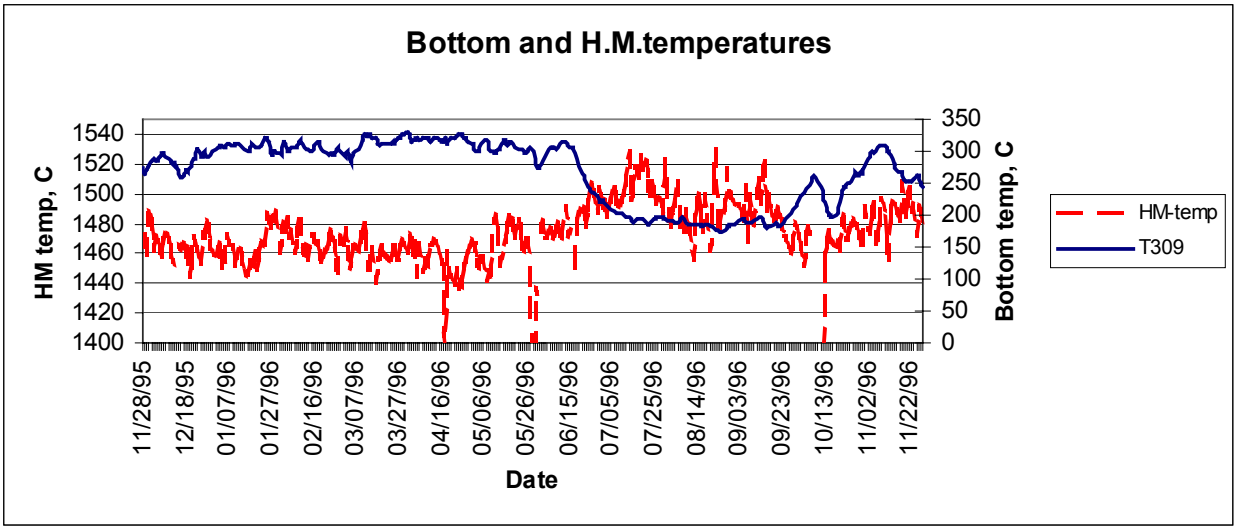

Fig. 5.3 *Typical inactivation, steadily decreasing bottom temperatures, starting on June 16 1996. Temperatures in bottom lining at point T309 (see Appendix 3) in Koverhar blast furnace. At the same time the hot metal temperature starts to rise.*

The thermocouples are located 1 to 3 m from the hot surface. That is why their readings are low, between 50 and 700 °C and also the time lag is in a magnitude of hours. Metal flow in the hearth can be simulated by numerical methods /14/. Depending on the geometry of the hearth and the shape of the lower part of the deadman, hot metal must flow in different ways to the tap hole. If the lower part of the deadman is floating and the coke is loose hot metal can flow under and through the lower part. This results in higher heat transfer to the bottom bricks and the steady state temperatures are higher in the bottom blocks, i.e. the 1150 °C isotherm lies deeper in the bottom lining. Typical inactivation with increasing hot metal temperature and steadily falling bottom temperature is shown in Fig. 5.3.

When the deadman is "sitting" on the bottom and the space between coke lumps is blocked by coke breeze and/or other solids hot metal cannot flow through the hearth centre. Hot metal must flow to the tap hole near the hearth walls. Consequently heat transfer to the middle of the bottom stays on a lower level and lower thermocouple readings are observed when the 1150 °C isotherm is rising.

5.2.2 Wall temperatures

A rise in the wall temperatures is sometimes observed at the same time as the bottom temperatures decline. When hot metal cannot flow through the furnace bottom centre it flows to the tap hole along the corners at the hearth walls. Heat transfer to the wall lining is higher. This circumferential flow of hot metal is detrimental to the hearth wall lining resulting in serious erosion - a so called elephant foot.

5.2.3 Desulphurization

Under normal operation conditions (slag basicity, fuel rate, burden distribution, reduction etc.) the sulphur partition lies on a certain level, e.g. 40 - 60. When the deadman becomes inactive, contents of FeO and MnO in the slag increase indicating increased oxygen potential and the sulphur partition declines. This phenomenon will be discussed later on.

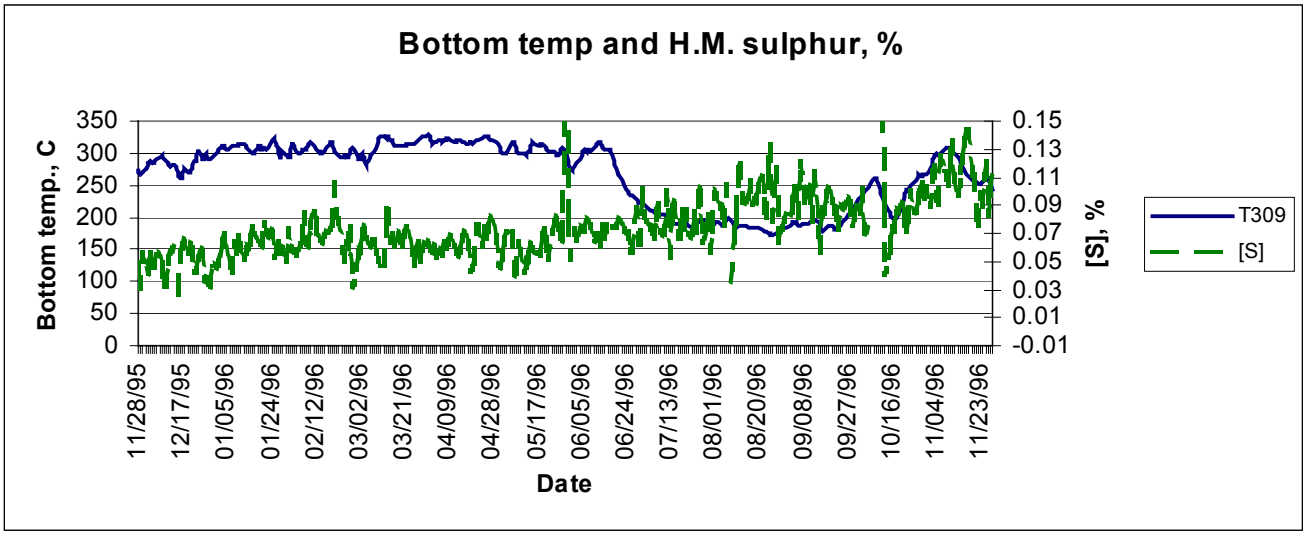

Fig. 5.4 *Hot metal sulphur during a typical inactivation on June 16, 1996. Temperatures in bottom lining at point T309 (see Appendix 3) in Koverhar blast furnace.*

5.2.4 Hot metal carbon

Hot metal carbon declines when sulphur increases - even though hot metal silicon and temperature remain on the normal level. This phenomenon will be discussed later in detail in chapter 7.

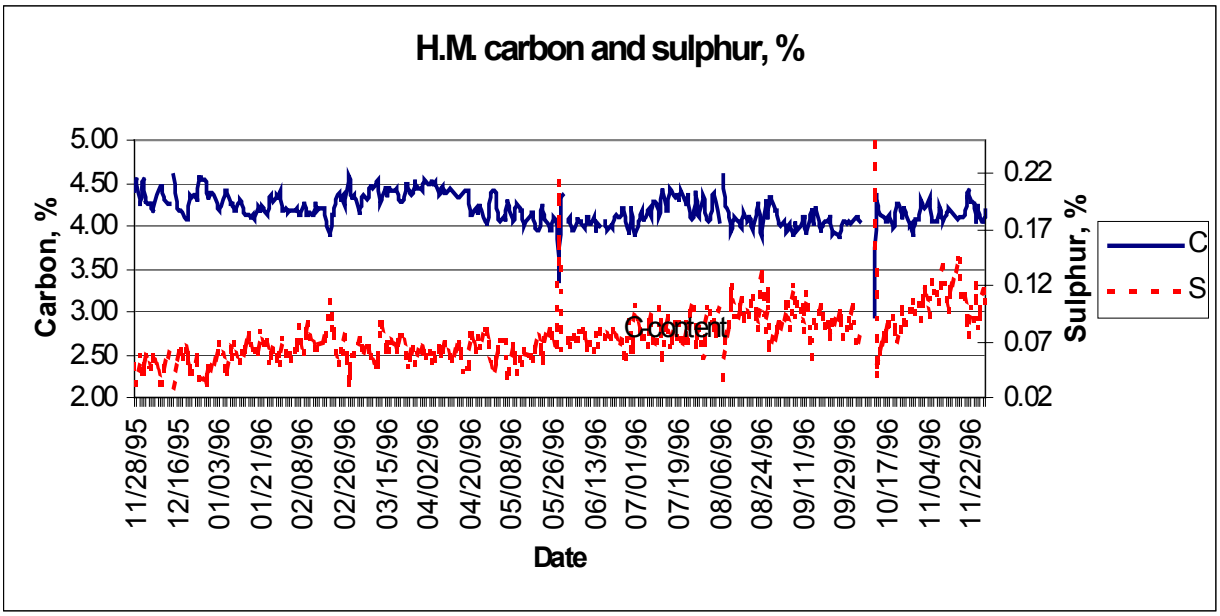

Fig. 5.5 *Hot metal carbon and sulphur during the inactivation on June 16, 1996 in Koverhar blast furnace.*

In Fig. 5.5 some kind of dependence of carbon content on sulphur content can be seen, but during October 17-November 20 1996 when the deadman was activated again this dependence was not as clearly observed as usually (Fig. 5.6). The reason is not known.

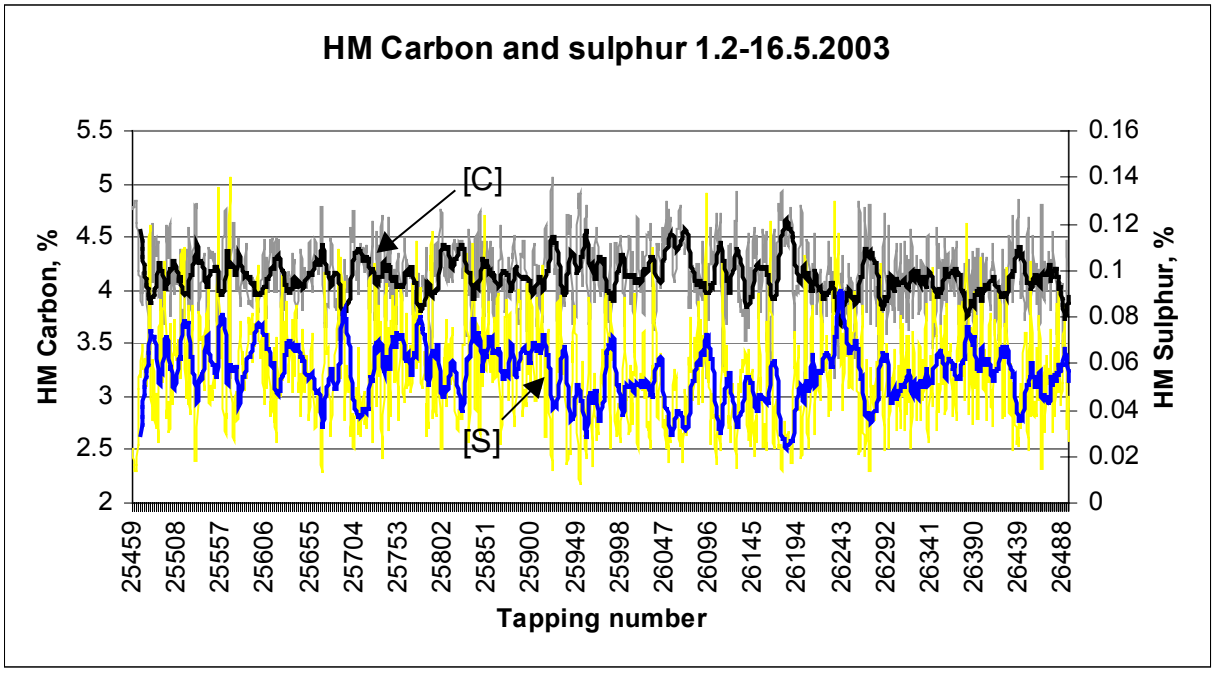

Fig. 5.6 *Hot metal carbon and sulphur contents in February - May 2003*

5.2.5 Slag ratio

Declining slag ratio is a clear consequence of an inactive deadman. Molten hot metal, slag and coke fill the space between the hearth walls and the inactive deadman. Because this space is narrow the slag/metal interface area becomes smaller and the slag flow is delayed (like in a chemist's separating funnel). The slag tapping time is quite short and the simultaneously tapped amount of hot metal relatively small. The amount of remaining slag in the hearth grows to a higher level due to rapid slag tapping.

5.2.6 Hot metal temperature

During a normal operation the molten metal below the tap hole level is cooled by conduction. Heat flows to the bottom and wall cooling systems. During tapping this cold metal is mixed with hot newly melted metal resulting in a certain hot metal temperature.

When the deadman becomes inactive a great part of the bottom metal is solid and cannot mix with the fresh hot metal. As described above, freshly melted hot metal is collected in the space between the deadman and the hearth walls. Mainly hearth walls cool this hot metal and the contact area is smaller in this case compared with the cooling from the hearth walls and bottom, resulting in a smaller temperature drop in hot metal. In this case the silicon content of hot metal and fuel rate remain practically unchanged but the hot metal temperature becomes higher. This rise in the hot metal temperature can be clearly seen in Fig. 5.3.

5.2.7 Deadman cleanliness index (DCI)

A widely discussed method to monitor the hearth condition is the Deadman Cleanliness Index, DCI. It has been developed by Nightingale et al. in Port Kembla, Australia /18,19/.
DCI is calculated as follows:

$$DCI = \theta_{HM} + \frac{[\Delta C]}{2.57 * 10^{-3}} - (1430 - 190 * (1.23 - (CaO)/(SiO_2))) \qquad (5.1)$$

Where $[\Delta C] = [\%C]_{sat} - [\%C]_{actual}$ and

$$[\%C]_{sat} = 1.3 + 2.57*10^{-3} \cdot \theta_{HM} - 0.31 \cdot [\%Si] - 0.33 \cdot [\%P] - 0.4 \cdot [\%S] + 0.028 \cdot [\%Mn] \qquad (5.2)$$

θ_{HM} = temperature of hot metal, °C

Expression (5.2) is the same presented by Neumann et al. /39/.

DCI indicates "the reserve range" of liquid hot metal and slag. The two first terms indicate the distance of hot metal from carbon saturation and the third term indicates the freezing and clogging property of slag (distance from liquidus temperature).
Attempts to control the hearth operation in Koverhar by using DCI as an indicator were not successful. When DCI was high the hearth operation was poor or the hearth got clogged.

Table 5.1 *Comparison of operating philosophies at Port Kembla and Koverhar*

	PORT KEMBLA	**KOVERHAR**
Low hot metal temp. High hot metal temp.	controlled controlled	tolerated desired
Low [Si] High [Si]	not so bad not good	controlled controlled
Big ΔC (≈ low [C]) High [C]	good not good	not good good
Low [S] High [S]	problem if < 0.010% not a problem	good not good
TARGET	High ΔC to ensure dissolution of coke fines. This keeps the deadman open.	High C-content and low S-content. Deadman control by CCC*) and coke CSR**)

**)* *CCC = Centre Coke Charging (method to charge only coarse coke in the middle of the furnace axis)*

***)* *CSR = Coke Strength after Reactivity test*

The difference between the works is mainly in raw materials and requirements of the steel plant. The difference in operating philosophies is presented in Table 5.1.

Another question is the ΔC hypothesis. This is certainly true for dripping hot metal below the cohesive zone. But if ΔC is still high in tapped hot metal it means that the ability of hot metal to dissolve carbon from the hearth coke has not been utilised, thus indicating deficient functioning of the hearth including the deadman.

5.3 Causes of inactivation

5.3.1 Coke properties

Coke properties play a central role in the deadman condition. The first important properties are cold strength (i.e. MICUM) and particle size. Coke particles are disposed to mechanical stress in the shaft and in the lower part of the blast furnace. Large and strong coke results in larger particle size and less fines in the hearth.

Coke lumps are weakened in the shaft by solution loss reaction:

$$C + CO_2 \rightarrow 2\ CO \qquad (5.3)$$

Tendency to this reaction is measured with the CRI/CSR test originally developed by Nippon Steel. The rate of reaction (5.3) depends on time, temperature, pressure, coke texture and amount of direct reduction.

CRI-test (Coke Reactivity Index): 200 g of 19 - 22.4 mm coke pieces are placed in a test retort and heated up to 1100 °C in pure N_2. Then 5 l/min pure CO_2 is led through the sample during 1 hour at 1100 °C. The loss in weight in % is the CRI index.

CSR-test (Coke Strength after Reaction with CO2): CSR is measured from the same sample immediately after CRI test. The sample is tumbled in a 700 mm long, 130 mm diameter tube rotating 30 minutes around its middle with 20 r/min speed. CSR-index is the percentage of +10 mm grains after the tumbling.

The test conditions are extreme and much harder than in a real blast furnace. Nevertheless they have been chosen in order to detect any differences between coke grades /20,21,22/. Beppler et al. /23/ have reported the correlation between CSR and the length of raceway cavity (Fig. 5.7).

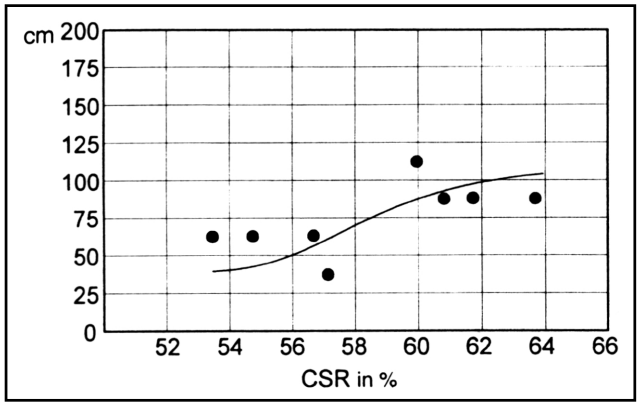

Fig. 5.7 *Influence of CSR on raceway length (from tuyere nose to < 6.3 mm coke bed). /23/*

With high injection rates the residence time of coke in the lower part of the blast furnace increases and the gasifying degree increases resulting in lower strength. Therefore coke properties become pronounced.

Coke is weakened also by an alkali attack - both by circulating alkali compounds and those present in the mineral phases of coke.

In the high temperature zone coke loses its alkalies and some SiO_2. It is also graphitized to some extent. These phenomena together with an abrasion in the raceway lead to a considerable formation of fines. High wind velocity makes the raceway act like a jet mill producing increasing amounts of coke dust.

Coke weakens from its surface and the core remains almost unreacted. Therefore coke lumps in the deadman represent more or less initial coke but the fines originate from the reacted and weakened surface. These observations stress the importance of large (stabilized) initial lump size because the specific surface is smaller for large coke. The steps in coke degradation are presented in Fig. 5.8.

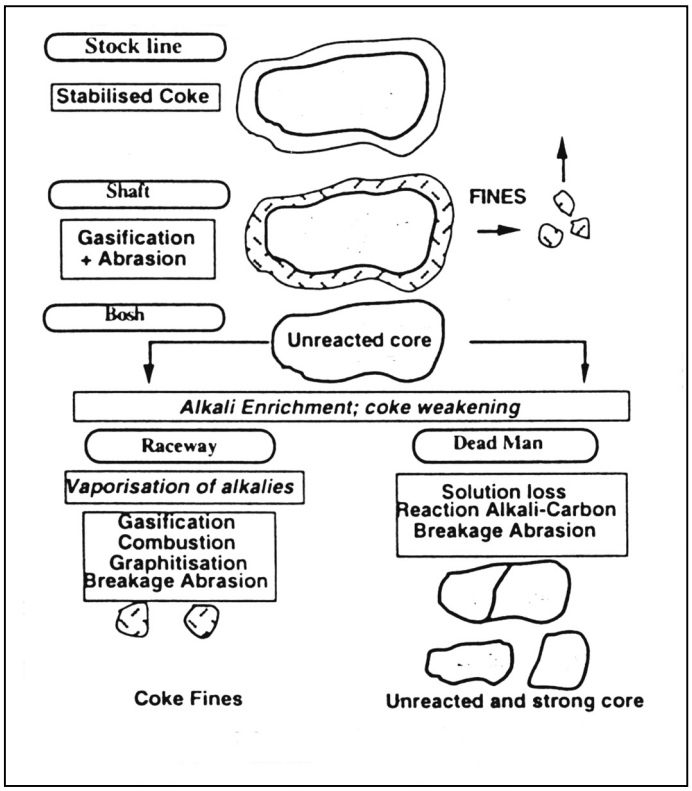

Fig.5.8 *Steps in coke degradation /24/*

When the degree of degradation increases the deadman becomes more and more filled with coke fines and successively becomes inactive.

5.3.2 Soot formation

Increasing amounts of oil or pulverised coal injection have become a new risk of a clogged hearth. If the amount of injectant is too high ascending gas to the shaft brings increasing amounts of soot or char. Usually the coke fines in the burden are consumed by solution loss reaction (5.3). In this case soot and char are more reactive and they are consumed instead of coke fines. These coke fines descend to the hearth and may clog the deadman.

An increased oil injection can have other effects on coke degradation, too. An early combustion inside the tuyeres produces more gas (CO and H_2) and thus increases the gas velocity in front of the tuyeres. Increasing velocity will increase the whirling speed of the tuyere coke and promote fines generation. In Koverhar the amount of dust in the top gas has increased with the amount of injected oil. Dust samples from the electric precipitator in the top gas cleaning system have been examined at Raahe Steel's laboratory to find the origin of carbon in the dust. The carbon in dust was identified to be coke fines. Too high injection rate retards the consumption of coke breeze in the raceway making the bottom and the back wall of the raceway tight (bird's nest). The raceway tends to shorten and to bend up towards the bosh wall. The complex of soot formation is illustrated in Fig. 5.9.

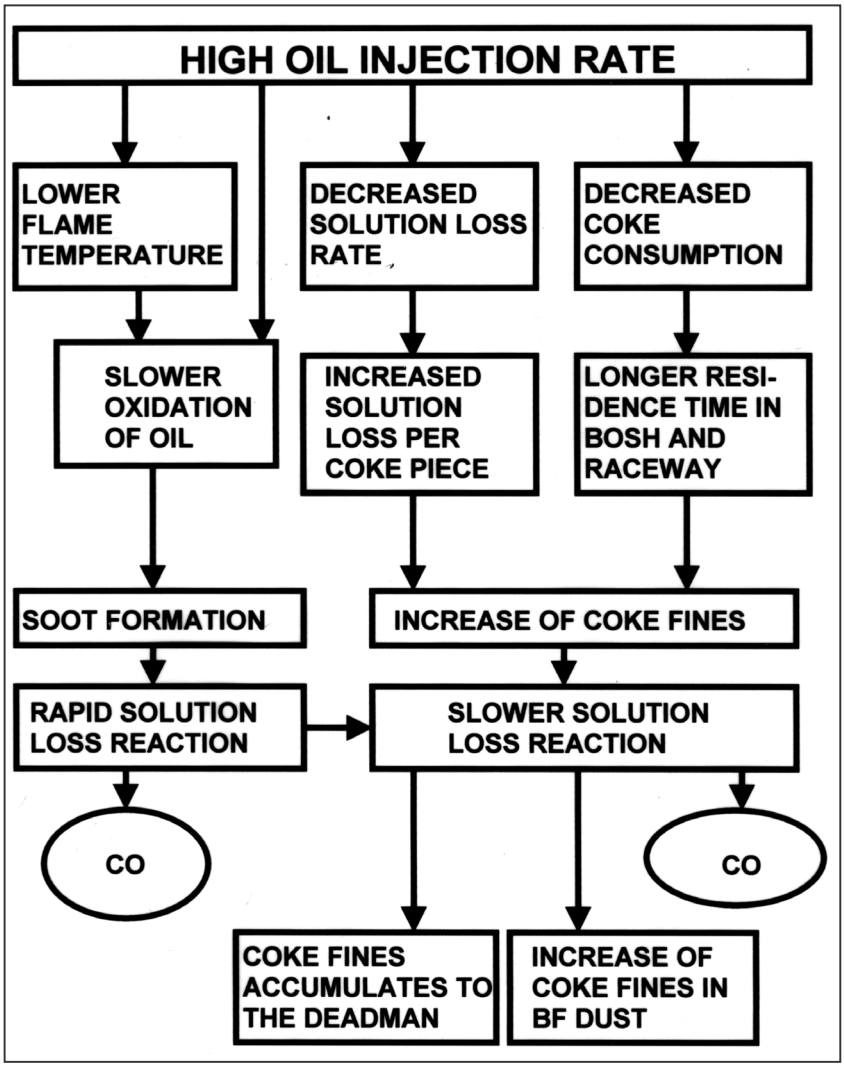

Figure 5.9 *Effect of high injection rate*

5.3.2 Burden properties

Poor burden properties may enlarge the risk of an inactive deadman. Low reducibility as well as poor high temperature properties like swelling and a wide softening temperature range may disturb gas permeability and result in a low reduction rate and consequently high FeO-content in the slag. Direct reduction cools the hearth and deteriorates coke strength. Low reducibility of the burden leads to the same result.

5.3.3 Burden distribution

An improper burden distribution may lead to a “hanging “ cohesive zone. From a hanging cohesive zone some parts extend very low or below the tuyere level where poorly reduced primary slag, high in FeO, drips in the hearth. In deadman core drillings residuals of unreduced sinter have been found /25/. If the amount of reaction (5.3) is large enough it cools the material in the deadman and the

space between the coke lumps gets filled with coke breeze and solidified slag. As long as FeO-containing slag is fluid, reaction (4.2) contributes to coke degradation as described in 4.2.1. Desulphurization is severely worsened by unreduced burden.

This kind of inactivation can be self-strengthening because an inactive deadman makes the burden distribution control more difficult by changing gas distribution in the bosh, belly and lower shaft.

5.3.4 Water leakage

Small water leakages are usually difficult to detect. With high injection rates and blast humidity control small water leakages do not show in the top gas H_2 content. Small water leakages give symptoms as sinking hearth bottom temperatures. Shortening of the tap hole and splashing of melt may occur during tapping. Small leakages, especially when they remain undetected, may lead to an inactive deadman when water does not evaporate completely but seeks its way to cooler parts in the bottom.

Large leakages are of course sudden and serious accidents leading to chilled hearth etc.

5.3.5 Maintenance stops

Maintenance stops may also be crucial to the deadman. When the metal below the tap hole level solidifies it has a large mass and good thermal conductivity to the cooled bottom. If other conditions are promoting inactivity a maintenance stop can lead to a long-standing inactivity of the deadman.

The sensitivity to maintenance stops depends on the furnace size, furnace cooling and hearth erosion. Large furnaces have a smaller cooling surface calculated per ton hot metal in the hearth, so they have a larger heat capacity. Too effective hearth cooling increases the risk of inactivation.

5.3.6 Low production rate

Low production rate increases the risk of an inactive deadman: the production rate being low the residence time of coke in contact with CO_2 and alkalies becomes longer and the coke properties weaken. Heat losses through the hearth lining are relatively constant at the beginning of the slow production period. Heat transport to the deadman slows down and a risk of solidification grows. A planned or unplanned stop during slow production may inactivate the deadman.

5.3.7 Hearth cooling

Hearth cooling itself is an essential factor in problems with an inactive deadman. Because the clogged deadman is maintained by solidified matter, it requires cooling to keep the temperature below melting points. One promoting factor is the thermal conductivity of the solidified material. Some suggestive values of thermal conductivity for materials in the hearth area are given in Table 5.2.

Table 5.2 *Typical values of thermal conductivity*

	W/(m·K)
Graphite (150 °C) /47/	116
Iron /48/	30
Carbon block /47/	13
Bottom scull /49/	12
Mullite /47/	2
Slag	1.4
Coke /50/	0.9

The exact composition of the deadman is unknown and the thermal conductivities of the materials change with time and temperature. That is why the calculation of deadman extension can be more or less suggestive.

A short report illustrates the influence of cooling area:

> From 1962 to 1995 the blast furnace in Koverhar was stopped for 3 to 5 weeks every summer for overhaul and summer vacancies. Until 1985 the stopping method was banking. From 1986 to 1994 the blast furnace was stopped for summer vacancies by blowing the stock line down to the tuyere level. The main part of the hearth was filled with fresh coke prior to blowing in. The furnace was in full production after 7 days. Oil injection was started when bottom temperatures exceeded 400 °C. Usually some bends were observed in the heating curves indicating deadman activation (Fig. 5.10).
>
> In January - June 1995, before the revamp of the blast furnace, all the three bottom temperatures stayed at a very low level, 350 - 400 °C and all attempts to get the bottom hot were useless. Heat losses were too large. When the bottom was torn apart, the magnitude of the salamander (= all material in the hearth below tap hole level, the deadman's foot) was revealed, Fig. 5.11.
>
> The ceramic plug in the middle was slightly eroded and the carbon blocks in the bottom were almost intact, but a huge elephant foot was formed at the hearth corners making a large cooling area for the deadman. This explains why it was so difficult to keep the bottom hot during the last operation year.

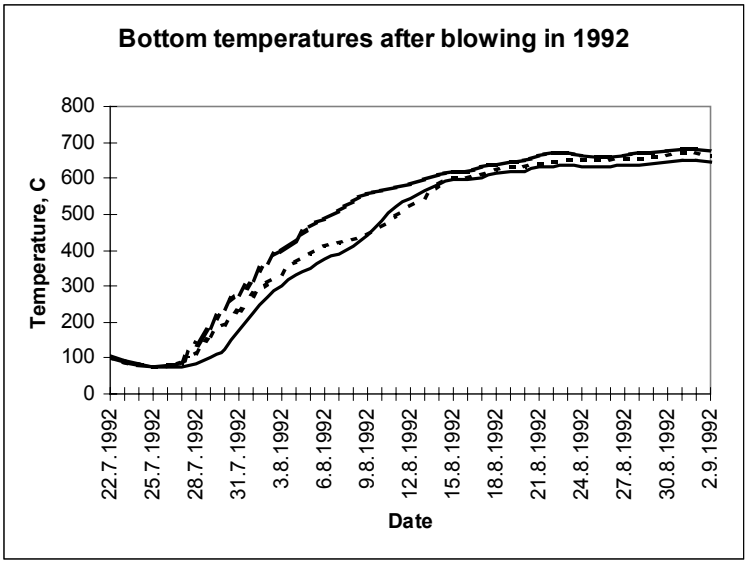

Fig. 5.10 *Bottom temperatures after blowing in 1992. (In this old construction there were only three thermocouples located between the two carbon block layers in the bottom of the hearth)*

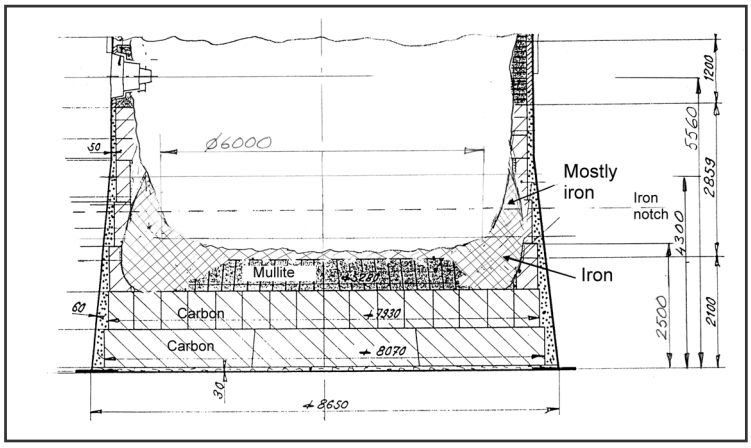

Fig. 5.11 *Salamander after campaign 1987-1995 / Koverhar*

5.3.8 Hearth construction

An improper hearth construction may promote solidification of the deadman by cooling its lower parts and also by leaving the corners free for hot metal flow towards the tap hole instead of an even flow through the deadman /26/. Common mistakes are e.g. too small well depth (from taphole to bottom), sharp corners between the hearth walls and the bottom and too efficient bottom cooling.

5.4 Deadman control

In this work great attention has been paid to an inactive deadman - a harmful phenomenon because the hot metal quality is poor with low carbon and high sulphur contents. There is also a great risk of an elephant foot formation which will reduce campaign life. Therefore it is important to get the deadman activated as soon as possible. During long lasting observations certain symptoms of inactivation could be found as listed in paragraph 5.2.

Shibaike et al. /25/ have presented an equation for estimating the deadman temperature (DMT). They have used a special tuyere level probe to measure the temperature in the deadman.

$$DMT = \frac{0.165 \times \theta_f \times \dot{V}_{bosh}}{d_H^3} + 2.445(FR - 483) + 2.91(\Delta\theta - 107) - 11.2(\eta_{CO,C} - 27.2) + \\ + 28.09(d_{pcoke} - 25.8) + 326 \qquad (5.6)$$

Where

DMT = Deadman temperature (°C),
θ_f = Adiabatic flame temperature (°C),
$\dot{V}_{bosh}$ = Bosh gas volume (m^3n/min),
d_H = Hearth diameter (m),
FR = Fuel rate (kg/t),
$\Delta\theta$ = slag fluidity index (°C),
$\eta_{CO,C}$ = η_{CO} at furnace centre, measured by shaft probe (-),
d_{pcoke} = Deadman coke size (mm) and $\Delta\theta$ = Slag fluidity index (°C),

$$\Delta\theta = \theta_{HM} - \{342 \times (CaO/SiO_2) + 11.0 \times [(Al_2O_3) + 1.4] + 819\} \qquad (5.7)$$

where θ_{HM} = Hot metal temperature,°C
(CaO/SiO_2) = (CaO/SiO_2) in slag
(Al_2O_3) = Al_2O_3 content in slag, %

Expression (5.6) illustrates some basic steps in the deadman control but it cannot be applied directly to other blast furnaces. It should also be noted that this expression is not valid when the deadman is inactive. It gives high values even when the hearth is clogged - only six maintenance stops can be observed as "blips" in the DMT-trend. As can be seen in Fig. 5.12 DMT does not show that the hearth is becoming clogged. Instead of clogging it shows a slightly increasing trend telling of efforts to get the hearth active again.

Nevertheless, the expression is valuable because it gives some ideas how to control the deadman. The high deadman temperature favours porous and open deadman structure. Picking out the positive terms in expression (5.6) gives some factors affecting DMT in a desired direction. High adiabatic flame temperature can be achieved by raising blast temperature, increasing oxygen enrichment, decreasing blast moisture and decreasing oil injection. The bosh gas volume can be increased by the wind rate. An increase of the fuel rate has a double effect as it elevates the heat level in general and also the slag fluidity index by raising the hot metal temperature. $\eta_{CO,C}$ can be controlled with the movable armours. The deadman coke size is mainly controlled by the centre coke size and also by the coke size in general. Slag fluidity index could be one possibility if the sulphur content of hot metal can tolerate a decrease in slag basicity.

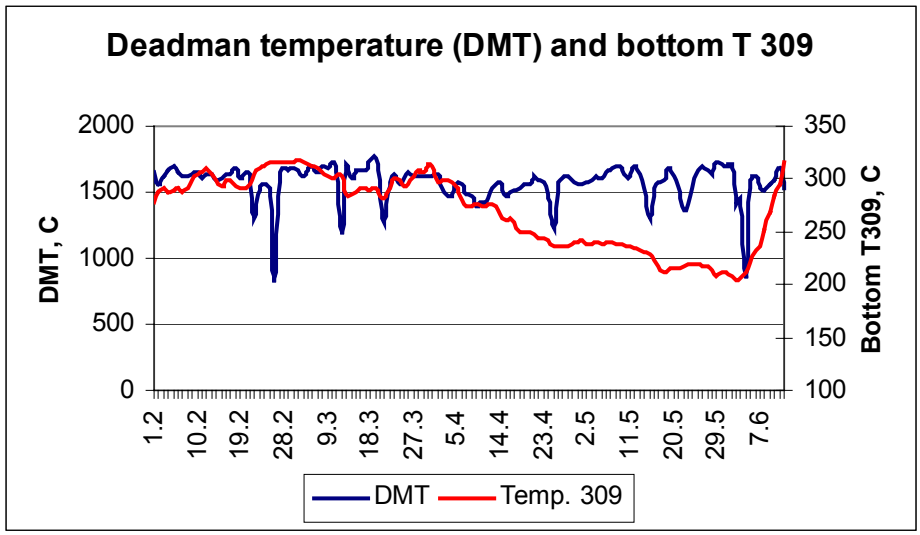

Fig.5.12 *Deadman temperature and bottom temperature at point 309 (see Appendix 3) in February - June 2003, when inactivation was identified at the end of March.*

At first when inactivation has been verified immediate measures are taken to maintain hot metal quality as good as possible; increasing slag rate and coke rate.

The first measure is to get coarse and good coke to the hearth. The oldest measure to control the blocked hearth has been coke size coarsening. Charging of nut coke (10-28 mm) has been stopped and the best quality coke has been used. It is also important to promote turnover of hearth coke. Therefore oil rate has been reduced to a minimum. Since 1995 coarse coke has been charged to the furnace centre, about 10 % of total coke. In July 1998 very coarse, + 60 mm, coke was used in Koverhar as centre coke to activate the deadman. The result was good and very coarse coke has been used since then as central coke.

The second measure is to push heat into the inactive deadman to break its structure. Maintaining the highest possible wind rate, high flame temperature and high oxygen enrichment does this. Reduced oil rate moves the maximum raceway temperature deeper in the furnace. Increasing heat level, i.e. fuel rate, is also adapted to get more heat to the deadman.

The third measure is to minimise bottom cooling. The cooling fan has been stopped and the cooling funnels are plugged up with rock wool.

The measures can be summarised as follows:

- ✧ Best quality of coke and no nut coke
- ✧ Large lump size of central coke (+60 mm)
- ✧ High wind rate and oxygen enrichment
- ✧ Reduced oil rate and possibly increased fuel rate
- ✧ Reduced bottom cooling.

These measures have been found to be effective and they are applied when needed. Activation of the deadman takes from three to five weeks - or even longer.

A clogged hearth phenomenon occurred in Koverhar at the end of March 2003. There was shortage of good quality centre coke and therefore reduced amount of a mixture of regular bell coke and centre coke (50:50) was used. Clogging started almost immediately after the use of the mixture began on March 28. The use of mixture continued till April 23. The hearth bottom continued to cool till June 2. The amount of centre coke was increased successively up to 35 kg/tHM. After that the bottom temperatures started to rise.

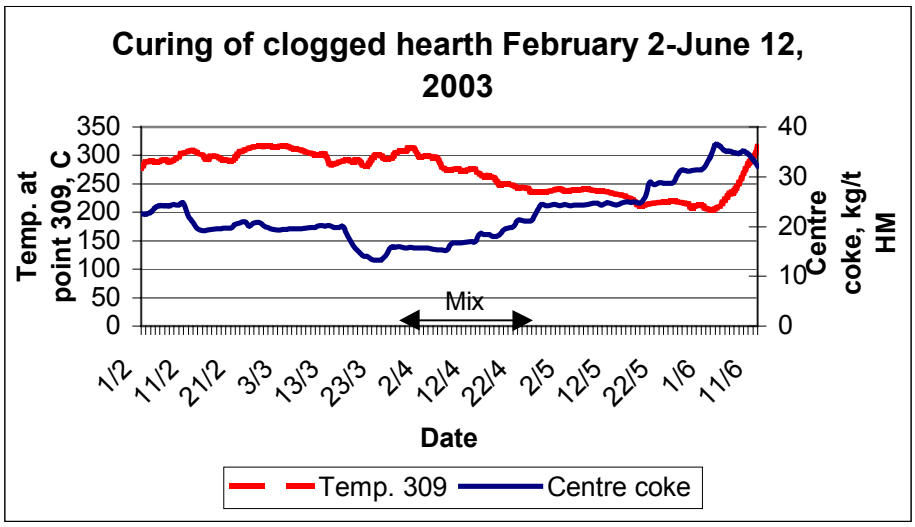

Fig.5.13 *Curing of clogged hearth*

5.5 Other methods to cure deadman

Soaking pit slag, manganese ore and fluorspar charging have been recommended by some authors /27/. A test period with manganese ore was done at BF 1 in Raahe Steel starting on October 28, 2001 and ending on August 24, 2002. No significant effect could be observed /52/.
Ichida et al. proposed a method to insert a heating probe (oxygen lance) in the deadman in order to rise the temperature inside the deadman /7/. No further advance has been reported.
Even use of explosives have been tried to blast the hard crust of the deadman, but not recommended /8/.

6 SULPHUR IN BLAST FURNACE

6.1 General

Usually sulphur has been considered to be the very impurity that must be eliminated in the blast furnace process – and that is true. At first glance it seems to be possible to control the sulphur content with slag basicity and also with carbon content because the correlation is so strong. A deeper study shows the complexity of the problem and will be discussed later. Fortunately, low sulphur and high carbon content are desired at the same time. Sulphide capacity C_S is a common way to express the desulphurization capability of the slag/28/:

$$C_S = (\text{wt\%S}) \sqrt{\frac{p_{O_2}}{p_{S_2}}} \tag{6.1}$$

where C_S = sulphide capacity
wt% S = sulphur content in the slag
p_{O2} = partial pressure of O_2
p_{S2} = Partial pressure of S_2

$$½\ S_2\ (g) = [S] \tag{6.2}$$

$$C\ (s) + ½\ O_2\ (g) = CO\ (g) \tag{6.3}$$

For reaction (6.2) $\Delta G^o_{6.2} = -131461 - 22.05 \cdot T$ J/mole /54/
and for (6.3) $\Delta G^o_{6.3} = -118050 - 84.39 \cdot T$ J/mole /28/

$$K_{6.2} = \frac{[a_S]}{p_{S_2}^{½}} = \frac{[\%S] \cdot f_S}{p_{S_2}^{½}} \tag{6.4}$$

$$K_{6.3} = \frac{p_{CO}}{a_C \cdot p_{O_2}^{½}} \tag{6.5}$$

$$\Delta G^o = -R \cdot T \cdot \ln K \tag{6.6}$$

Where $[a_S]$ = activity of sulphur in hot metal
[%S] = sulphur content in hot metal
f_S = activity coefficient of sulphur
p_{CO} = partial pressure of CO in hearth atmosphere
a_C = activity of carbon
ΔG^o = Standard free energy
R = gas constant
T = temperature
K = equilibrium constant

By substituting ΔG^o values into (6.4) and (6.5), taking logarithms, combining with (6.1), (6.2) and rearranging gives

$$\ln\frac{(\%S)}{[\%S]\cdot f_S} = \ln C_S - \ln\frac{p_{CO}}{[a_C]} - \frac{1613}{T} + 12.80 \qquad (6.7)$$

In this formulation p_{CO} in the hearth atmosphere determines the oxygen potential. But the slag contains unreduced FeO making conditions fuzzy. If FeO controls the oxygen potential in the slag, sulphur distribution can be calculated in similar way:

$$Fe\ (l) + ½\ O_2 = (FeO)\ \ (l) \qquad (6.8)$$

For reaction (6.8) $\Delta G^{o}_{6.8} = -51975 - 8.855\cdot T$ J/mole /38/

$$K_{6.8} = \frac{a_{FeO}}{a_{Fe}\cdot p_{O_2}^{½}} \qquad (6.9)$$

Where $[a_{FeO}]$ = activity of FeO in slag
p_{O2} = partial pressure of O_2 in hearth atmosphere
a_{Fe} = activity of iron
ΔG^{o} = Standard free energy
R = gas constant
T = temperature
K = equilibrium constant

By substituting ΔG^{o} value into (6.6) and (6.9), taking logarithms, combining with (6.1) and rearranging gives

$$\ln\frac{(\%S)}{[\%S]\cdot f_S} = \ln C_S - \ln a_{FeO} + \ln a_{Fe} + \frac{10360}{T} - 1.81 \qquad (6.10)$$

Common observations at the blast furnace show the effect of slag FeO on desulphurization. If the FeO content is high in the slag (e.g. 0.3%) the hot metal sulphur is also high. Iwamasa and Fruehan observed increased desulphurisation of hot metal with decreasing FeO in the slag /29/.
On the other hand Smith and Fruehan have found that high sulphur content in hot metal retards FeO reduction from slag by carbon in hot metal /30/. Those experiments were made with an initial carbon content of 2 – 4.5% to keep the sulphur activity constant and slag FeO = 5%.

Sulphur retards carbon dissolution in many ways, but which of them is dominant is not clear:

- ✧ Sulphur increases carbon activity in hot metal (high positive interaction coefficient).
- ✧ Sulphur is a surface-active element blocking the hot metal surface.
- ✧ Sulphur decreases carbon diffusion coefficient in hot metal /51/.
- ✧ Sulphur in the slag increases the wettability of the slag making the contact area between coke and hot metal smaller /9/.
- ✧ Sulphur in hot metal decreases the wettability between carbon and hot metal /31/.

All these factors prolong the time needed to reach equilibrium.

6.2 Sulphur load

The sulphur load itself doesn't seem to have an influence on carbon content, but it is difficult to be verified with statistical methods because hot metal sulphur is controlled by slag basicity. Hot metal sulphur depends on the sulphur load:

$$[S] = \frac{100 \times TS}{L_S \times SR + 1000} \quad , \tag{6.11}$$

Where TS = sulphur load (kg/tHM),
SR = slag rate (kg/tHM),
L_S = sulphur partition (–) and
[S] = hot met sulphur (%).

There are several expressions for L_S based on hot metal analysis, slag composition, temperature, optical basicity, hearth gas composition etc. One of the most common formulas is the Tamura expression presented by Hori /32/. This formula has given good estimates for sulphur distribution in Koverhar blast furnace:

$$\begin{aligned} L_S = (\%S)/[\%S] = \exp\{&0.263 \times [\%C] + 0.145 \times [\%Si] - 0.060 \times [\%Mn] \\ &+ (3.45 \times (CaO)/(SiO_2) + 2.39 \times (MgO)/(SiO_2))/(1 + 0.197 \times (Al_2O_3)/(SiO_2)) \\ &- 20033/\theta_{HM} + 10.30\}/p_{CO} \end{aligned} \tag{6.12}$$

Where () refers to slag component, %
[] refers to hot metal component, %
θ_{HM} = hot metal temperature, °C
p_{CO} = partial pressure of CO

6.3 Sulphur circulation

Most of the sulphur to the blast furnace comes from coke, where it is bound as organic sulphur and as FeS. Common blast furnace coke contains around 0.6 % S. Injected oil contains normally 1.8 % S, but it may be up to 3 % S. Iron bearing materials, sinter and pellets contain minor amounts of sulphur, 0.001 to 0.01 %.

Table 6.1 *A typical sulphur balance for Koverhar blast furnace*

SULPHUR IN	kg/tHM	SULPHUR OUT	kg/tHM
Pellets	0.14	Hot metal	0.56
Slag formers	0.52	Slag	3.74
Coke	2.31	BF dust	0.35
Oil	1.92	Balance	0.24
Sum	4.89	Sum	4.89

Dissection investigations show how sulphur circulates from the combustion zone up to the cohesive zone and is adsorbed to the metal and ore (Fig. 6.1). The sulphur content of freshly reduced iron is around 0.02 % and can increase up to 0.15 - 0.20 % near the cohesive zone /33/. Similar observations have been made in the experimental blast furnace at LKAB.

Sulphur is gasified mainly in the combustion zone from coke and injected fuels and is absorbed mainly in the dripping zone, cohesive zone and slightly above it /33/. Some gasification can take place from molten slag.

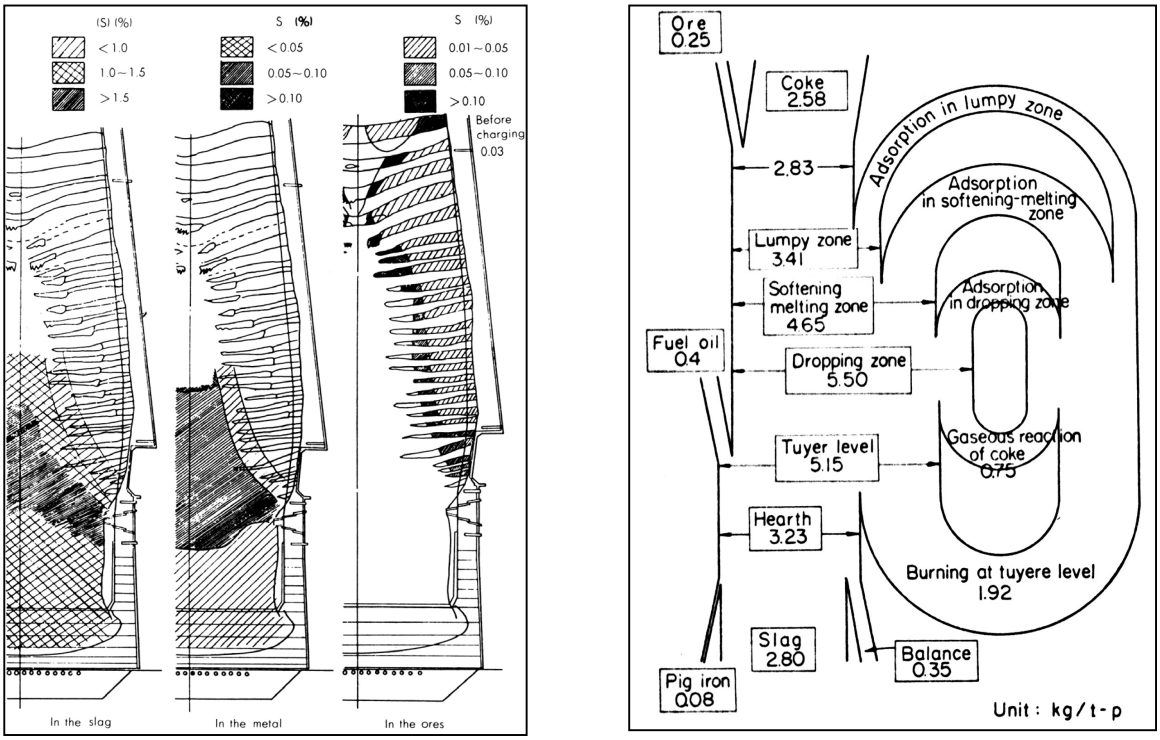

(a) (b)

Fig. 6.1 *Sulphur distribution (a) and sulphur circulation (b) in Hirohata Nr.1 blast furnace /33/*

6.4 Sulphur precipitation in blast furnace hearth

6.4.1 Experiences at Raahe blast furnace

The hearth of blast furnace Nr.1 in Raahe was clogged frequently and for long periods of time since the blowing in 1995. Numerous efforts were made to get the deadman active and the hearth open but without success. When the blast furnace was blown down for an intermediate repair in July 2002 a huge scab, weighing about 410 tons, was found in the hearth (Fig. 6.2). The scab consisted of iron, slag, calcium sulphide CaS and some coke. The sulphur content in the scab was 8.8%, which corresponds to 20% of CaS in a network of metallic iron and slag.

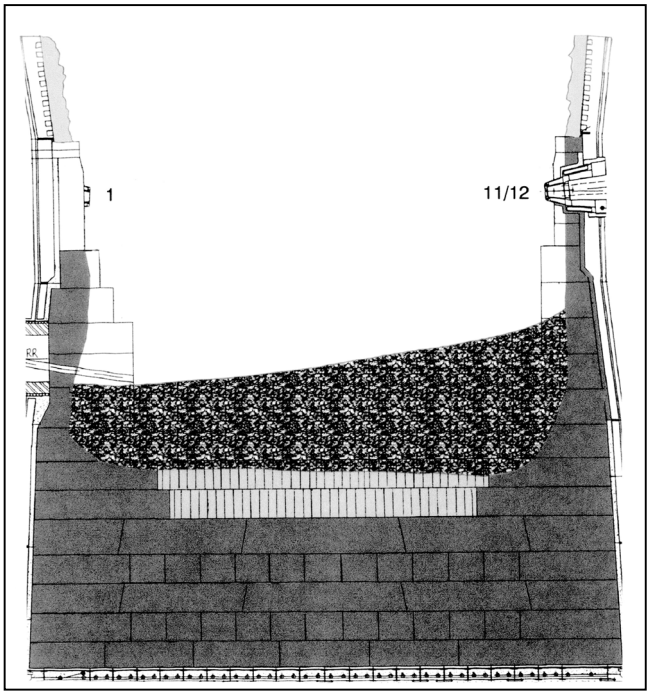

Fig. 6.2 *Estimated location of bottom scab in Raahe Nr. 1*

Table 6.2 *Bulk samples from the bottom scab (Raahe Nr.1, 2002)*

Nr.	CaO	Fe*)	MgO	MnO	P	SiO_2	Ti	V	Al_2O_3	S
1	16.7	48	6.7	0.70	0.022	2.07	0.07	0.05	13.7	8.37
2	18.6	39	7.3	0.29	0.015	3.19	0.10	0.04	16.9	9.36
3	20.3	57.6	1.52	1.3	0.038	6.91	0.50	0.14	1.48	9.12
4	18.5	49.6	4.04	0.48	0.026	8.41	0.17	0.08	5.87	7.96
5	22.7	41.9	4.53	0.52	0.018	4.58	0.13	0.05	7.95	12.0
6	18.3	48.1	4.11	0.91	0.022	5.84	0.17	0.07	6.55	9.3
7	21.1	52.3	2.77	1.08	0.031	6.53	0.17	0.08	5.89	9.31
8	17.8	55.3	3.18	0.54	0.025	4.38	0.09	0.07	6.38	8.9
9	18.9	51.7	5.12	1.94	0.029	6.19	0.27	0.09	9.88	9.37
10	7.93	67.4	1.76	1.51	0.035	4.15	0.10	0.08	3.6	4.31
MV	**18.08**	**51.1**	**4.10**	**0.93**	**0.03**	**3.88**	**0.17**	**0.07**	**7.82**	**8.8**

**) Fe mainly as metallic iron*

The main minerals in Raahe bottom scab were metallic Fe, calcium sulphide, magnesium aluminate (spinel), crystalline slag (melilite) and carbon.

Results of recalculation of S to CaS and P, Ti and V to oxide slag components and subtraction of iron are presented in Table 6.3.

Table 6.3 *Contents of slag components in the bottom scab (Raahe Nr.1, 2002)*

Nr.	MgO	MnO	P_2O_5	SiO_2	TiO_2	V_2O_5	Al_2O_3	CaS	CaO
1	15.12	1.58	0.11	4.67	0.26	0.20	30.91	42.51	4.63
2	14.26	0.57	0.07	6.23	0.20	0.14	33.02	41.17	4.34
3	4.12	3.52	0.24	18.72	1.35	0.68	4.01	55.61	11.76
4	9.70	1.15	0.14	20.19	0.41	0.34	14.09	43.01	10.97
5	9.73	1.12	0.09	9.84	0.28	0.19	17.08	58.02	3.66
6	10.09	2.24	0.12	14.34	0.42	0.31	16.09	51.41	4.98
7	6.53	2.55	0.17	15.39	0.40	0.34	13.89	49.40	11.34
8	8.59	1.46	0.15	11.83	0.24	0.34	17.24	54.12	6.02
9	10.84	4.11	0.14	13.11	0.57	0.34	20.92	44.66	5.30
10	8.21	7.05	0.37	19.36	0.47	0.67	16.80	45.26	1.81
MV	**9.72**	**2.53**	**0.16**	**13.37**	**0.46**	**0.35**	**18.40**	**48.52**	**6.48**

When comparing the compositions of the scab, coke ash and blast furnace slag it can be seen that the scab is not a simple mixture of coke ash and slag. The proportion of calcium in the scab is much higher than in slag or coke ash and the silica content lower than in them (Table 6.4).

Table 6.4 *Percentages of slag components in the scab, typical coke ash and blast furnace slag*

	MgO	MnO	P_2O_5	SiO_2	TiO_2	V_2O_5	Al_2O_3	CaS	CaO
Scab	9.72	2.53	0.16	13.37	0.46	0.35	18.40	48.52	6.48
Coke ash	1.70	0.08	0.76	62.32	0.15	0.01	31.97	2.32	0.69
Slag	10.62	0.70	0.00	38.09	1.99	0.07	9.47	1.81	37.25

Further examinations have revealed a special layered structure: there were iron rich layers, Ti(C,N) rich parts, CaS rich zones, all mixed with spinel and melilite. These layers had no sharp boundaries, but the impression was clear; their thickness being 5 to 10 mm. The layer structure brought in mind certain operation periods giving their special contribution to the layers.

Even though the focus has now been on CaS it must be kept in mind that Ti(C,N) is a common salamander compound (in the blast furnace dialect salamander means all liquid and solidified materials in the hearth below the tap hole level) (Fig.6.3). It precipitates on colder parts of the hearth and Ti-compounds like ilmenite and rutile are used to generate a protecting layer in eroded blast furnace hearths. The occurrence of Ti(C,N) tells about low temperature.

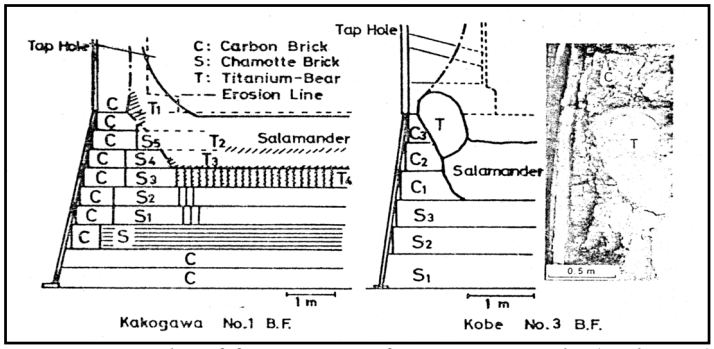

Fig. 6.3 *Mode of formation of Ti-compounds (Ti bears) in the blast furnace hearth /34/*

6.4.2 Experiences at Koverhar blast furnace

The blast furnace in Koverhar had also an intermediate repair in August 2002. There was no big scab in the hearth and the remainings of the deadman were small. Some samples were taken from the deadman. The upper part of it was coke and slag containing alkali cyanides. The lower part of the deadman consisted of 20-30 mm coke particles embedded in slag and iron matrix with thin (5 mm) seams. Samples from this lower part (marked with number 3) were examined with XRD, optical microscope and SEM.

Three chemical analyses were made from the slag phase of sample 3 (Table 6.5).

Table 6.5 *Samples of slag phase from the bottom of deadman (Koverhar, 2002)*

Nr.	**CaO**	**Fe**	**MgO**	**MnO**	**P_2O_5**	**SiO_2**	**TiO_2**	**V_2O_5**	**Al_2O_3**	**S**
3-1	26.9	2.5	17.3	0	0.00	24.4	0.59	0.08	20.2	3.02
3-2	25.7	3.7	19.9	0	0.01	25.0	1.57	0.62	20.6	3.10
3-3	26.4	2.6	17.3	0	0.00	23.9	0.65	0.08	21.9	3.00
MV	**26.3**	**2.9**	**18.2**	**0**	**0**	**24.4**	**0.94**	**2.6**	**20.9**	**3.04**

For mineral identification by XRD the sample 3 was divided in two parts: 1) general, consisting both coke and slag matrix and 2) slag matrix. The results are presented in Table 6.6:

Table 6.6 *XRD results of Koverhar sample 3*

		General	Slag matrix
Fe	Iron	X	
$MgAl_2O_4$	Spinel	X	X
$CaMgSiO_4$	Monticellite	X	X
C	Graphite	X	
CaS	Oldhamite		X
$Ca_2Al_2SiO_7$	Gehlenite	X	X

By optical microscopying some Ti(C,N) crystals could be found. They appeared as bronze coloured needles in the slag phase, though not in plenty. Iron droplets were carburated and they were in many cases in contact with a pink coloured (in optical microscope) phase. In larger iron inclusions there were graphite flakes implying carbon saturation.

The pink coloured phase was identified by SEM microanalysis to be CaS (Oldhamite). The iron in contact with CaS contained only 0.01 – 0.02% S. Phosphorus and vanadium seem to concentrate in the bottom iron. The contents 0.3 - 0.4% P and 0.5 – 0.6% V are much higher than in hot metal (0.025% P and 0.15% V). Typical microstructures are shown in Fig.6.5 and Fig. 6.6.

The dominating appearance of CaS in the bottom scab of Raahe Nr. 1 furnace and also in Koverhar was surprising. Several hypotheses were proposed to explain this phenomena. Because transport of CaS from the slag through the hot metal layer to the bottom seems difficult due to a large difference in densities precipitation from the hot metal was taken as a working hypothesis.

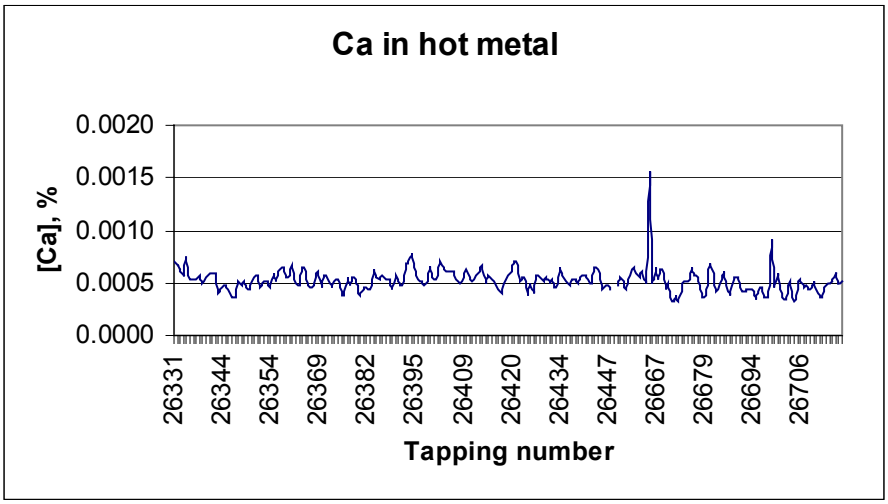

Fig.6.4 *Calcium content in hot metal (Koverhar April 30, 2003-June 9, 2003)*

Common factors in both furnaces are the use of heavy bottom oil (ERP) and high sulphur load. Hot metal in Koverhar contains 0.0004-0.0008% Ca (Fig. 6.4). Soluble calcium in the hot metal in Raahe has been analysed to 0.0003-0.0008%. When the sulphur content in the hot metal is high enough CaS can precipitate on colder parts of the hearth as will be shown later.

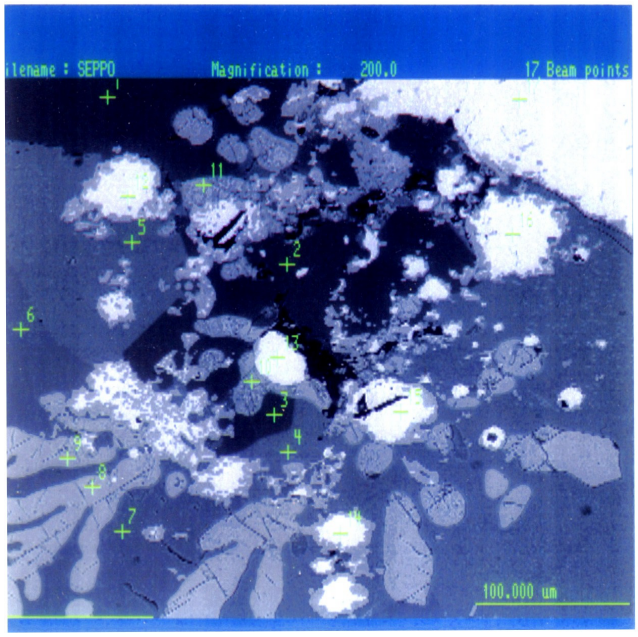

Fig. 6.5 *SEM-picture of sample 3; middle of the hearth, tap hole level:*
Points 1 – 3: Spinel ($MgO \cdot Al_2O_3$)
Points 4 and 5: about 10% MgO + 10% Al_2O_3 + 40% CaO + 40% SiO_2 (Melilite)
Points 6 and 7: Monticellite ($CaO \cdot MgO \cdot SiO_2$)
Points 8 – 11: Oldhamite (CaS), containing some 0.5% Mg
Points 12 – 17: metallic Fe, containing 0.16% Si, 0.41% P, 0.02% S, 0.31% Ti and 0.62% V (Carbon content could not be analysed with SEM).

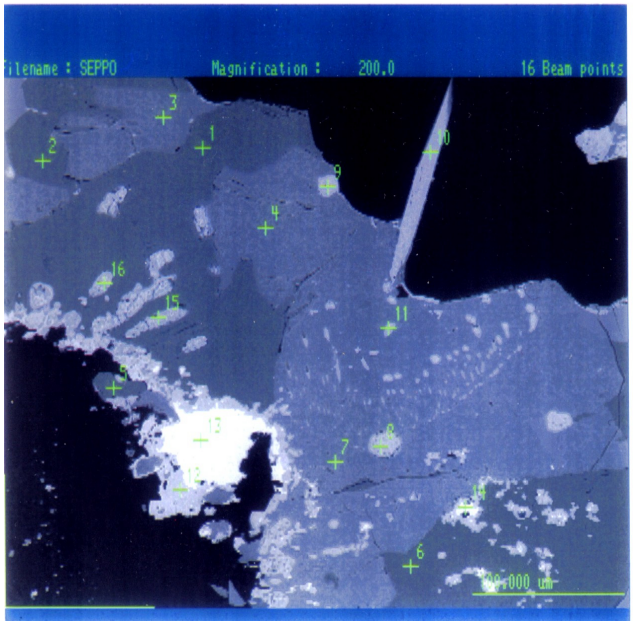

Fig. 6.6 *Another SEM-picture of sample 3; middle of the hearth, tap hole level:*
Points 1,2,5 and 6: Spinel ($MgO \cdot Al_2O_3$)
Points 3, 4 and 7: Monticellite ($CaO \cdot MgO \cdot SiO_2$)
Points 8, 9, 11, 15 and 16: Oldhamite (CaS), with 2.8% (Mg+Si+Al+Mn+Fe)
Point 12: Wüstite (FeO)
Points 13 and 14: Metallic Fe, containing 0.30% P, 0.01% S, 0.59% Ti and 0.47% V
Point 10: Titanium carbonitride (Ti(C,N))

6.4.3 Calculation of conditions for CaS precipitation

To calculate ΔG for the reaction

$$CaS(s) = [Ca] + [S] \qquad (6.13)$$

Starting from

$$CaS(s) = Ca(g) + ½\ S_2(g) \qquad (6.14)$$

$$\Delta G^{o}_{6.14} = 551\,736 - 102.33 \cdot T \ \text{J/mole} \qquad /35/$$

$$Ca(g) = [Ca] \qquad (6.15)$$

$$\Delta G^{o}_{6.15} = -39\,481 + 49.4 \cdot T \ \text{J/mole} \qquad /36/$$

$$½S_2(g) = [S] \qquad (6.16)$$

$$\Delta G^{o}_{6.16} = -135\,150 + 23.4 \cdot T \ \text{J/mole} \qquad /36/$$

$$\Delta G^{o}_{6.13} = \Delta G^{o}_{6.14} + \Delta G^{o}_{6.15} + \Delta G^{o}_{6.16} = 377\,110 - 29.5 \cdot T \ \text{J/mole}$$

The equilibrium constant for the reaction (6.13) is

$$K_{6.13} = \frac{a_{[Ca]} \cdot a_{[S]}}{a_{CaS(s)}} \qquad (6.17)$$

The activity of component i on weight-% scale is

$$a_i = f_i \cdot [\%i] \qquad (6.18)$$

Where a_i is the activity of component i,
f_i is the activity coefficient of component i and
[% i] the percentage of component i in the melt.

Because there are several components in considerable amounts in the hot metal their interactions must be taken into account.

$$\log f_i = \sum_{j=2}^{n} e_i^j \cdot [\%j] + \sum_{j=2}^{n} r_i^j [\%j]^2 + \sum_{j=2}^{n} \sum_{k=2}^{n} r_i^{j,k} [\%j] \cdot [\%k] \qquad (6.19)$$

Where f_i is the activity coefficient of component i,
e_i^j is the first order interaction parameter,
r_i^j is the second order interaction parameter and
% j , %k the percentage of component j resp. k in the melt.

Several first order interaction parameters can be found tabulated in literature, but only a few second order parameters.
In this case we calculate with the main components in hot metal: C, Si, Mn, Ti and S and their influence in formation of CaS.

$$\log f_{[Ca]} = [\%Ca]\cdot e_{Ca}^{Ca} + [\%S]\cdot e_{Ca}^{S} + [\%C]\cdot e_{Ca}^{C} + [\%Si]\cdot e_{Ca}^{Si} + [\%Mn]\cdot e_{Ca}^{Mn} + \\ + [\%Ti]\cdot e_{Ca}^{Ti} + [\%Ca]^2\cdot r_{Ca}^{Ca} + [\%S]^2\cdot r_{Ca}^{S} + [\%C]^2\cdot r_{Ca}^{C} + [\%Si]^2\cdot r_{Ca}^{Si} + \\ + [\%Mn]^2\cdot r_{Ca}^{Mn} + [\%Ti]^2\cdot r_{Ca}^{Ti} \qquad (6.20)$$

$$\log f_{[S]} = [\%Ca]\cdot e_{S}^{Ca} + [\%S]\cdot e_{S}^{S} + [\%C]\cdot e_{S}^{C} + [\%Si]\cdot e_{S}^{Si} + [\%Mn]\cdot e_{S}^{Mn} + \\ + (\%Ti)\cdot e_{S}^{Ti} + (\%Ca)^2\cdot r_{S}^{Ca} + (\%S)^2\cdot r_{S}^{S} + (\%C)^2\cdot r_{S}^{C} + (\%Si)^2\cdot r_{S}^{Si} + \\ + [\%Mn]^2\cdot r_{S}^{Mn} + [\%Ti]^2\cdot r_{S}^{Ti} \qquad (6.21)$$

$$\Delta G^{o}_{6.13} = -\,R\cdot T\cdot \ln K_{6.13} = -2.30259\cdot R\cdot T\cdot \log K_{6.13} \qquad (6.22)$$

$$\log K_{6.13} = -\frac{\Delta G^{o}_{6.13}}{2.30259\cdot R\cdot T} \qquad (6.23)$$

Substituting into equation (6.17), taking logarithms and rearranging

$$0 = \log f_{[Ca]} + \log[\%Ca] + \log f_{[S]} + \log[\%S] - \log K_{6.6} = g \qquad (6.24)$$

$$g = \log[\%Ca] + [\%Ca]\cdot(e_{Ca}^{Ca} + e_{S}^{Ca}) + [\%Ca]^2\cdot(r_{Ca}^{Ca} + r_{S}^{Ca}) + \\ \log[\%S] + [\%S]\cdot(e_{Ca}^{S} + e_{S}^{S}) + [\%S]^2\cdot(r_{Ca}^{S} + r_{S}^{S}) + \\ [\%C]\cdot(e_{Ca}^{C} + e_{S}^{C}) + [\%C]^2\cdot(r_{Ca}^{C} + r_{S}^{C}) + \\ [\%Si]\cdot(e_{Ca}^{Si} + e_{S}^{Si}) + [\%Si]^2\cdot(r_{Ca}^{Si} + r_{S}^{Si}) + \\ [\%Mn]\cdot(e_{Ca}^{Mn} + e_{S}^{Mn}) + [\%Mn]^2\cdot(r_{Ca}^{Mn} + r_{S}^{Mn}) + \\ [\%Ti]\cdot(e_{Ca}^{Ti} + e_{S}^{Ti}) + [\%Ti]^2\cdot(r_{Ca}^{Ti} + r_{S}^{Ti}) - \frac{\Delta G^{o}_{6.13}}{2.30259\cdot R\cdot T} \qquad (6.25)$$

Partial differentiation of (6.25) gives

$$\frac{\partial g}{\partial[\%Ca]} = g' = \frac{1}{[\%Ca]} + (e_{Ca}^{Ca} + e_{S}^{Ca}) + 2\cdot[\%Ca]\cdot(r_{Ca}^{Ca} + r_{S}^{Ca}) \qquad (6.26)$$

Equation (6.27) can then be solved by a numerical method:

$$x_{n+1} = x_n - \frac{g(x_n)}{g'(x_n)} \qquad (6.27)$$

The results are illustrated in Fig.6.7 at some temperatures.

The influence of the temperature on interaction coefficients are estimated with (6.28) /54/

$$e_i^j(T) = \frac{T'}{T} \cdot e_i^j(T') \tag{6.28}$$

Where e_i^j = interaction coefficient
T' = reference temperature, K
T = temperature, K

6.4.4 Discussion

As can be seen in Fig.6.7 there is a strong potential for CaS to precipitate on the colder parts of the hearth. Similar precipitates have been found in Koverhar in 1996 in the bottom of the iron runner below the skimmer. The compositions of those samples are presented in Table 6.5.

Table 6.5 *Samples from the bottom of iron runner (Koverhar, 1996)*

Nr.	CaO	Fe	MgO	MnO	P_2O_5	SiO_2	TiO_2	V_2O_5	Al_2O_3	S
1	38.5	4.6	13.7	0.22	0.001	1.1	3.40	0.13	28.65	18.1
2	28.0	17.4	14.4	0.21	0.006	10.6	4.45	0.18	14.38	9.7
3	36.5	5.4	15.1	0.24	0.001	9.4	2.23	0.10	22.90	15.5
4	30.2	11.4	13.7	0.23	0.005	6.0	3.47	0.17	20.46	15.0
5	31.1	9.4	17.4	0.20	0.009	11.7	5.72	0.23	17.25	10.4
6	32.2	6.4	17.0	0.21	0.001	9.8	7.27	0.21	20.61	12.9

The high content of sulphur remained mysterious for many years, but now it seems reasonable owing to CaS precipitation.

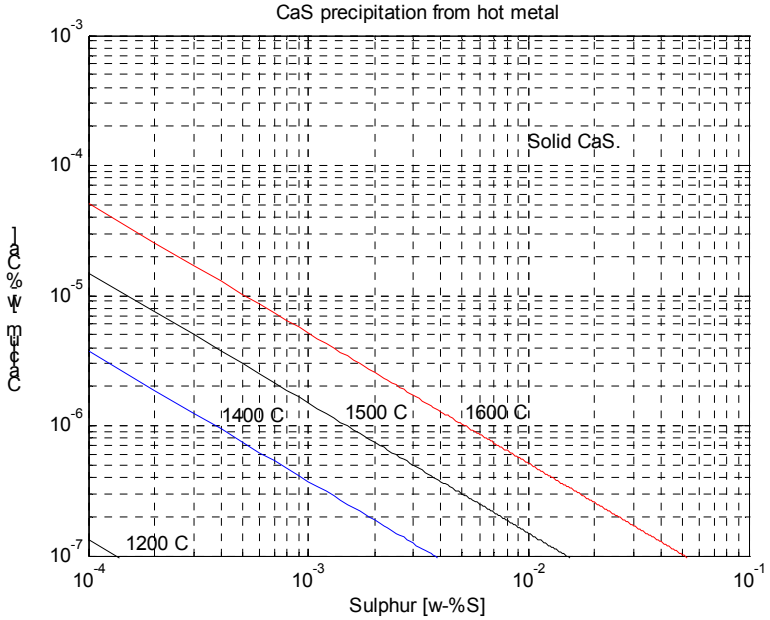

Fig. 6.7 *CaS precipitation from hot metal as a function of Ca and S contents*

Ca content in hot metal is 0.0004 - 0.0008 % (Fig. 6.4). Very low Ca contents are difficult to analyse. The XRF determinates total Ca while soluble Ca is unknown. The XRF is calibrated with standard samples of raw iron. Common sulphur contents in hot metal are 0.02 - 0.06 %. In Fig. 6.7 the potential of CaS precipitation can be deduced. The Ca and S contents are so high that the hot metal should be saturated with CaS.

The solubility of CaS in slag must also be taken into account. With a high sulphur load the sulphur content of slag is 2.0 – 2.5 % which means it being close to saturation (Fig.6.8). Precipitated CaS can be dissolved by the hot metal from hot slag according to reaction (6.13) and precipitate later in the colder parts of the hearth.

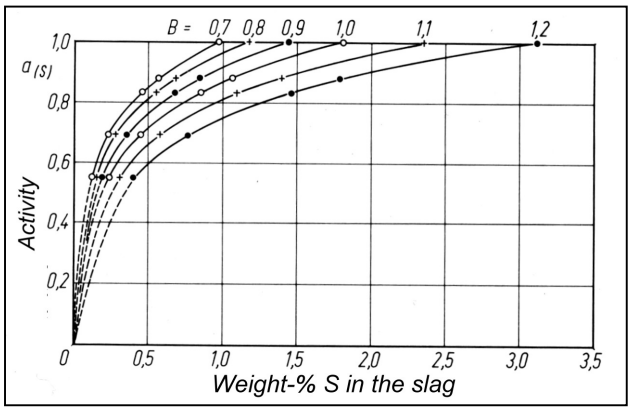

Fig. 6.8 *Activity of Calcium sulphide in CaO-SiO_2 system. B=(CaO)/(SiO_2). H. Schenck and T. El Gammal. /38/*

Other hypotheses for scab formation have been suggested during discussions at Raahe and Koverhar plants:
-Mechanical transport by peeling scaffolds from the bosh walls. As can be seen in Fig. 6.1 sulphur content in the root of the cohesive zone may be high containing CaS. Peeling takes place irregularly and sometimes gives rise to a clogged hearth.
-Mechanical transport of CaS from the slag by the deadman coke. This hypothesis cannot completely explain the selective transport of CaS instead of other minerals. Slag and CaS have lower density than hot metal.
-Secondary slag dripping down from the cohesive zone has a high basicity and can dissolve more sulphur than the final slag which has dissolved the coke ash. When the slag basicity decreases due to acid coke ash CaS precipitates if the solubility of CaS in the slag at this lower basicity is exceeded (Fig. 6.8). Precipitated CaS may then be transported to the bottom on the surface of the deadman coke.

Precipitation explains why problems occur with high sulphur contents in hot metal. The sulphur load as well as the sulphur content in the slag may be high without the hearth clogging when the sulphur content in hot metal is below a certain limit. Controlling the sulphur content in hot metal can prevent hearth clogging. Mechanical hypotheses do not explain why CaS scab does not occur when the sulphur content of the slag is nearly saturated with CaS, and hot metal sulphur is below a certain limit. This limit has not been found in literature, but experiences in Koverhar give some guidelines. Before relining in summer 1995 hot metal sulphur was kept between 0.06 - 0.10 %. Clogging of the hearth was a common problem and the problems continued after the relining when the injection of oil with 1.9 - 2.8 % sulphur content increased and the sulphur content in hot metal rose to a level between 0.07 -0.08 %. Clogging of the hot metal runner below the skimmer was also a common problem. After a difficult disturbance with a chilled hearth the operation practice was radically improved by increasing slag basicity CaO/SiO_2 from 0.9 - 1.0 to 1.15 - 1.25. This was done in week no. 39/1997 (Fig. 6.9). Hot metal sulphur settled down to a level 0.05 % and below. Problems with the skimmer were eliminated almost completely, and the hearth was in good condition when inspected in August 2002. The sulphur content of slag has grown with the sulphur load without any adverse effects on the hearth condition (Fig. 6.10).
At least in case of Koverhar, the hearth clogging problems are well under control when the hot metal sulphur content is below 0.05%.

The precipitation hypothesis also explains the clogging of the hot metal runner below the skimmer in 1996, as described at the beginning of this chapter.

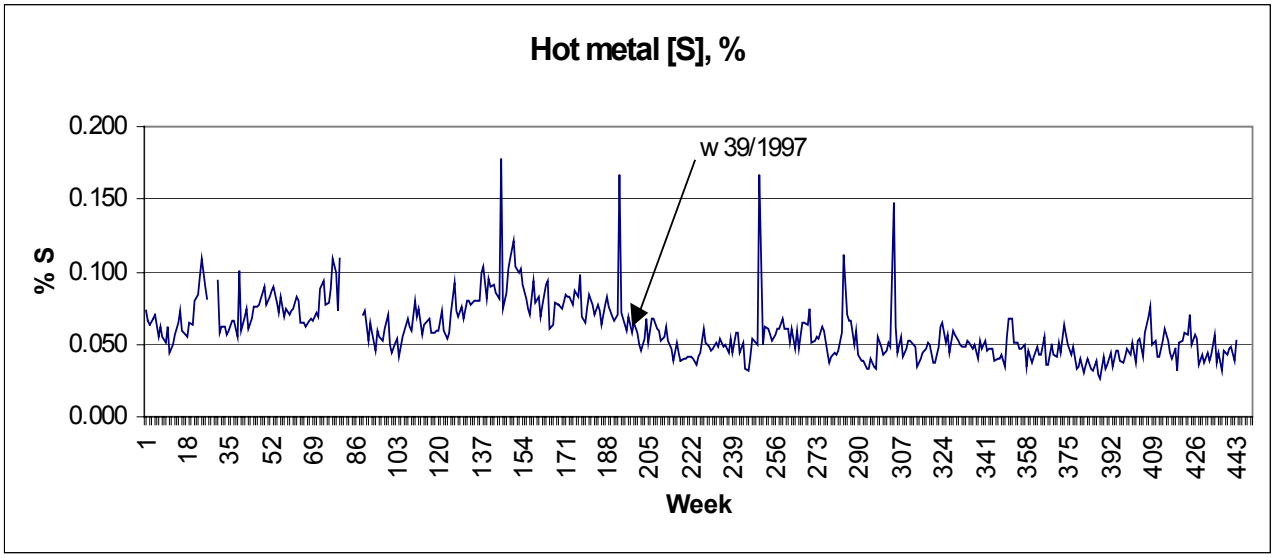

Fig.6.9 *Sulphur content of hot metal in Koverhar January 1,1994 - May 19, 2002*

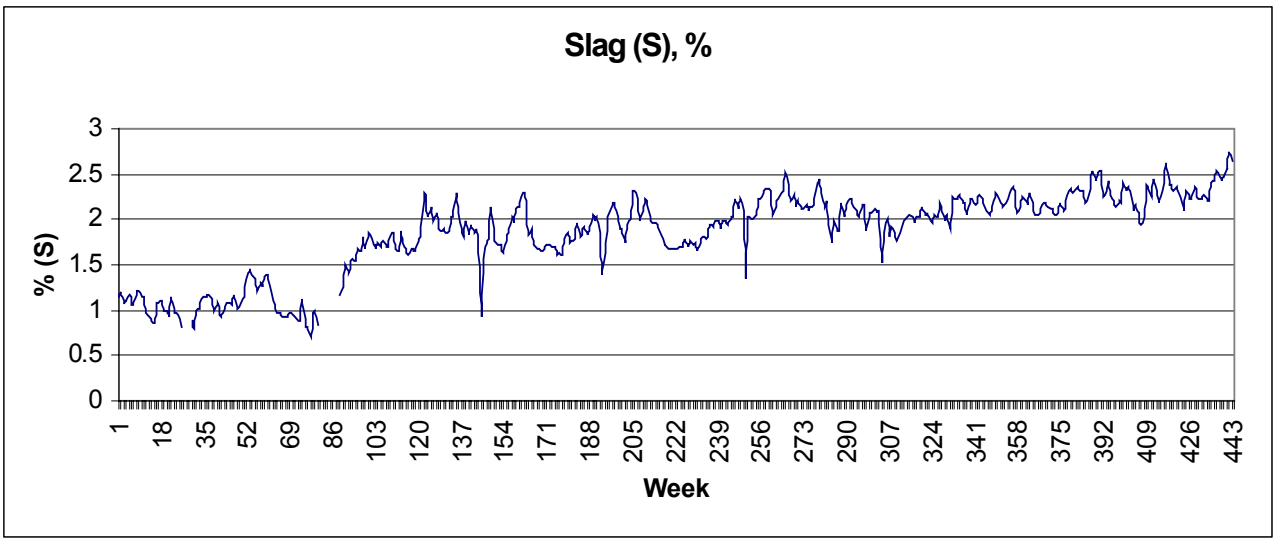

Fig. 6.10 *Sulphur content of slag in Koverhar January 1.1994 - May 19, 2002*

6.4.5 Sulphur's role in hearth problems, summarised

A clogged hearth makes the deadman impermeable and the hot metal and slag flow along the hearth walls to the tap hole. Heat transfer to the deadman decreases and it gets colder and gains in volume. The expanding deadman distorts the raceways upwards.

The cohesive zone becomes "hanging": the hot gases flow more towards the bosh walls and the cohesive zone reaches lower at 2 – 3 meters from the tuyeres and also between the tuyeres. More unreduced FeO, MnO etc. melt and dissolve into the slag. Oxygen potential in the slag increases resulting in lower sulphide capacity. The sulphur content of hot metal gets higher [high sulphur load and low slag basicity are contributing factors]. CaS precipitates on the deadman and other colder parts in the hearth and the vicious circle goes on and on.

Once the hearth has been severely clogged it can be extremely difficult to open it again. Because the scab consisting of CaS, Ti(C,N), metallic iron, slag and coke has a very good contact with the cooled carbon lining it gives a good ground for further precipitation of CaS and the scab grows. Later in Fig. 8.1 the vicious circle of scab evolution is illustrated. There are several initiating factors from coke of inferior quality to a long maintenance stop, but the growing process is self-propagating. Peeling of shaft scaffolds may also cool or even chill the hearth.

Corrective actions can be deduced from Fig. 8.1, but they all have a very long time constant. It may take weeks or months to see the effect. The most important thing is to avoid initiating factors. Lower sulphur load and low sulphur content in hot metal have shown to be beneficial in hearth control.

7 CARBON IN HOT METAL

7.1 Solubility of carbon

The following relation gives the solubility of carbon in pure iron /28/

$$\log N_C = -\frac{560}{T} - 0.375 \qquad (7.1)$$

Where N_C = atomic fraction of carbon
T = temperature, K

Chipman et al. /in 55/ give the solubility as

$$[\%C] = 1.34 + 2.54 \times 10^{-3} \times \theta \qquad (7.2)$$

Where θ = temperature in °C

Other elements dissolved in hot metal have an influence on carbon solubility. Bodsworth and Bell have collected the influence of some other elements on the carbon solubility in Table 7.1

Table 7.1 *Carbon solubility factors /28/*

X	Temp. °C	$\frac{\Delta\%C}{\%X}$	$\frac{\partial \ln N_C}{\partial N_X}$	$\frac{\partial \ln N_C}{\partial N_X}$
	REF	/41,42/	/42/	/41/
Al	1600	-0.25	-2.7	-2.7
Cr	1600	+0.9	+1.3	+0.97
Co	1600	-0.03	-0.4	
	1550			-0.50
Cu	1600	-0.2	-4.2	-4.1
Mn	1600	+0.04	+0.5	
	1500			+0.5
Ni	1600	-0.07	-0.5	
	1490			-0.99
Nb	1600	+0.12		+4.1
P	1600	-0.35	-4.6	-4.6
Si	1600	-0.30	-3.7	-4.0
S	1600	-0.40	-3.7	-4.0
V	1600	+0.13	+2.3	
	1560			+2.2
Ti	1600	+0.17	+3.3	

Factors presented by Neumann et al. /39/ for expression 5.2 are similar to values in Table 7.1.

Another method to calculate the carbon solubility is to use thermodynamic data and interaction coefficients to calculate carbon in balance with graphite.

As an example carbon content in hot metal with 0.05 % Mn, 0.515 % Si at 1500 °C as a function of sulphur content can be calculated:
Starting from

$$[C]_{Fe} = C_{Gr} \qquad \Delta G_{1500\,^\circ C} = 52\,360 \ \text{J/mol} \tag{7.3}$$

$$K_{7.3} = \frac{a_{C_{Gr}}}{a_{[C]}} \tag{7.4}$$

$$g = \ln f_C + \ln[\%C] - \frac{\Delta G}{RT} = 0 \tag{7.5}$$

By applying interaction parameters

$$g = \ln[\%C] + e_C^C \cdot [\%C] + e_C^{Si} \cdot [\%Si] + e_C^S \cdot [\%S] + e_C^{Mn} \cdot [\%Mn]$$

$$+ r_C^C \cdot [\%C]^2 + r_C^{Si} \cdot [\%Si]^2 + r_C^S \cdot [\%S]^2 + r_C^{Mn} \cdot [\%Mn]^2 - \frac{\Delta G}{RT} = 0 \tag{7.6}$$

and taking partial differentiation

$$\frac{\partial g}{\partial [\%C]} = \frac{1}{[\%C]} + e_C^C + 2 \cdot r_C^C \cdot [\%C] \tag{7.7}$$

and solved as presented in chapter 6.4.3.

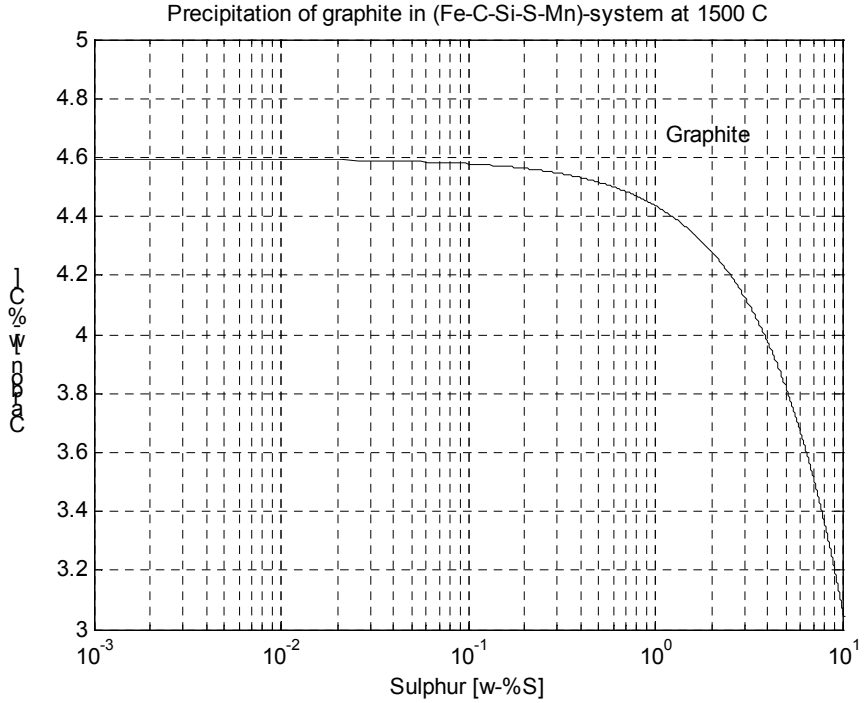

Fig. 7.1 *Equilibrium precipitation of graphite as a function of sulphur in hot metal at 1500 °C.*

Fig. 7.1 shows a moderate influence of sulphur on carbon solubility up to about 0.2 % sulphur content. The result is congruent with expression 5.2.

7.2 Actual data from blast furnaces

As mentioned in chapter 1, carbon content is an important part of the total quality of hot metal. Nearly 80% of the total reaction energy in the BOF process comes from oxidation of carbon in hot metal. That is why carbon content should be as high as possible. Hot metal for steel making is not saturated with carbon as foundry iron usually is. Fig. 7.2 shows the difference between the carbon content at saturation (calculated with expression 5.2) and the actual carbon content. The difference has been in average 0.77 % during January1 - May 22, 2003.

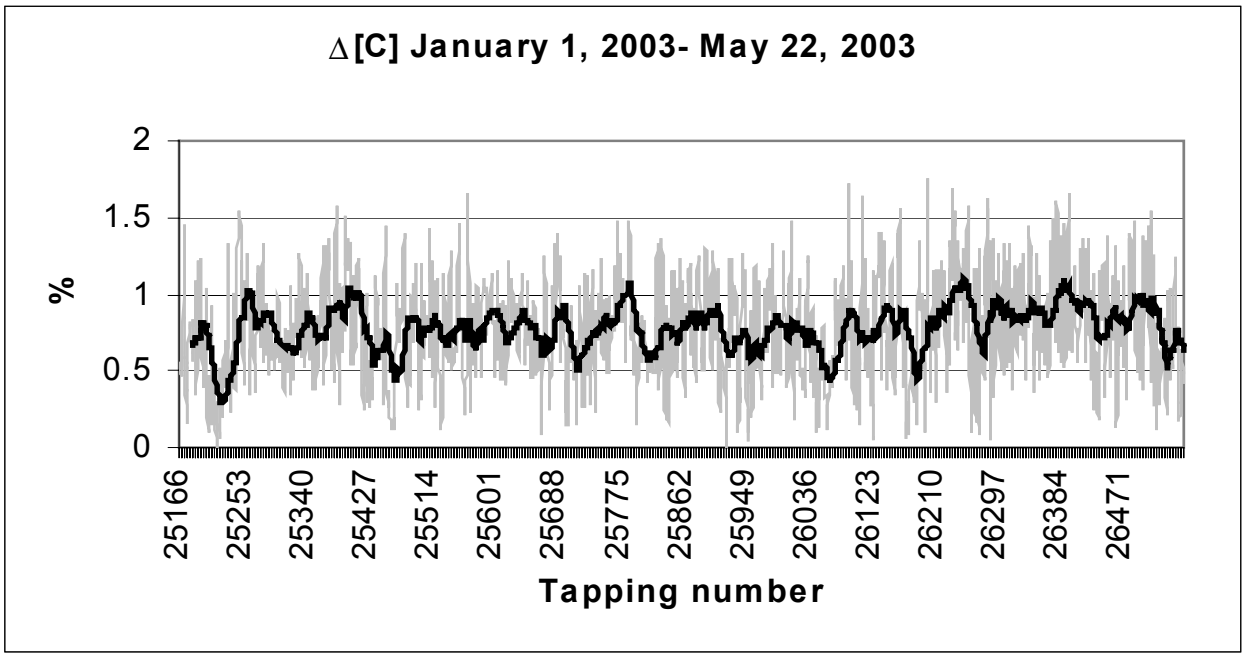

Fig. 7.2 *Difference* $[\Delta C] = [\%C]_{sat} - [\%C]_{actual}$ *in hot metal during 1.1 - 22.5.2003 in Koverhar. Moving average for 20 tappings added.*

In order to find an explanation to the large and varying difference between carbon saturation and actual carbon content a comparison was made together with Swedish and Finnish blast furnace plants. A regression study of hot metal compositions at the different plants was made. 1000 to 3000 tappings from five Swedish and Finnish blast furnaces were analysed. Data from periods of seriously disturbed operation have been removed. The regression formulas are presented in the same way as the carbon solubility in expression (5.2).

$$[\%C]_{actual} = k_0 + k_{\theta HM} \cdot \theta_{HM} + k_{Si} \cdot [\%Si] + k_P \cdot [\%P] + k_S \cdot [\%S] + k_{Mn} \cdot [\%Mn] \qquad (7.8)$$

The results are presented in Table 7.2 as coefficients for the terms in (7.8)

Table 7.2 *Results from regression $\%C_{actual}$ analysis*

BF PLANT	k_0	$k_{\theta HM}$	k_{Si}	k_P	k_S	k_{Mn}	R^2	n
A	0.095	0.00306	0.206	-0.594	-5.48	0.629		3000
A	0.405	0.00288	0.171	-0.903	-6.01	0.650	0.580	3359
A	0.181	0.00322	0.156	-4.91	-5.68	0.440	0.584	1679
A	0.423	0.00286	0.174	-0.649	-6.07	0.642	0.607	3359
B	4.36	0.00006	0.606	-4.40	-4.63	0.553		1600
B	1.44	0.00351	0.540	3.96	-1.33	0.819	0.399	1239
C	-0.47	0.00347	0.294	-8.92	-2.14	0.159	0.730	1926
C	1.82	0.00215	0.231	-10.7	-4.59	0.114	0.604	1775
D	3.50	0.00098	0.130	-18.3	-6.53	1.45	0.818	3473

R^2 = Multiple R square
n = Number of observations

There are some striking differences between the factors in the solubility formula and those in the multiple regression formulas. Some comments about the factors:

k_0: The constant has no special significance. It depends on the model as a whole.

$k_{\theta HM}$: Most of the values are consistent with the corresponding coefficient in expression (5.2)

k_{Si}: The strong interaction between [Si] and temperature is generally known. In these data sets the variation of [Si] has been small, the effect of the temperature also shows in the coefficients of [Si] turning them positive. The basic effect of [Si] (Fig. 7.13) cannot be seen.

k_P: Also the variations of [P] in these data sets are small. The significance of [P] is small and it can be neglected.

k_S: The coefficients of [S] are significant and a decade larger than in expression (5.2). The difference in sulphur coefficients k_S compared to -0.36 in expression (5.2) needs to be more deeply investigated.

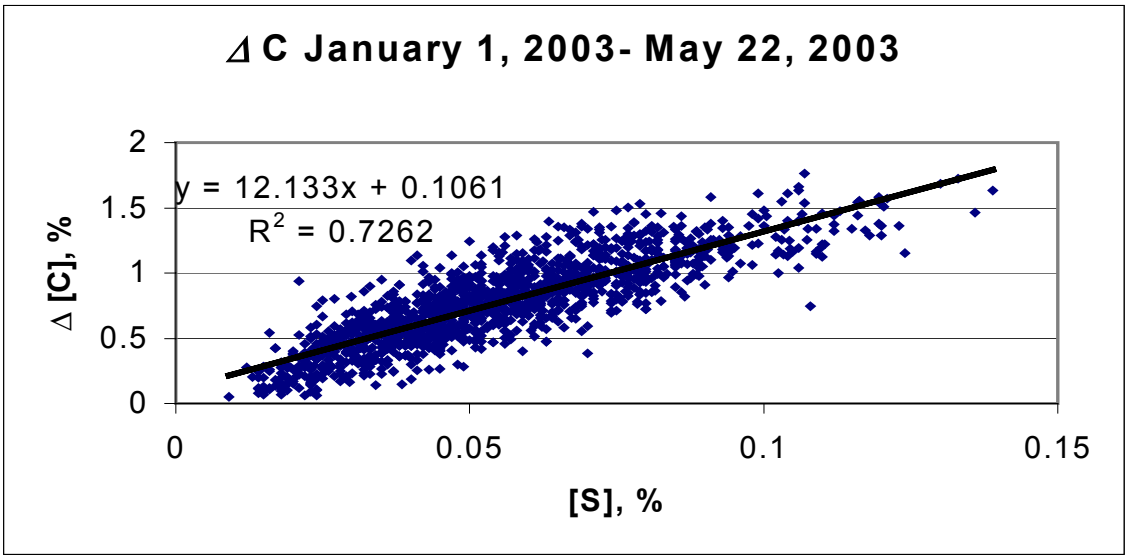

Fig. 7.3 *Difference $[\Delta C] = [\%C]_{sat} - [\%C]_{actual}$ as a function of sulphur content in hot metal. Same data as in Fig. 7.2*

The difference $[\Delta C] = [\%C]_{sat} - [\%C]_{actual}$ increases faster than the sulphur content in hot metal predicts. As shown in Fig. 7.2, the influence of sulphur should be almost linear up to 0.2%. For

example, if the hot metal sulphur content is 0.08 % then the expected value of the carbon content with a given hot metal composition and temperature is 4.57% but in Koverhar's conditions the measured carbon content is 3.6%. So there must be some kinetic factors governing carbonisation which will be discussed later.

Carbon and sulphur have a strong interaction. By controlling the heat level of the blast furnace process one can control carbon content to some extent, but it means more fuel consumption. Controlling sulphur by slag basicity is a better way because it results in hot metal with lower sulphur and higher carbon contents.

Kinetics in the blast furnace process is extremely complicated making it interesting to find the route how the carbon content is determined.

As mentioned earlier, the deadman and hearth phenomena play key roles in hot metal quality. The condition of the deadman has a strong influence on hot metal temperature and composition. The conditions are good for desulphurisation and carbonisation of hot metal when hot metal can flow freely towards the tap hole and the deadman is a porous coke bed. High sulphur content indicates deficient hearth operation with high FeO content in the slag even though the hot metal temperature is high /40/.

Oil injection was adapted in Raahe and Koverhar at the end of the sixties. In Koverhar heavy fuel oil was used 30 – 60 kg/tHM. Extra heavy bottom oil with 1.5 – 3.0 % S has been used in Koverhar since 1994. The oil rate remained on a level of 50 – 70 kg/tHM for five years. Now when injection technique has been improved, oil rates of 120 kg/tHM have been reached with oxy-oil technique during 2002. Even higher rates are planned. External desulphurisation has been in use since 1986. Though sulphur content of treated hot metal is managed it is still a costly operation.

During 1986 – 1988 six different coke grades were used in Koverhar in many various mixtures. Also here significant differences in carbonising effect could be observed, but no explanation could be found.

Carbon content of hot metal is an important subject because the energy content of hot metal is of great importance in BOF process and also because it is an indicator of the hearth operation and possible erosion of the hearth lining.

7.3 Beginning of carbonisation

Carbonisation is a complicated process starting in solid phase when metallic iron is formed. The carbonising agent is most probably CO gas (in $CO/CO_2/H_2O/H_2/N_2$-atmosphere) in the shaft. Direct carbonisation at some contact points with freshly reduced iron and coke carbon may also take place. Carbonisation continues in contact with coke carbon and CO gas when the metal melts and trickles down through the bosh coke layer to the hearth where it gets its final tapping composition.

At least the following factors play their role in the carbonisation of hot metal:

- Gas phase composition and temperature $\left(p_{CO}, p_{O_2}\right)$
- Coke (and char) properties (reactivity)
- Hot metal composition, especially sulphur and silicon
- Hot metal temperature
- Sulphur load

- ✧ Slag composition on different process steps
- ✧ Reduction of iron oxides
- ✧ Deadman condition
- ✧ Retention time.

In September-October 2002 a test campaign was run at the experimental blast furnace of LKAB in Luleå, Sweden. During the campaign samples were taken from the shaft with probes at different levels: higher shaft probe①, lower shaft probe③ and inclined probe⑥ which could reach to the cohesive zone (Fig.7.4). During sampling the furnace was always on full blast. The hollow probe was pushed in with slow rotation and the material was collected in the probe. When the probe was pulled out nitrogen was purged in it cooling the sampled material.
The great value of this kind of samples comes from the fact that the samples are from a furnace on full blast and they have been cooled rapidly so that most of the chemical reactions have been interrupted quite fast.

Rem.: In chapter 7.3 the carbon contents in iron phases of the pellets are approximations based on recognised structures and their amounts. Carbon could not be analysed using SEM from the phases.

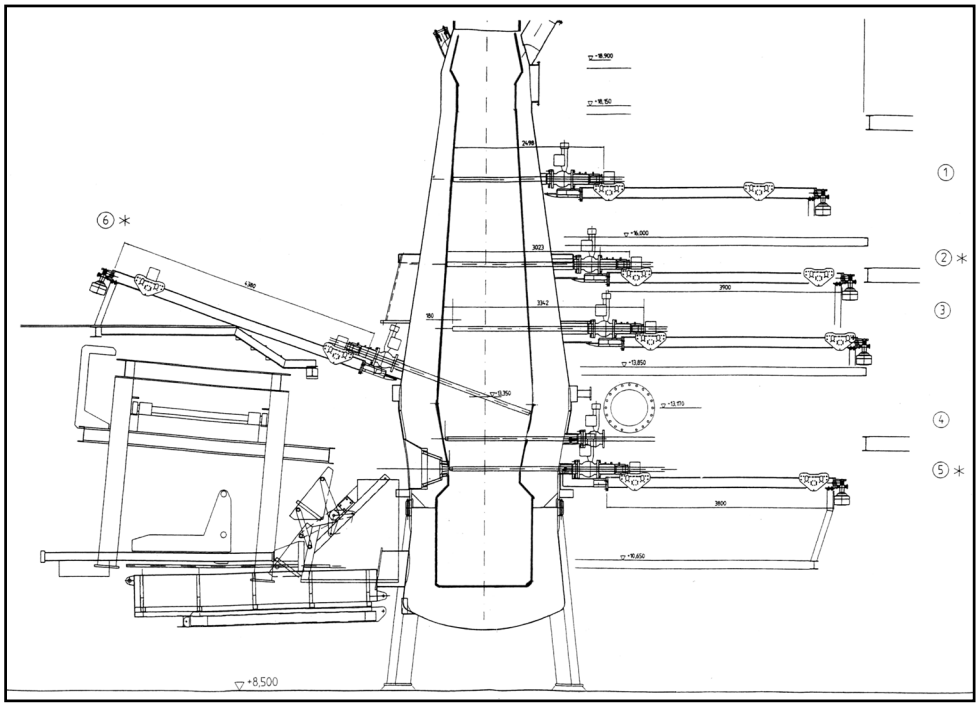

Fig. 7.4 *The experimental blast furnace of LKAB*

The higher shaft probe① is located 1 m below the stock level. The temperature at this level is about 600 - 700 °C. The lower shaft probe③ is located 2.5 m below the stock level and the temperature at that level is between 1000 and 1100 °C. Measured gas compositions are presented in a Baur-Glaessner diagram in Fig. 7.5. Hydrogen content in the gas was 12 % through the centre and wall side. In the mid radius it was 10% at 1000 °C and 6 % at 660 °C.

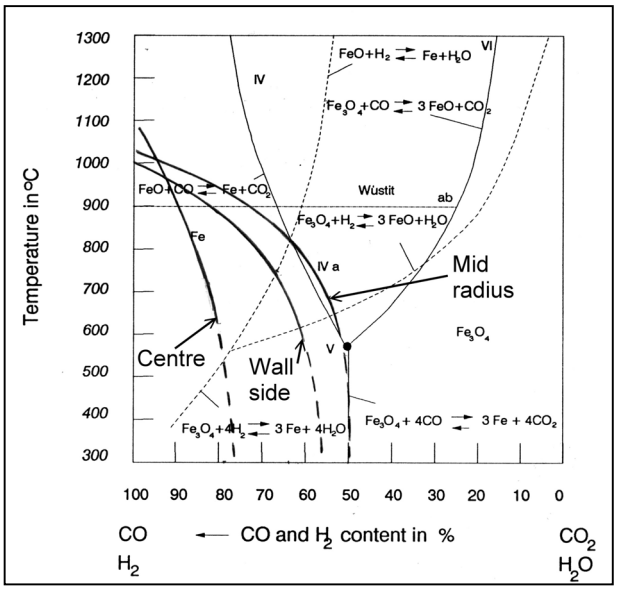

Fig. 7.5 *Gas compositions and temperatures in the experimental blast furnace plotted in a Baur-Glaessner diagram.*

In a sample from probe① iron oxides were almost completely reduced. Some FeO-rich residual slag was left on ferrite grain boundaries and no signs of carbonisation were seen (Fig.7.6).

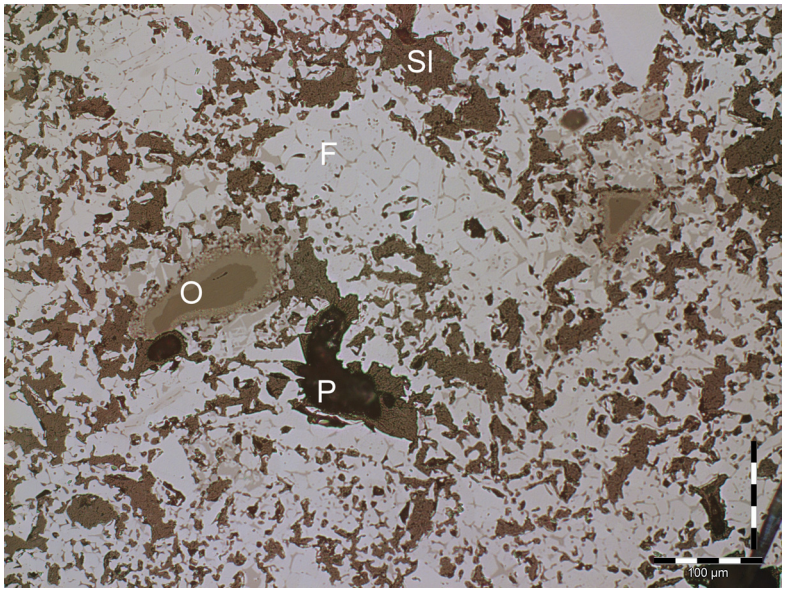

Fig. 7.6 *Pellet sample from higher shaft probe①. F = ferrite grains with interstitial slag on grain boundaries, Sl = slag, O = olivine grain, P = pore. Sampled September 30, 2002. Scale bar 100 µm.*

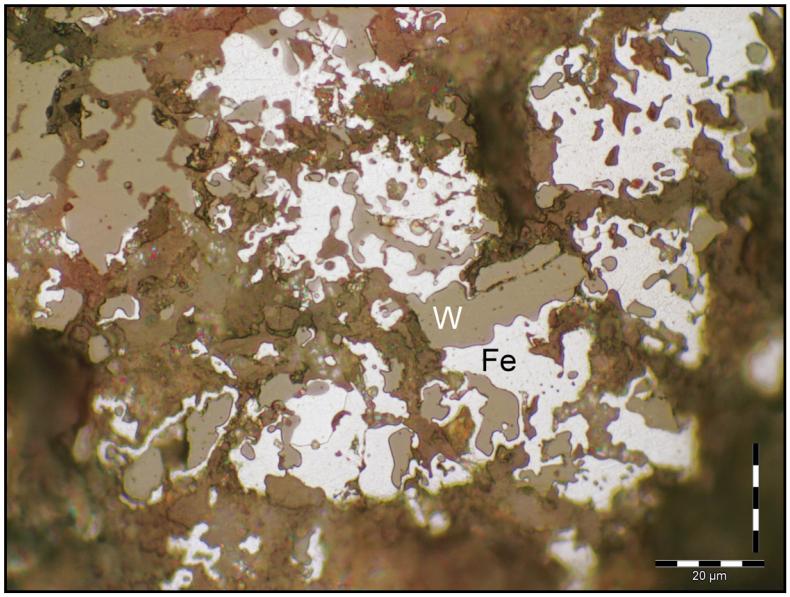

Fig. 7.7 *Sample of weakly clumped pellets from lower shaft probe③. Beginning softening, but still open and porous structure. Wustite and iron (ferrite) are in close contact and there are no signs of carbonisation. Sampled October 5, 2002. Scale bar 20 µm*

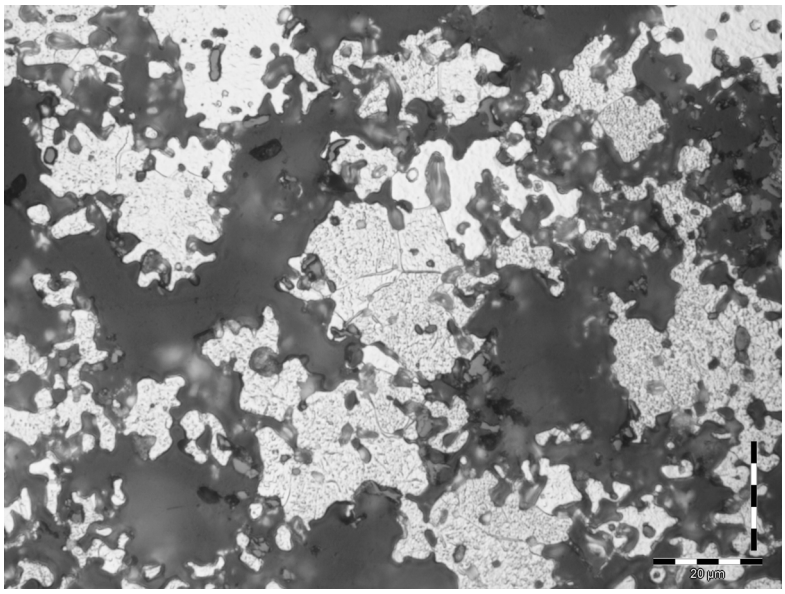

Fig. 7.8 *Another sample of weakly clumped pellets from lower shaft probe③. Similar structure as in Fig. 7.7. Sampled October 11, 2002. Scale bar 20 µm*

The inclined probe⑥ may reach the cohesive zone assuming that the cohesive zone extends high enough at the moment samples are taken. Anyway, the probe penetrates some loose layers before it hits the cohesive zone. Temperatures in this region are 1100 -1400 °C.

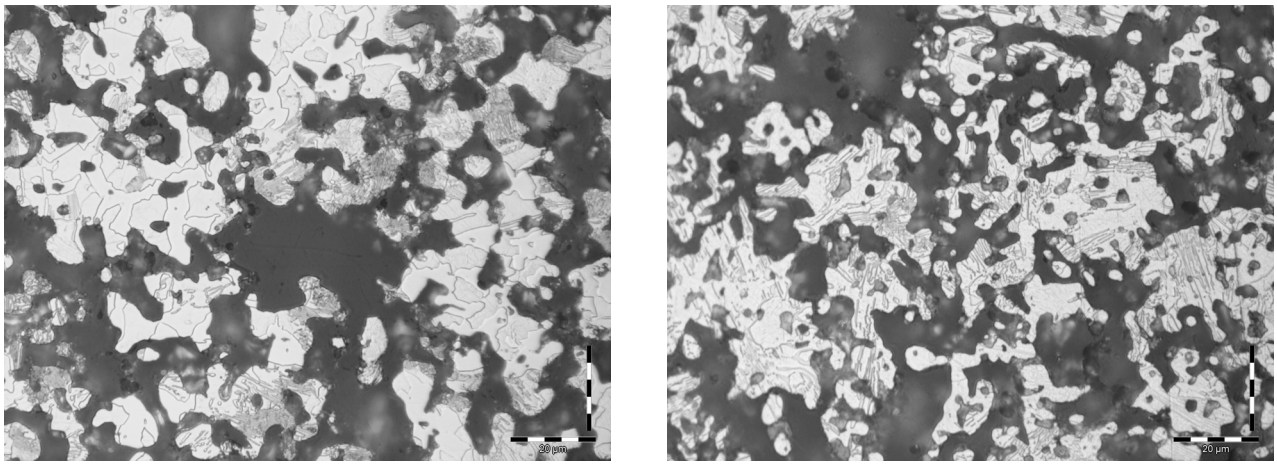

(a) (b)

Fig. 7.9 *Two pellets from same sampling with inclined probe⑥. These pellets were porous and equally reduced from surface to core. In (a) about 0.3 % C (40% pearlite) and in (b) about 0.6 %C (80% pearlite). Sampled October 4, 2002. Scale bar 20 µm*

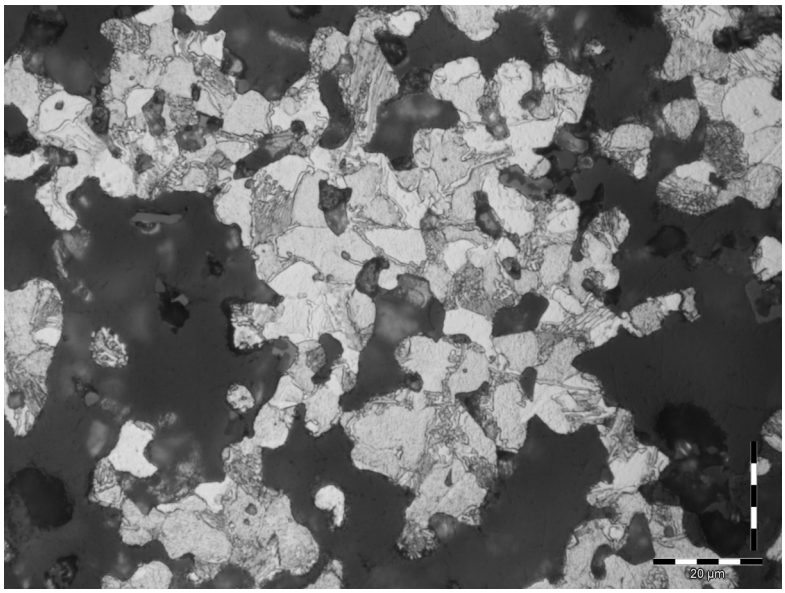

Fig. 7.10 *Sampled with inclined probe© five days later than in Fig.7.8.*
Porous pellet with about 0.1 % C throughout the pellet.
Sampling October 9, 2002. Scale bar 20 µm

With an optical microscope pearlite was not found in iron grains when wustite was present. It means that carbon content remains very low as long as there is wustite present. Solid freshly reduced iron grains contain only traces of carbon. Carbon pick-up from gas phase takes place when there is reduced iron in contact with gas and temperature at about 1000-1100 °C.

Carbonisation of steels for hardening is made at temperatures of 920 - 1100 °C in CO rich atmospheres /43/. The reactions are:

$$2CO \rightarrow CO_2 + C \qquad (7.9)$$

$$C \rightarrow [C] \qquad (7.10)$$

Obviously the reactions are the same in a blast furnace because the conditions are similar.

Investigation of samples from an operating blast furnace (Experimental blast furnace of LKAB) have revealed how the carbon pick-up and reduction can proceed in a same pellet (Fig. 7.11):

on the surface there is about 10 µm layer of cementite
on some places also 50 µm of ledeburite
then 200 µm of pearlite with cementite on grain boundaries
then 100 µm of pearlite
then 150 µm of pearlite with ferrite on grain boundaries
then 2000 µm of ferrite and slag phase
and innermost 6000 µm in diameter melt rich in FeO.

Approximating with these dimensions gives an average carbon content 0.5 - 1 % for the metal in one pellet.

Liquidus temperature of iron containing carbon equivalent to cementite-ledeburite layer is 1148 °C. The temperature of this pellet has been very close to this temperature.
The carbon content of melting and trickling iron is above 2.1 % rising rapidly in contact with coke and CO according to the Fe-C phase diagram.

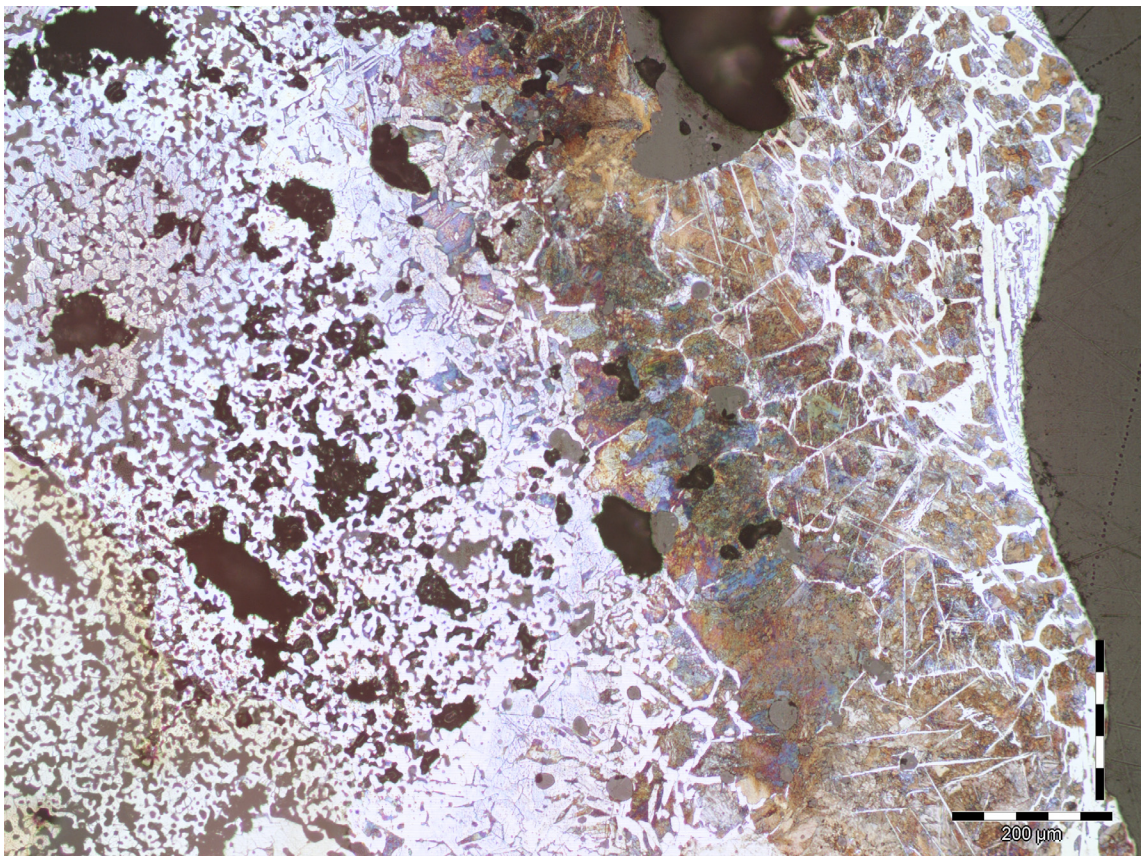

Fig. 7.11 *Polished and etched sample of a reduced pellet from little above the cohesive zone. Sampled October 14, 2002. Scale bar 200 µm.*

Some indication for the hypothesis that the carbon for the first carbonisation comes from the gas phase are that cementite and pearlite covers the pellet all around, except in some places where adhered slag covers the surface as can be seen in Fig. 7.12.

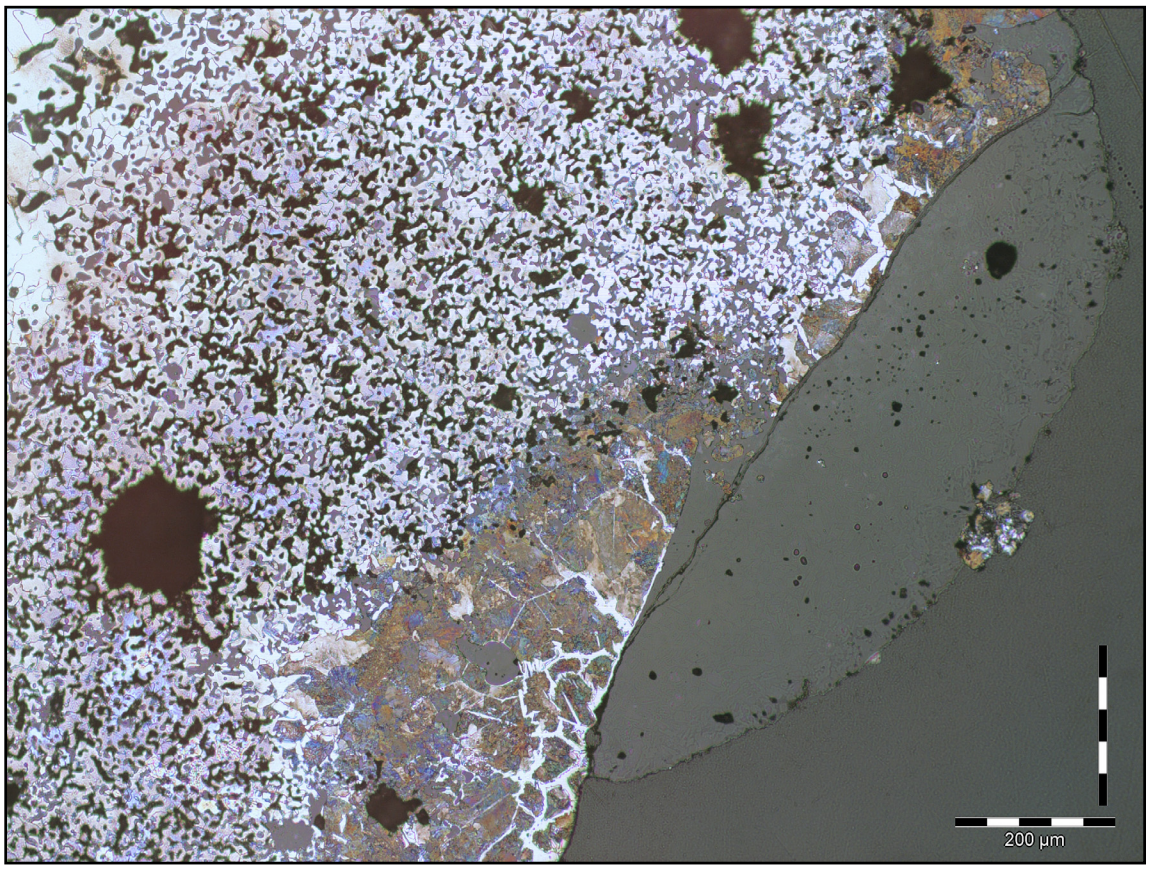

Fig. 7.12 *The same pellet as in Fig. 7.11. Covering grey slag drop on the right retarding the contact with CO. Scale bar 200 µm.*

7.4 Carbonisation by solid carbon

As described in the preceding chapter carbonisation begins to a significant amount when there is fresh iron without FeO at sufficient temperature and CO pressure. Anyway, coke, coal or oil char are the main carbonising agents when molten iron trickles down from the cohesive zone. The dissolution rate of solid carbonaceous material can be expressed

$$\ln\frac{([C]_s-[C]_t)}{([C]_s-[C]_0)}=-\frac{A\times k}{V}\times t \qquad (7.11)$$

where $[C]_s$, $[C]_t$ and $[C]_0$ are carbon content in weight percent at saturation, at time t and in initial melt. A is the contact area (m^2) between carbonising agent and the melt, V is the total volume (m^3) of the melt, k the mass transfer coefficient (m/s) and t the time (s). The mass transfer coefficient k can further be expressed:

$$k = k_0 \times v^n \qquad (7.12)$$

where k_0 is a constant and v the melt velocity (m/s). The value of n varies from 0.5 to 0.75 in laminar flow. Gudenau et al. have studied the carbonising effect of different cokes and significant differences in their carbonising effects have been found /44/.
For practical measurements Gudenau et al. have defined an index n^*, "ash factor", to characterise coke qualities. When $n^* = 1$, the coke reacts like graphite and when $n^* = 0$, carbon pick-up will not happen.

$$\ln\frac{([C]_s-[C]_t)}{([C]_s-[C]_0)}=-\frac{A\times k_0\times v^n\times}{V}\times t^{n^*} \qquad (7.13)$$

Gudenau et al. reported results of 13 industrial grades of coke and 10 test coke grades. They observed that high MgO and Al_2O_3 contents inhibit carbon dissolution considerably whereas high Fe_3O_4 and CaO favour it. In these tests the metal had an initial composition of 2.2-2.5% C, 0.01-0.03% S, 0.3-0.4% Si, 0.06% Mn and 0.035% P. The temperature was 1540±10 °C.

Wu and Sahajwalla studied carbon dissolution from different graphite and coal grades into iron with different sulphur contents /45/. They defined the overall dissolution rate constant K (s^{-1}) with an expression (7.14):

$$K=\frac{A\times k}{V} \qquad (7.14)$$

In their experiments they found a significant correlation between hot metal sulphur and the rate constant:

$$K\times 1000 = 0.523\times\left(\frac{1}{\%S}\right)+9.92 \qquad \text{When } 0.034 < \%S < 1.15 \qquad (7.15)$$

The carbon dissolution rate from graphite is greater than from coal. There are considerable differences between coal grades as well as between graphite grades. The carbon dissolution rate constant is dependent on crystallite size of carbonising agent. It is high for graphite with around 200 Å and low for coal with low C content having around 10 Å.

As the final carbon content develops in the hearth the condition of the deadman plays an important role. Looking only at the specific coke area it would be desirable to have small size coke in the hearth giving a large specific surface (A/V), but small coke size makes the deadman prone to be clogged with coke breeze and slag. Therefore large coke size is preferable enabling free flow of hot metal through the deadman. A floating deadman and the coke free corners in the hearth reduce the contact area between coke and hot metal, too. This phenomenon can be monitored e.g. with the slag ratio (4.1).

It is very difficult to obtain good desulphurisation and carbon pick-up when the deadman is inactive /40/. Centre coke charging has been the key to control the deadman.

7.5 Silicon and temperature

Silicon decreases carbon solubility in hot metal (Fig. 7.13). This can be observed especially when foundry iron is produced; hot metal is saturated with carbon as can be deduced from graphite precipitation (kish graphite) during tapping.

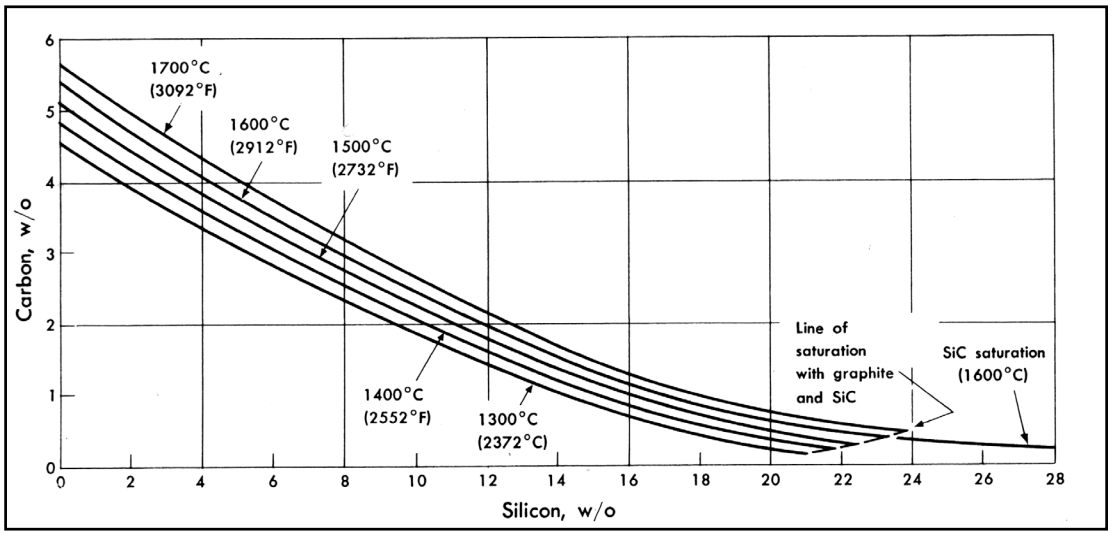

Fig. 7.13 *Carbon solubility in iron-silicon alloys /3/*

In basic iron operation it looks like it would be the opposite – higher carbon with higher silicon content. This can also be seen in Table (7.2). Probably, the explanation is that a high hot metal temperature and a high silicon content are only indicators of the high heat level in the blast furnace.

Not only the heat level determines the hot metal temperature but it also depends on the deadman condition. If the deadman is inactive the hot metal temperature can be higher than normal because the metal is not mixed with larger amounts of colder sump iron.

7.6 Role of sulphur

The sulphur content has usually been considered a result of slag basicity, hot metal carbon, temperature etc. and the carbon content an outgrowth. However, the very strong correlation between sulphur and carbon contents in hot metal (Fig.7.14) has aroused the question if the opposite could be possible; could the carbon content be controlled by the sulphur content in hot metal and how?

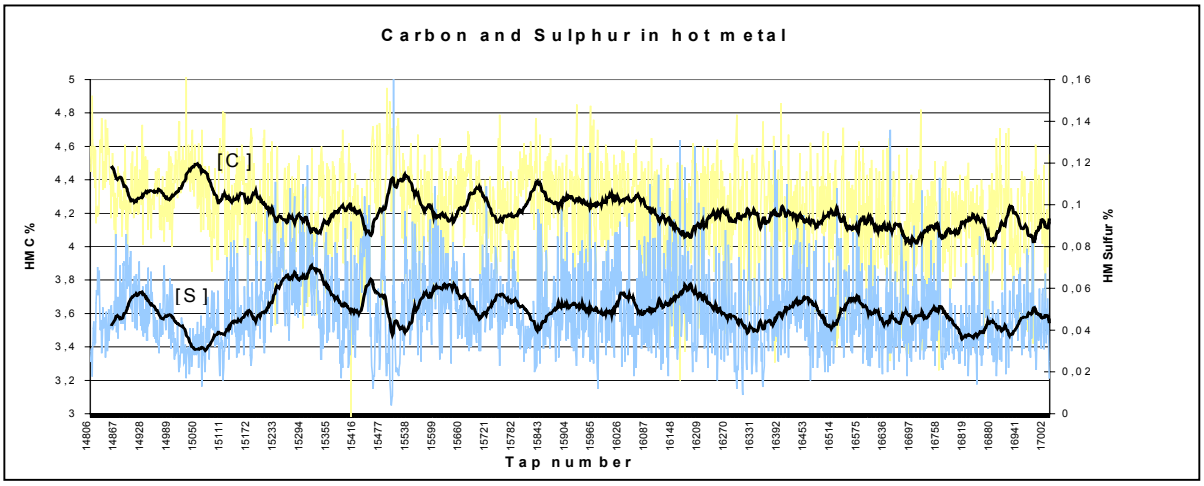

Fig. 7.14 *Carbon and sulphur contents in hot metal during 01-Jan-2000 – 31-July-2000 in Koverhar*

The interaction coefficients work in both directions. Recently Sahajwalla and Khanna /51 and 55/ have shown by mathematical simulation how sulphur retards carbon dissolution from graphite and also carbon diffusion in iron melt. These results confirm their earlier experimental results /45/. In Fig. 7.15 it is shown how carbon dissolves into iron melt and how sulphur moves from the interface deeper into the melt. Sulphur does not block the interface. Fig. 7.16 shows how sulphur affects retarding on carbon dissolution rate. Difference in rate constant between 0% S and 4% S does not look very large, but it reveals a clear trend. 4% S in hot metal also seems extremely high but it can be locally accurate in the cohesive zone.

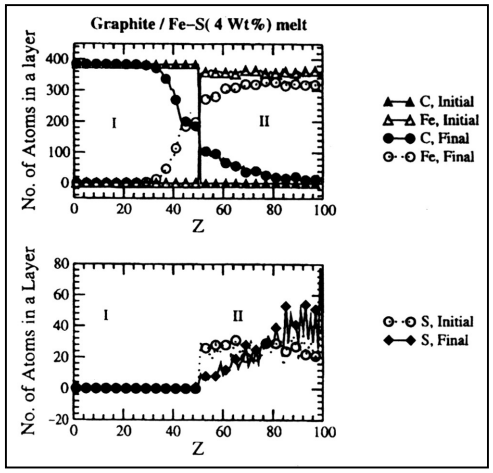

Fig. 7.15 *Atomic distribution at graphite /Fe-S interface. Z = atomic layer number /55/.*

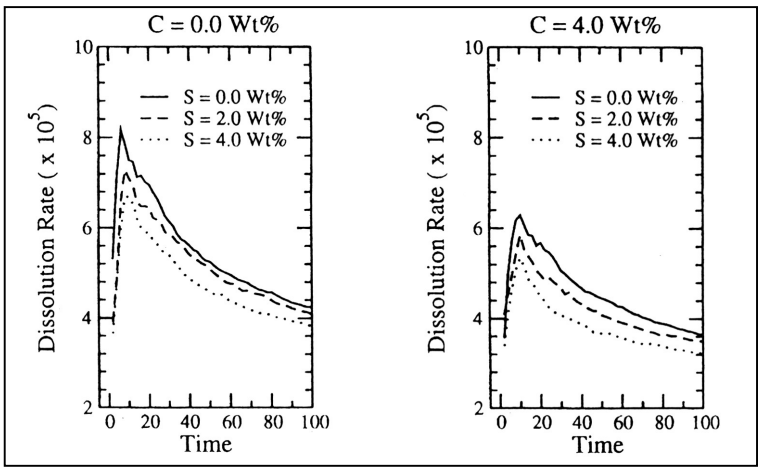

Fig. 7.16 *Carbon dissolution rate as function of time /55/.*

The retarding effect of sulphur on carbon dissolution can explain the difference between carbon content at saturation and actual carbon content of hot metal to a large extent. The residence time in the hearth is too short for the hot metal to reach carbon saturation.

The following hypothesis seems to work. Just before melting the metal contains above 2% C and over 0.1% S. The primary slag is high in FeO, depending on the degree of reduction, and the desulphurisation power is very low. When the first metal droplets form in contact with coke the carbon pick-up takes place, but because the sulphur content is high the dissolution is retarded. Concurrently, the reduction of FeO proceeds and desulphurisation of metal droplets becomes more effective.

Here the surface phenomena may also have their role: sulphur will decrease the contact surface between coke and hot metal by increasing the contact angle. Slag sulphur will increase the slag wettability with coke covering its surface from hot metal and carbon pick-up. Both phenomena hinder carbon uptake.

Desulphurisation takes place mainly during trickling through the bosh coke in contact with slag and when hot metal settles through the slag layer into the hearth. Some desulphurisation takes place in the hearth in contact with the slag layer and also during tapping when hot metal and slag come to contact in the tap hole. The sulphur content of hot metal varies during the tapping. In an investigation at bast furnace Raahe nr.2 it was observed a clear descending trend of hot metal sulphur content, but after 40 minutes from the sulphur content began to rise /57/. The descending trend can be explained by a layer-wise filling of the hearth: the first tapped hot metal had a shorter time to react with the slag. The freshly produced hot metal came out at about 40 minutes from the tapping start and trickled through a thicker slag layer. The increasing trend after 40 minutes from tapping start can be explained by mixing with old hot metal below the tap hole level. The remaining slag on the opposite of the taphole side displaces older hot metal and pushes it to the tap hole. Floating deadman has a similar effect at the end of a tapping. Waller et al. have observed a similar trend when examining ladle analyses from Raahe nr.1 and 2 /58/.

7.7 Other factors affecting carbonisation

The effect of reduction degree can be anticipated with time series analysis. The following model (R^2=0.77, F_{Tot} =379) illustrates the idea:

$$[C]_t = 2.63 - 9.8\times10^{-4}\times O_{SL,t-2} + 0.80\times[Si]_t + 1.14\times(CaO/SiO_2)_{t+2} \qquad (7.16)$$

where $O_{SL,t-2}$ = Solution loss oxygen at time t-2 hours , Nm^3/tFe
$[Si]_t$ = Si% in hot metal at time t, hours
$(CaO/SiO_2)_{t+2}$ = Slag basicity at time t+2, hours

Solution loss oxygen is calculated continuously from oxygen balances. It tells how complete the indirect reduction of iron oxides have been when the hot metal in this actual tapping has been melted. If, for example, the reduction of the burden has been poor, then the reaction 4.2 has been pronounced, which can be observed as increased solution loss oxygen and two hours later as decreased carbon content in hot metal. Burden properties and distribution control are used to get good reduction. This affects carbonisation in two ways: carbonisation by CO gas has been retarded because there has been larger amount of FeO in contact with reduced Fe (Fig. 7.6 - 7.8) and higher FeO content in the slag decreases the sulphur partition.

The effect of slag basicity can be seen better in the next tapping about two hours later because there is always residual slag in the hearth. The residual slag is mixed with the slag that has been melted at the same time with hot metal at time t.

This expression is an approach to show how the hot metal carbon can be controlled with slag basicity and also with heat level (indicated by hot metal $[Si]_t$) of the blast furnace. For blast furnace operation and desulphurisation CaO/SiO_2 = 1.15 –1.2 gives good conditions.

The final carbon content is formed in the hearth where deadman condition is of great importance. The larger the contact area between hot metal and coke is, the better are the conditions for carbonisation. If the deadman is clogged, the hot metal is in contact with the inactive deadman, the hearth walls and the coke between the deadman and the walls, resulting in poor carbonisation conditions.

MgO in slag has been reported to influence the contact area between the hot metal droplets and the bosh coke (Ref. /9/, page 561). It has a tendency to depress wetting of coke by slag thus leaving more area for hot metal to contact coke. To study these factors a regression analysis was made. A regression formula was determined (n=2206, F=868, R^2=0.81) based on tapping data:

$$[C]_{HM} = -0.487 + 0.00285 \times \theta_{HM} + 0.104 \times [Si] - 8.17 \times [S] + 0.0543 \times (MgO) + 0.140 \times \rho \qquad (7.17)$$

where θ_{HM} = hot metal temperature, °C
ρ = slag ratio, (expression 4.1)

A large value of ρ means a short slag delay and loose structure of the hearth coke and consequently large free volume for hot metal and slag as described in chapter 4.2.2.
The positive effect of MgO in slag can be seen from the positive coefficient of (MgO).
The significance of the other coefficients is commented in chapter 7.2.

8 DISCUSSION

Regarding hot metal quality there are many sources of disturbances starting from raw materials handling through the blast furnace process ending in the casting of the hot metal. This study has concentrated on three closely interconnected problems: hearth operation and hot metal sulphur and carbon. The main purpose is to show that there are applicable methods to control the hot metal quality.

Fig. 8.1 shows some of the most common reasons for a clogged hearth or an inactive deadman on the left side. The list can be completed with peeling scaffolds from the shaft, burdening failures etc. If the symptoms are identified in an early stage severe problems can be avoided by taking appropriate measures. Sudden disturbances are usually cured by fixing the reason, but a slowly developing inactivation is not so easy to detect and requires patience and special insight, which were discussed in chapter 5.4.

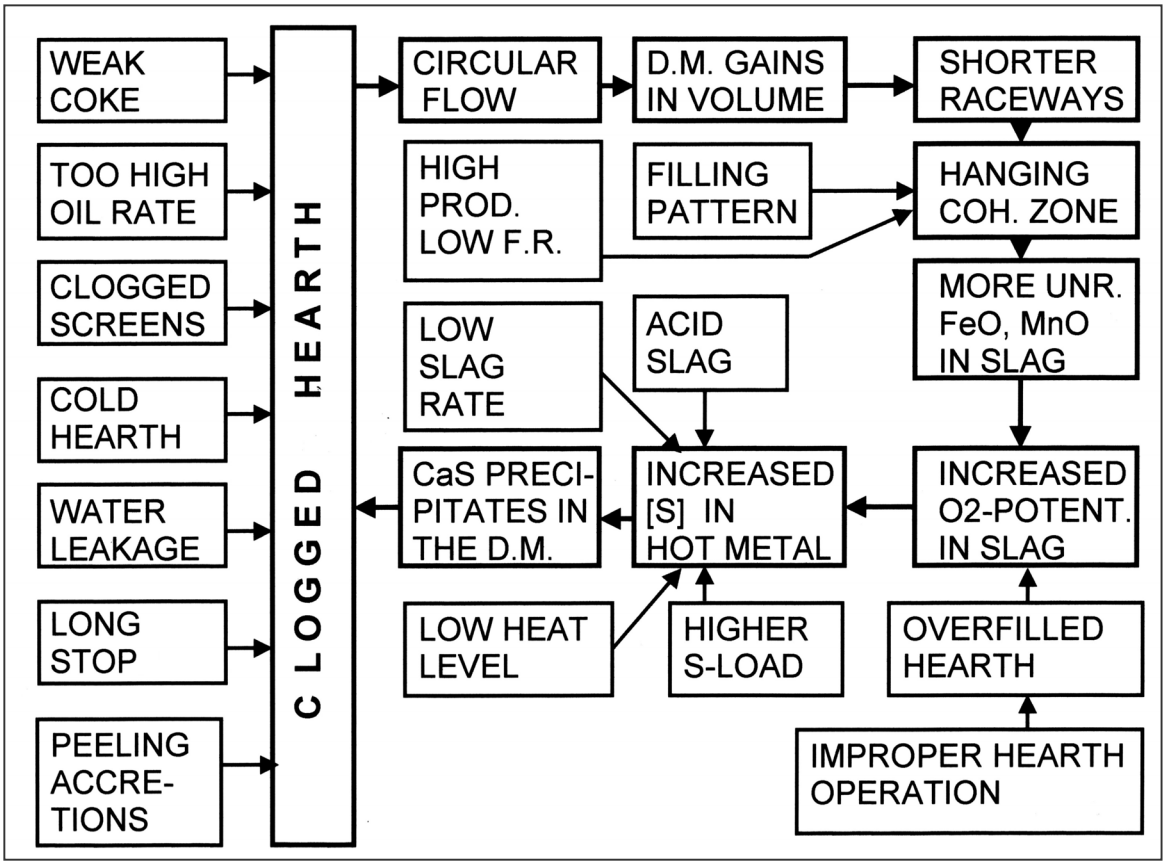

Fig. 8.1 *Evolution of clogged hearth problem*

Clogging of the hearth starts from the bottom and gives soon clear signs such as high sulphur content, low carbon and high hot metal temperature. Slag ratio is shortened and bottom temperatures start to decline (Chapter 5.2). A circular flow of hot metal around the deadman due to its impermeable structure slows down the heat transfer to the deadman because freshly melted hot slag and metal do not bring heat into it. The deadman starts to expand when slag and coke fines adhere to the relatively cooler surface.

When the deadman expands the raceways become shorter, they bend upwards and further towards the bosh walls leading to a hanging cohesive zone. The melting rate at the peripheral areas grows and more unreduced FeO and MnO drop below the tuyere level increasing the oxygen potential of the slag-metal system.

A high production rate as well as a low fuel rate has a similar effect lowering the location of the cohesive zone. Changing movement of the burden in the bosh makes adjustment of the burdening pattern problematic. An overfilled hearth distorts the raceways, too, retards descending of the burden or even stops it. At the end of the tapping the burden slips down bringing excess FeO and MnO into the final slag.

Sulphur causes special problems in the blast furnace operation. It can be an essential factor in the chain of a vicious circle as is shown on the right side of Fig. 8.1. Increasing oxygen potential of the slag-metal system deteriorates sulphur removal and the sulphur content of hot metal gets higher. Conditions for precipitation of CaS on colder parts of the deadman become favourable.

The last phase of carbon pick-up from about 2-3 % to the final over 4.5 % takes place in the hearth. Carbon pick-up depends on many coke properties, but also on the sulphur content of hot metal, because there is a strong interaction between carbon and sulphur. Possibilities to control coke properties lie outside this study. Experience from blast furnace operation shows that it is possible to control the carbon content by controlling hot metal sulphur with slag basicity.

Although carbon and sulphur have a strong interaction the order of cause and consequence is not always clear in the blast furnace process. However, the hypothesis of taking care of desulphurisation and reduction efficiency in order to get higher carbon content in hot metal has been successful even when the sulphur load has been very high. Relatively high slag basicity was adapted and a special attention to hearth conditions has been paid together with the burden distribution control.

Sulphur control together with a careful hearth operation control is an effective tool to achieve good final quality of hot metal.

9 SUMMARY

The main purpose of this work has been to find the factors influencing the hot metal carbon content and to develop methods to control the hot metal sulphur content and to operate the blast furnace hearth properly.

Physical conditions in the hearth define the prerequisites and thus the chemical reactions which then determine the hot metal quality. The hearth coke, deadman, should not be clogged and inactive to secure the proper hearth operation. The deadman should be loose and slightly floating. Methods to monitor the hearth condition have been developed mainly based on temperature measurements in the hearth lining. Hot metal composition and temperature also give clear signals of the hearth operation. If the deadman becomes inactive it can be activated again within a reasonable time frame by applying certain operational methods. Both carbonisation and desulphurisation are strongly dependent on the hearth operation. A good hearth operation prolongs the campaign life of the hearth lining thus improving the total economy.

Regarding the hot metal quality there are many sources of disturbances starting from raw materials handling through the blast furnace process ending to the casting of the hot metal. Sulphur can also be a harmful element participating in clogging of the deadman and accelerating its precipitation in the deadman forming a vicious circle. The sulphur content of hot metal retards carbonisation of hot metal. The sulphur content of hot metal can be controlled by increasing slag basicity and improving the reduction of iron oxides and by selecting raw materials with low sulphur content, too.

The carbon content of hot metal is an important part of the total quality of hot metal. Almost 80% of total reaction energy in the BOF process comes from oxidation of carbon in hot metal. That is why a high and even (stable) carbon content is most desirable. Carbonisation of solid iron starts in the shaft by CO gas and also by coke carbon when the molten metal trickles down to the hearth through the coke layer. The final carbon content of hot metal is formed in the hearth and it is favoured by a loose, active deadman, coke with good carbonising properties and low sulphur content in hot metal.

REFERENCES

1. Jockenhövel, A., Willms, Chr., "Archaeological Investigations on the Beginning of Blast Furnace Technology in Central Europe. In: Crew, P. / Crew, S. (Eds): Early Ironworking in Europe. Archaeology and Experiment. Abstracts of the International Conference at Plas Tan y Bwlch 19-25 Sept. 1997. Plas Tan y Bwlch Occasional Papers No 3 (Plas Tan y Bwlch 1997) 56-58.

2. Ramm, A.N., "Sovremennyj Domennyj Protsess", Metallurgija, Moskva 1980. 303 pages p. 34

3. Elliot, J.F., Gleiser, M. and Ramakrishna, V., "Thermochemistry for Steelmaking", Addison-Wesley, London, 1963. 846 pages p. 485

4. Kowalski, W., Lüngen, H.B. and Stricker, K.P., "State of the art for prolonging blast furnace campaigns". La Revue de Métallurgie-CIT, Avril 2000. p.493-505

5. Liu, B., Liu, F. and Zhang, L., "Blast furnace carbon block wear and application of hot-pressed carbon brick at Bengang", Iron and Steel Engineer, December 1992. pp 36-39

6. Miyashita, T., Nishio, H, Shimotsuma, T., Yamada, T., and Ohtsuki, M., "Limits of Oxygen Enrichment, Tuyere Fuel Injection, and Prospect of Stack Gas Injection in an Experimental Furnace", Transactions ISIJ, Vol 13, 1973. pp 1-10

7. Ichida, M., Kunimoto, K., Kamiyama, H., Okada, T. and Nishio, K., "Development of Blast Furnace Dead-man Dynamic Control Technology", The First International Congress of Science and Technology of Ironmaking, 1994, Sendai, ISIJ. pp 278-283

8. Sanui, M., "Final meeting report 17-21.3.1997", Consultant report, Rautaruukki Oy, Raahe, 1997

9. ISIJ, “Blast Furnace Phenomena and Modelling”, Elsevier 1987. 631 pages p. 561

10. Kanbara, K., Hagiwara, T., Shigemi, A., Kondo, S., Kanayama, Y., Wakabayashi K. and Hiramoto, N., "Dissection of Blast Furnaces and Their Internal State", Transactions ISIJ, Vol 17, 1977. pp 371-380

11. Nicolle, R., Steiler, JM., Helleisen, M., Venturini, MJ., Jusseau, N., Van Crayelinghe, M., Metz, B. and Duperray, P., "The Internal State of the Blast Furnace Hearth", Proceedings of The Sixth International Iron and Steel Congress, 1990, Nagoya, ISIJ. pp 430-438

12. Sunahara, K., Inada, T. and Iwanaga, Y., "Disintegration of blast furnace deadman coke due to molten FeO", Ironmaking and Steelmaking 1993 Vol 20 No. 3. pp 207-214

13. Iwanaga, Y, "Coke properties sampled at tuyere and control of deadman zone", Ironmaking and Steelmaking, 1991 Vol. 18 No.2.pp 102-106

14. Brännbacka, J. and Saxén, H., "Modeling the liquid levels in the blast furnace hearth", ISIJ International 41 (2001) 1133-1140.

15. Torrkulla, J., Brännbacka, J., Saxén, H. and Waller, M., "Indicators of the internal state of the blast furnace hearth", ISIJ International 42 (2002) 504-511.

16. Brännbacka, J. and Saxén, H., "On the operation of the blast furnace hearth with a sitting and floating deadman", submitted to ISIJ International.

17. Saxén, H., J. Brännbacka, J., J. Torrkulla, J. and M. Waller, M., "On the detection of the state of the blast furnace hearth", Proceedings of International Blast Furnace Lower Zone Symposium, AusIMM, Wollongong, Australia, (2002), pp 7.1-7.12.

18. Nightingale, R.J., Dippenaar, R.J. and Lu, W-K., "Developments in Blast Furnace Process Control at Port Kembla Based on Process Fundamentals". Metallurgical and Materials Transactions B, Volume 31B, October 2000. pp 993-1003

19. Nightingale, R.J., Tanzil, F.W.B.U., Beck, A.G.J., Dunning, J.D. and Vardy, S.K., "Operation Guidance Techniques For Blast Furnace Casting And Liquids Management", ICSTI/Ironmaking Conference Proceedings, 1998. p. 567-579

20. BS 4262

21. ASTM D5341-93

22. ISO/FDIS 18894

23. Beppler, E., Grosspietsch, K-H., Louis, G. and Nelles, L., "Einfluss der Koksqualität auf das Betriebsverhalten des Hochofens", Stahl und Eisen 119 (1999) Nr. 5. pp 69-76

24. Negro, P., Steiler, J.M., Beppler, E., Jahnsen, U., Bennington, C.R., Willmers, R.R., "Assessment of Coke Degradation in the Blast Furnace from Tuyere Probing Investigations", 3rd International Cokemaking Congress, Gent Belgium September 16-18,1996. pp. 20-27.

25. Shibaike H., Ogata, I., Naito, M., Sasaki, S., Yasunaga, S. and Hashimoto, S., ”Long-Term High-Efficiency Operation of Sakai No. 2 Blast Furnace (Third Campaign)”, Nippon Steel Technical Report No. 43 October 1989. pp 41-53

26. Kurita, K. and Ogawa, A., "A Study of Wear Profile of Blast Furnace Hearth Affected by Fluid Flow and Heat Transfer", The First International Congress of Science and Technology of Ironmaking, 1994, Sendai, ISIJ. pp 284-289

27. Ostrouhov, M. Ja., Shparber, L. Ja., "Ekspluatatsija Domennyh Petshej", Metallurgija, Moskva, 1975. 264 pages pp 114-115

28. Bodsworth, C. and Bell, H.B., "Physical chemistry of iron and steel manufacture", Longman, London 1972, 529 pages pp 180-181

29. Iwamasa, P.K. and Fruehan, R.J., "Effect of FeO in the Slag and Silicon in the Metal on the Desulfurization of Hot Metal", Metallurgical and Materials Transactions, Volume 28B, February 1997. pp 47 – 57

30. Smith, R. and Fruehan, R.J., “ The effect of carbon content on the rate of reduction of FeO in slag relevant to iron smelting”, Steel Research 70 (1999) No 8+9. pp 283 - 295

31. Wu, C. and Sahajwalla, V., “Influence of Melt Carbon and Sulphur on the Wetting of Solid Graphite by Fe-C-S Melts”, Metallurgical and Materials Transactions, Volume 29B, April 1998. pp 471 – 477

32. Hori, R., Maki, T. and Goto, T., “Blast Furnace Operation with Sinter, Pellets and Lump Ore Mixture by the Control of Movable Armour and Centre Coke Charging”, Seminar on Sinter and Pellets, IISI, Brussels, Belgium – June 1-2, 1999. pp 258-269

33. Shimomura, Y., Nishikawa, K., Arino, S., Katayama, T., Hida, Y. and Isoyama, T., “On the Internal State of Lumpy Zone of Blast Furnace”, Transactions ISIJ, Vol 17, 1977. pp 381 – 390

34. Narita, K., Maekawa, M., Onoye, T., Satoh, Y. and Miyamoto, M., "Formation of Titanium Compounds, So-called Titanium Bear, in the Blast Furnace Hearth", Transactions ISIJ, Vol. 17, 1977. pp. 459-468

35. Kubaschewski, O., Alcock, C.B., "Metallurgical Thermochemistry", Pergamon Press, 1979. 449 pages

36. Sigworth, G.K. and Elliot, J.F., "The Thermodynamics of Liquid Dilute Iron Alloys", Metal Science, Vol 8, 1974. pp. 298-310.

37. Julin, Y. and Härkki, J., "[Fundamentals of inoculation of foundry irons] (in Finnish)", Report TKK-V-C 28(1982) p 21

38. "Grundlagen des Hochofenverfahrens , Physikalisch-chemische und physikalische Zusammenhänge" , Verlag Stahleisen m.b.H. Düsseldorf 1973, 240 pages

39. Von Neumann, F., Schenck, H. and Patterson, W., “Eisen-Kohlenstoff-Legierungen in Thermodynamischer Betrachtung”, Giesserei 23 (1959). pp 1217-1246

40. Raipala, K., ”Deadman and hearth phenomena in the blast furnace”, Scandinavian Journal of Metallurgy 2000, 29. pp 39-46

41. Fuwa, T. and Chipman, J., Trans. Amer. Inst. min. (metall.) Engrs., 1959, Vol.215, p.708

42. Ohtani, M. and Gocken, N.A., Trans. Amer. Inst. min. (metall.) Engrs., 1960, Vol 216, p 533

43. Lindroos, V., Sulonen, M. and Veistinen, M.,"Uudistettu Miekk-ojan Metallioppi (in Finnish)", Otava 1986. 841 pages

44. Gudenau, H., Mulanza, J.P. and Ganpath Ram Sharma, D., “Carburization of hot metal by industrial and special cokes”, Steel Research 61 (1990) No. 3. pp 97-104

45. Wu, C. and Sahajwalla, V., ”Dissolution Rates of Coals and Graphite in Fe-C-S Melts in Direct Ironmaking: Influence of Melt Carbon and Sulphur on Carbon Dissolution”, Metallurgical and Materials Transactions, Volume 31B, April 2000. pp 243-251

46. Rosing, K., "A model for estimating of blast furnace hearth wear" (in Swedish), Graduate thesis, Åbo Akademi, 2000.

47. Koverhar BF Revamp, Information given by suppliers, 1995

48. "Anhaltszahlen für die Wärmewirtschaft in Eisenhüttenwerken", Verlag Stahleisen m.b.H., Düsseldorf, 1957. 472 pages

49. Kawasaki Steel, Internal report, Mizushima 1984

50. "Ruhrkohlen Handbuch", Verlag Glückauf GmbH, Essen, 1984. 404 pages

51. Sahajwalla, V. and Khanna, R., "Effect of sulfur on the dissolution behaviour of graphite in Fe-C-S melts: A Monte Carlo simulation study", Scandinavian Journal of Metallurgy 2003; 32, pp 53-57

52. Paananen, T., "The use of manganese in the blast furnace as added in sinter and as lump ore", (In Finnish), Internal Report, Rautaruukki Steel, 17.3.2003. 41 pages

53. Richardson, F.D. and Jeffes, J.H.E., "ΔG (formation) of metal oxides: assesment J. Iron and Steel Inst. 1948 **160** 261; 1949 **163** 150

54. Matsushita, Y. and Sakao, H. (eds.), "Steelmaking Data Sourcebook", Gordon & Bleach, New York 1988

55. Sahajwalla, V. and Khanna, R., "Fundamental investigation of basic mechanism of carbon dissolution in molten iron", Yazawa International Symposium, METALLURGICAL AND MATERIALS PROCESSING: PRINCIPLES AND TECHNOLOGIES, Volume I: MATERIALS PROCESSING FUNDAMENTALS AND NEW TECHNOLOGIES, TMS (The Minerals, Metals & Materials Society), 2003. pp 825-840

56. Rist, A. and Meysson, N., "Recherche graphique de la mise au mille minimale du haut fourneau a faible température de vent", Revue de Métallurgie 61, no 2, 1964, pp 121-145

57. Raipala, K., "Composition of hot metal - measured from the taphole" (In Finnish), Internal Report TR01290, Rautaruukki Oy, 5.3.1990. 15 pages

58. Waller, M., Torrkulla, J. and Saxén, H., "Using ladle-wise analyses of pig iron composition", Poster presentation, The 4th European Coke and Ironmaking congress. Paris, 2000. 7 pages

59. Negro, P., Eibes, C., Didelon, F. and Eymond, JL., "French experience about coke quality at high coal injection rate", European Blast Furnace Committee, Koverhar/Finland, September 18 and 19,1997.

APPENDIX 1

Source /36/

First order interaction parameters e_i^j *at 1600 °C*

$j \rightarrow$ $i \downarrow$	C	Ca	Mn	S	Si	Ti
C	0.14	-0.097	-0.012	0.046	0.08	
Ca	-0.34	-0.002			-0.097	
Mn	-0.07		0.0*)	-0.048	-0.0327*)	-0.05*)
S	0.11		-0.026	-0.028	0.063	-0.072
Si	0.18	-0.067	0.002	0.056	0.11	
Ti				-0.11	2.1*)	0.042*)

*) Source /54/

Temperature dependence of certain interaction parameters:

$$e_C^C = \frac{158}{T} + 0.0581$$

$$e_C^{Si} = \frac{162}{T} - 0.008$$

$$e_S^S = \frac{233}{T} - 0.153$$

$$e_{Si}^C = \frac{380}{T} - 0.023$$

$$e_{Si}^{Si} = \frac{34.5}{T} - 0.089$$

Second order interaction parameters r_i^j *at 1600 °C*

$j \rightarrow$ $i \downarrow$	C	Ca	Mn	S	Si	Ti
C	0.0074				0.0007	
Ca	0.012				0.0009	
Mn						
S	0.0058		0.0	-0.0009	0.0017	0.0001
Si					-0.0021	
Ti						-0.001

APPENDIX 2

Blast Furnace Profile at Fundia Wire Oy Ab, Koverhar.

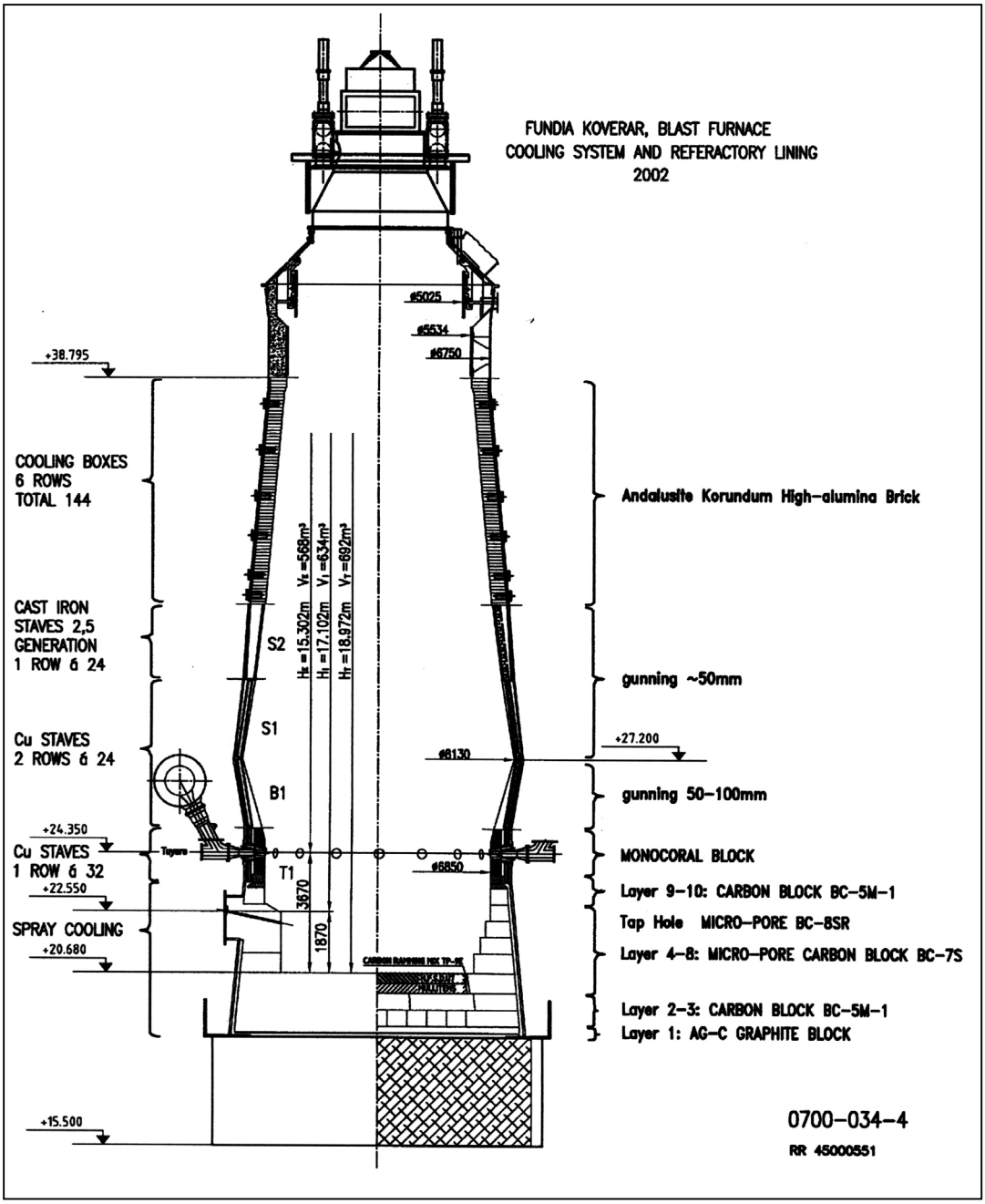

APPENDIX 3

Hearth construction of Koverhar blast furnace 1995 -